

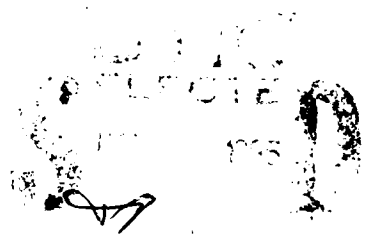
MICROCOPY RESOLUTION TEST CHART
NATIONAL BUREAU OF STANDARDS-1963-A

2

AD-A161 023

NAVAL POSTGRADUATE SCHOOL

Monterey, California



THESIS

OTIC FILE COPY

TEST AND EVALUATION OF AN IMPROVED
SEA, SWELL AND SURF PROGRAM

BY

Michael J. Gill

September 1985

Thesis Advisors:

E.B. Thornton
C.S. Wu

Approved for public release; distribution unlimited.

85 11 08 020

UNCLASSIFIED

SECURITY CLASSIFICATION OF THIS PAGE (When Data Entered)

REPORT DOCUMENTATION PAGE		READ INSTRUCTIONS BEFORE COMPLETING FORM
1. REPORT NUMBER	2. GOV. ACCESSION NO.	3. RECIPIENT'S CATALOG NUMBER
	AD-A161023	
4. TITLE (and Subtitle): Test and Evaluation of an Improved Sea, Swell and Surf Program	5. TYPE OF REPORT & PERIOD COVERED Masters Thesis September 1985	
	6. PERFORMING ORG. REPORT NUMBER	
7. AUTHOR(s) Michael J. Gill	8. CONTRACT OR GRANT NUMBER(s)	
9. PERFORMING ORGANIZATION NAME AND ADDRESS Naval Postgraduate School Monterey, California 93943-5100	10. PROGRAM ELEMENT PROJECT, TASK AREA & WORK UNIT NUMBERS	
11. CONTROLLING OFFICE NAME AND ADDRESS Naval Postgraduate School Monterey, California 93943-5100	12. REPORT DATE September 1985	13. NUMBER OF PAGES 128
14. MONITORING AGENCY NAME & ADDRESS (if different from Controlling Office) Naval Postgraduate School Monterey, California 93943-5100	15. SECURITY CLASS. (of this report) Unclassified	
	15a. DECLASSIFICATION DOWNGRADING SCHEDULE	
16. DISTRIBUTION STATEMENT (of this Report) Approved for public release; distribution unlimited		
17. DISTRIBUTION STATEMENT (of the abstract entered in Block 20, if different from Report)		
18. SUPPLEMENTARY NOTES		
19. KEY WORDS (Continue on reverse side if necessary and identify by block number) Sea; Swell; Surf; Wave prediction; Surf prediction; Breakers; Wind generation; Longshore currents. ←		
20. ABSTRACT (Continue on reverse side if necessary and identify by block number) A sea, swell and surf program is improved, tested and evaluated on a micro-computer (HP-9845B). Sea swell is calculated by a two dimensional spectral model. The energy balance equation is tested for different cases of wind velocities and water depths. Satisfactory agreement is observed between the offshore model and expected wave heights		

DD FORM 1473
1 JAN 73

EDITION OF 1 NOV 65 IS OBSOLETE

UNCLASSIFIED

FORM 1473-15-014-6601

1

SECURITY CLASSIFICATION OF THIS PAGE (When Data Entered)

for a 15 knot wind, but the model overbuilds wave energy for a 30 knot wind. Wave transformation is described by a one dimensional random wave model in which the wave heights are described using the Rayleigh distribution. The obtained solution of the random wave field is used to predict the longshore currents. An empirical formula for determining the breaker parameters is developed, based on beach slope and incident wave steepness. The improved model is tested using an undulated bathymetry to validate the model physics. The model outputs of wave height and current are compared with data acquired from a wave tank and natural beaches. The model is found to accurately forecast wave heights, breaker location, breaker type and longshore currents for several sets of conditions. Model limitations are discussed and recommendations for further improvement are made.

A-1



Approved for public release; distribution unlimited.

Test and Evaluation of an Improved
Sea, Swell and Surf Program

by

Michael James Gill
Lieutenant, United States Navy
B.S., University of Washington at Seattle, 1978

Submitted in partial fulfillment of the
requirements for the degree of

MASTER OF SCIENCE IN METEOROLOGY AND OCEANOGRAPHY

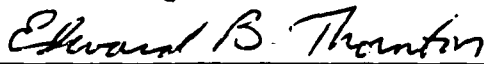
from the

NAVAL POSTGRADUATE SCHOOL
September, 1985

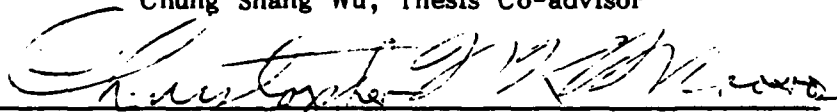
Author:


Michael J. Gill

Approved by:


Edward B. Thornton, Thesis Advisor


Chung Shang Wu, Thesis Co-advisor


Christopher N.K. Mooers, Chairman,
Department of Oceanography


John N. Dyer
Dean of Science and Engineering

ABSTRACT

A sea, swell and surf program is improved, tested and evaluated on a micro-computer (HP-9845B). Sea swell is calculated by a two dimensional spectral model. The energy balance equation is tested for different cases of wind velocities and water depths. Satisfactory agreement is observed between the offshore model and expected wave heights for a 15 knot wind, but the model overbuilds wave energy for a 30 knot wind. Wave transformation is described by a one dimensional random wave model in which the wave heights are described using the Rayleigh distribution. The obtained solution of the random wave field is used to predict the longshore currents. An empirical formula for determining the breaker parameters is developed, based on beach slope and incident wave steepness. The improved model is tested using an undulated bathymetry to validate the model physics. The model outputs of wave height and current are compared with data acquired from a wave tank and natural beaches. The model is found to accurately forecast wave heights, breaker location, breaker type and longshore currents for several sets of conditions. Model limitations are discussed and recommendations for further improvement are made. *Keywords: sea, swell, surf*

TABLE OF CONTENTS

I.	INTRODUCTION -----	8
A.	OPERATIONAL REQUIREMENT FOR WAVE FORECASTING --	8
B.	WAVE THEORY BACKGROUND -----	9
C.	CURRENT MODELING TECHNIQUES -----	10
D.	OBJECTIVES -----	11
II.	OVERVIEW OF THE SSSP MODEL -----	12
A.	OVERALL PROGRAM DESIGN -----	12
B.	SSSP FLOWCHART -----	13
C.	PROGRAM MODULES -----	17
1.	Offshore Module -----	17
2.	Wave Height Transformation -----	24
3.	Longshore Currents -----	30
4.	Surf Zone -----	30
III.	MODEL IMPROVEMENTS -----	32
A.	OFFSHORE WAVE HEIGHT GROWTH -----	32
B.	WAVE REFRACTION MODULE -----	38
1.	Model Experiments -----	42
2.	Improvement Of Numerical Scheme -----	53
3.	Boundary Conditions -----	58
4.	Results -----	59
C.	ONE DIMENSIONAL WAVE HEIGHT CALCULATIONS -----	63
D.	LONGSHORE CURRENT CALCULATIONS -----	71
E.	IMPROVEMENTS TO THE SURFCON MODULE -----	74

F.	DEVELOPMENT OF AN OPERATIONAL USER'S GUIDE	----	80
IV.	DISCUSSION	-----	81
A.	SENSITIVITY TEST OF THE BREAKER PARAMETERS	----	81
B.	CHOOSING THE BREAKER PARAMETERS	-----	94
C.	MOTIVATION FOR THE RANDOM WAVE MODEL SUBSTITUTION		102
V.	TEST AND EVALUATION OF THE IMPROVED MODEL	-----	104
A.	WAVE HEIGHT AND BREAKER LOCATION	-----	104
B.	LONGSHORE CURRENT DISTRIBUTION	-----	112
VI.	SUMMARY AND CONCLUSIONS	-----	118
A.	SUMMARY	-----	118
B.	CONCLUSIONS	-----	121
	LIST OF REFERENCES	-----	123
	INITIAL DISTRIBUTION LIST	-----	127

ACKNOWLEDGEMENTS

The author wishes to express his appreciation to Dr. E.B. Thornton, thesis advisor, for his guidance and assistance throughout the course of this thesis project. Dr. Thornton's patience and confidence is gratefully acknowledged. Dr. C.S. Wu provided invaluable help in optimizing the numerical methods used in the SSSP model as well as co-advising the thesis effort. Dr. C.N.K. Mooers reviewed the manuscript and provided timely advice. The graphics generation and programming assistance provided by Ms. Donna Burych is gratefully recognized. All are members of the Department of Oceanography, Naval Postgraduate School, Monterey, CA.

The author wishes to express his special thanks to his wife, Virginia, who managed to keep her sense of humor throughout the entire NPS experience.

I. INTRODUCTION

A. OPERATIONAL REQUIREMENT FOR WAVE FORECASTING

Wave and surf forecasting has been an important part of Naval Amphibious operations since the beach landings of World War II. The need for the prediction of ocean and surf waves for military purposes led to the first real attempt to quantitatively model ocean and beach waves. Ocean engineers and physical oceanographers, such as M.P. O'Brien, H.U. Sverdrup and W.H. Munk, made great strides in sea, swell and surf modeling during the 1940 - 1955 time period (Bascom, 1980). The wave and surf predictions made by the U.S. Navy are still based on these works. During the intervening time period, significant advances in knowledge of ocean wave dynamics have occurred, and it is time to update prediction techniques.

Although warfare technology has advanced along all fronts, the standard amphibious beach assault is still a viable and preferable method of projecting forces ashore for many tactical scenarios. However, amphibious assault craft are vulnerable to many types of wave dynamics. In general, landings are affected by the initial ocean sea and swell where the boats are launched as well as by the breaking waves in the surf zone, along with the accompanying longshore currents. Since in a major landing tens of thousands of lives are at risk, an accurate assessment of the sea, swell and surf is vital to a successful amphibious landing operation (Joint Surf Manual, 1976).

In addition to the assault landing itself, an amphibious operation normally concludes with the construction of a temporary harbor facility to accommodate the resupply of the troops ashore. The survivability and design

characteristics of these structures depend in large part on the environment around them. The ability to model wave height and direction, and longshore currents is necessary to operational planners and coastal engineers in designing and emplacing these facilities.

In the past twenty years, separate models have been developed to deal with ocean waves, breaking surf and longshore currents. In 1981, the U.S. Navy contracted to have a model developed which would combine three complementary models. The goal of this comprehensive Sea, Swell and Surf Program (SSSP) model was to predict the wind generated wave height, calculate the surf zone characteristics based on the wind generated energy propagation, and use a two dimensional grid to compute the longshore current field. The model, developed by Wang and Chen (1983), was written in FORTRAN and designed to run on a main frame computer. To facilitate the model's use by Naval Oceanographers in the fleet, the model was converted into BASIC and implemented on the HP-9845B/275 micro-computer (Devendorf, 1985). The primary goal of this thesis is to modify the SSSP model to improve its computational efficiency.

B. WAVE THEORY BACKGROUND

The water surface elevation in the ocean can be viewed as a large number of individual wavelets at various frequencies. The waves that contribute the most energy to the ocean wave system are wind generated waves with periods of 1 to 30 seconds. The size and period of these waves are a function of the velocity of the wind, the duration of the storm and the distance over which the wind blows (fetch).

The simplest theory is linear, small amplitude wave theory. Sea water is assumed to be incompressible and homogeneous, and surface tension forces are assumed to be negligible. The solutions of this theory describe the behavior of the individual components of ocean wind waves (Phillips, 1977). As waves enter into shallow water, wave speed varies with the local water depth and refraction occurs.

Initially, refraction of monochromatic waves was modeled using wave ray theory of a single wave (Arthur, 1949). It was not until the mid 1960's that the development of fast computers and the implementation of better physics enabled numerical analysts to study the generation of wind waves over an entire frequency spectrum. Early researchers in the wave spectral analysis field introduced direction variables to study straight and parallel contour wave spectrum transformation (Karlsson, 1969) and included the effects of bottom dissipation and local wind generation.

As computers advanced, more complex refraction models were developed. Noda et al. (1974), using a relaxation finite differencing scheme, solved for the stationary wave spectral transformation. The model that is under study by this thesis was originally developed by Wang and Yang (1981) and included the effects of bottom friction. Chen and Wang (1983) improved the model by including the effects of non-stationary waves.

C. CURRENT MODELING TECHNIQUES

Two numerical modeling techniques are currently used in wave and surf forecasting applications. The finite element method, while highly complex, has the advantage of being able to incorporate irregular localized bathymetry and has stable non-linear convergence properties. Wu and Liu (1985) introduced the method in their study of wave induced nearshore currents.

The finite difference method is a widely used numerical method. It is based on a linear differencing approach. Finite differencing normally uses a rectangular computational grid. This method was used by Noda et al. (1974) and Shaiu and Wang (1977) in their studies of nearshore circulation and wave energy transformation, respectively. The method is easier to implement than the finite element method due to its use of a regular grid describing the bathymetry, and is employed in the development of the SSSP (Wang and Chen, 1983).

D. OBJECTIVES

The objective of this thesis is to improve a sea, swell and surf program which is implemented on the HP 9845-B/275 micro-computer. The program is divided into subroutines, which include the open water wave generation module, wave transformation, the surf zone breaker calculations and the longshore current routines. To test the model, the output from the improved model is compared with data bases acquired from two natural beaches as well as several wave tank experiments. A users manual has been prepared and an attempt has been made to interface graphic output with the current model. Limitations of the model are discussed and future improvements suggested. This model is proposed for use by operational planners and Naval Oceanographers at sea.

II. OVERVIEW OF THE SSSP MODEL

A. OVERALL PROGRAM DESIGN

The Sea, Swell and Surf Program (SSSP) was developed by Wang and Chen (1983). The SSSP is essentially three complementary models which are merged to calculate offshore wave height fields, surf zone information and longshore current velocities. The three modules, ocean, surf and longshore currents, can be run independently or the offshore wave energy can be used as input to the surf and current models. The SSSP is a numerical model which uses finite differencing to solve the governing equations.

The original version, as written by Wang and Chen, was written in FORTRAN and designed to run on a mainframe computer. The version discussed in this thesis was converted to BASIC and implemented on an 16 bit HP 9845-B/275 micro-computer (Devendorf, 1985). The micro-computer version consists of a control program with subroutines to calculate wave direction, height, and number, and output surf, swell and current information.

The SSSP considers an offshore wind generated energy spectrum which is used to estimate the wave growth based on initial inputs of wind speed and wave height or spectral energy bands. As the waves traverse down the user defined grid, changes in the deep water energy spectrum due to bottom friction and irregular bottom changes, are taken into account. If the surf zone model is to be run, a significant wave height, calculated from the area under the wave spectrum, and the peak frequency are used to provide a monochromatic wave height input into the surf model. It is also possible to

input monochromatic wave data directly into the surf module to compute the surf zone characteristics without running the computationally intensive offshore module (Wang and Chen, 1983).

B. SSSP FLOWCHART

The SSSP is controlled by one main program which, in turn, can call any of twelve subroutines. A general flowchart of the entire SSSP shows that the SSSP is divided into two main modules (Fig. 2.1). The user is prompted for all required information in a menu-driven, interactive fashion. Initially, the user chooses whether to run the offshore or the surf model. General and specific input is requested for the module being run. The open water or surf condition modules are calculated and the proper output is generated by either the OUTSW or OUTSRF routines.

A more detailed flowchart of the open water condition module is presented as Figure 2.2. OPEN computes the wavenumber as a function of depth and then loops through a calculation series for each energy band. An adjustment is made for the angle of the swell/waves with respect to the grid axis. The DIRECT and HEIGH2 subroutines are called and the energy from each spectral band is summed and converted to wave height.

The original SURFCON subroutine (Figure 2.3) used the most energetic energy band computed by the OPEN module as its frequency input, or used data entered directly by the user. The wavenumber was computed, the DIRECT and HEIGH2 subroutines were called, the average wave height was calculated and a series of breaker height and locations were predicted.

If longshore currents were desired, the NEARCIR subroutine was invoked. The model, as implemented on the HP-9845, used an iterative process on a

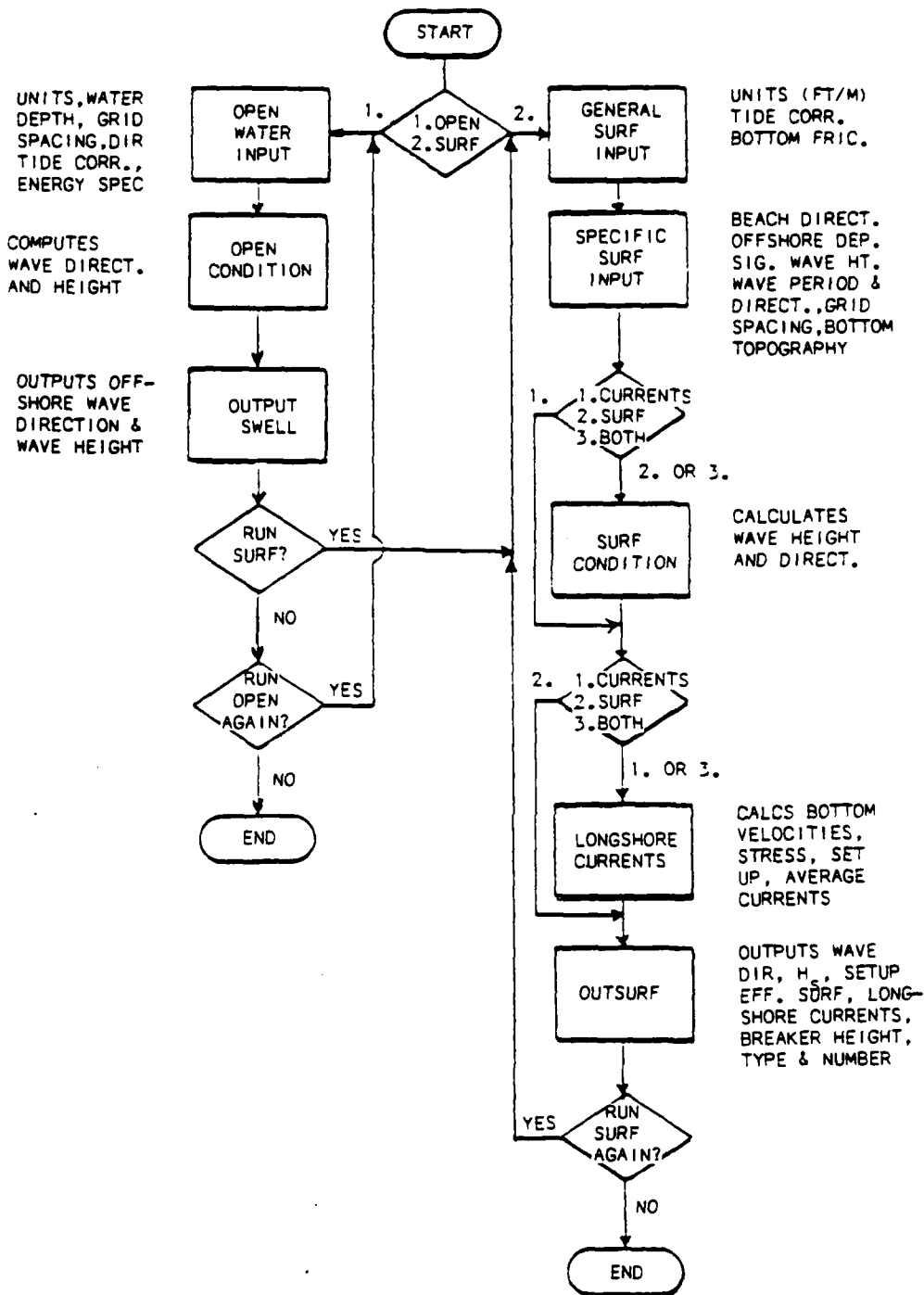


Figure 2.1. General flowchart of the Sea, Swell and Surf Program (SSSP).

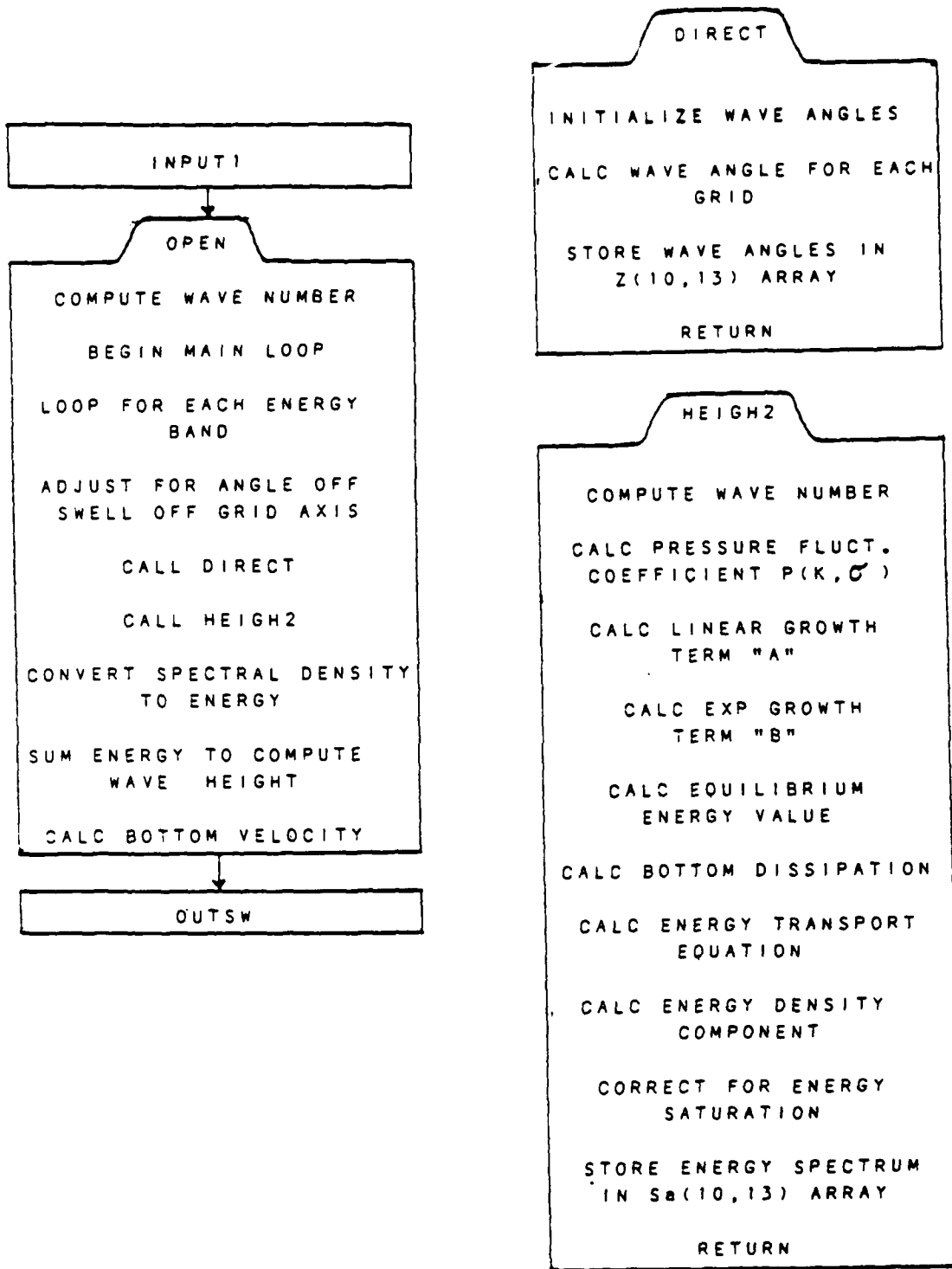


Figure 2.2. Flowcharts of the Open water, Wave Direction and Wave Height subroutines (OPEN, DIRECT and HEIGH2).

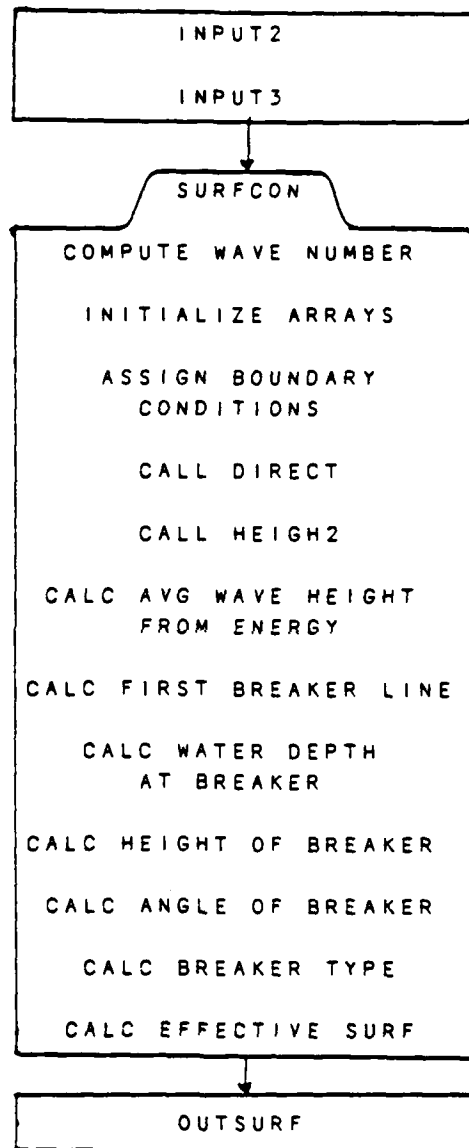


Figure 2.3. Flowchart of the original Surf Condition subroutine (SURFCON).

two dimensional grid to solve for the mean horizontal velocities. It was found that this scheme was computationally unstable as well as requiring as long as twenty-three hours to converge to a solution (Devendorf, 1985).

To take advantage of the most recent advances in breaker height modeling, and increase the computational speed, the SURFCON and its ancillary subroutines were revised to use a one dimensional random wave model. A detailed flowchart of the new SURFCON module (Fig. 2.4), which replaces the original, shows the simplifications implemented by the new model. DIRECT2 is a simple Snell's law calculation, applicable over straight and parallel contours. HEIGH3 uses a random wave model which incorporates the probability density function for breaking waves. The output of the new SURFCON module includes breaker height, number of breakers, wave direction and surf zone width.

LONSHOR is a new longshore current subroutine (Figure 2.4), which was implemented in place of the unstable NEARCIR to simplify and speed the calculation of the longshore currents. This model uses a simple radiation stress balance to calculate the current parallel to the beach. The next section will discuss the physics of the SSSP modules in detail.

C. PROGRAM MODULES

1. Offshore Module

When the SSSP is run, a menu of initial choices is presented. If the user chooses the "OPEN WATER" option, the OPEN subroutine is invoked. This offshore module computes the wave height and direction fields as a function of water depth, wind speed and direction, fetch, and the initial energy field. The initial energy can be described by a single significant wave height, direction and period, or as an implicitly entered energy

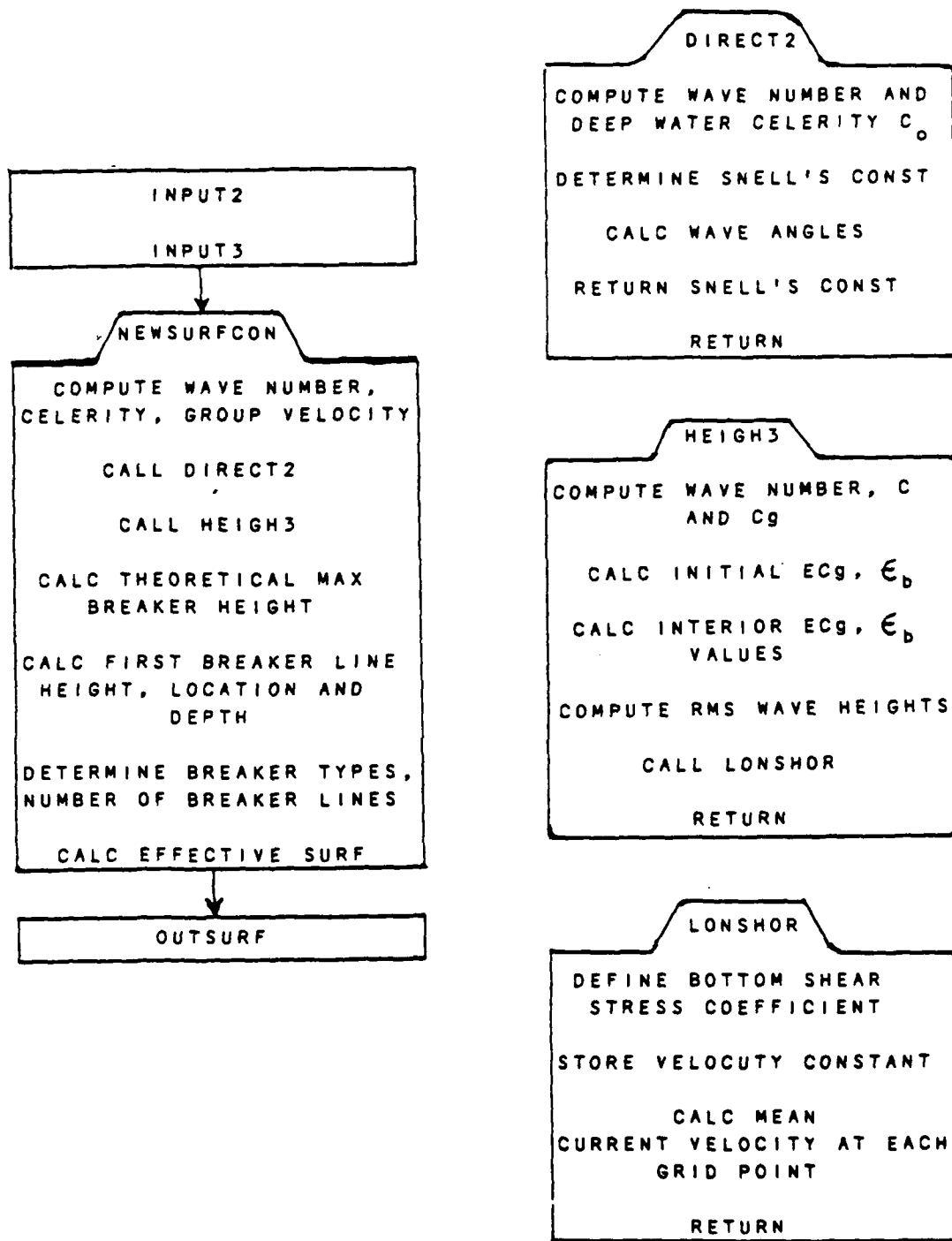


Figure 2.4. Flowcharts of NEWSURFCO, DIRECT2, HEIGH3 and LONSHOR subroutines used in the new model.

spectrum. Water depth for the matrix can be read in from a data file or entered directly from the keyboard. A tidal height correction constant can be added to the depth field to take into account the state of the tide. The bottom type can be specified, which determines the coefficient of friction for the wave height calculations.

a. Wave Refraction

Once all the required input is entered, the program begins its calculation cycle. The first field that is calculated is the wave direction matrix, using a steady state conservation of wavenumber (Phillips, 1977):

$$\frac{\partial}{\partial X}(k \cos \theta) - \frac{\partial}{\partial Y}(k \sin \theta) = 0 \quad (1)$$

where:

$$k = \text{wavenumber} = \frac{2\pi}{L} \quad (\text{m}^{-1})$$

$$L = \text{wavelength} \quad (\text{m})$$

$$\theta = \text{wave direction (clockwise angle from the X axis to the wave ray (see Figure 7))}$$

$$X = \text{offshore grid spacing (user specified (see Figure 5))}$$

$$Y = \text{longshore grid spacing (user specified (see Figure 5))}$$

The wavenumber is calculated, for the frequency band being considered, using the linear dispersion relation:

$$\sigma = (g k \tanh(k h))^{1/2} \quad (2)$$

where:

$$\begin{aligned}\sigma &= \text{angular frequency} = 2\pi f \quad (\text{sec}^{-1}) \\ g &= \text{acceleration of gravity} \quad (\text{m sec}^{-2}) \\ h &= \text{water depth (m)} \\ f &= \text{frequency} = \frac{1}{T} \quad (\text{sec}^{-1}) \\ T &= \text{wave period (sec)}\end{aligned}$$

Since (2) is transcendental in k , a sixth order polynomial fit of (2) is used (Hunt, 1979) to provide a faster method of computing k than the iterative Newton's method used in the original Wang and Chen (1983) version of the SSSP. The wavenumber k is given as:

$$\begin{aligned}k &= \frac{\sigma}{(gh)^{1/2}} [S + (1 + 0.66667S + 0.35550S^2 \\ &\quad + 0.16084S^3 + 0.06320S^4 + 0.02174S^5 \\ &\quad + 0.00654S^6 + 0.00171S^7 + 0.00039S^8 \\ &\quad + 0.00011S^9)^{-1}]^{1/2} \quad (3)\end{aligned}$$

where:

$$S = \sigma^2 \left[\frac{h}{g} \right]$$

Once the wavenumber is determined, subroutine DIRECT is called to compute the wave refraction of the wave components over the specified grid. DIRECT starts with initial values of the wave angles for each grid point, and uses a finite differencing scheme developed by Noda (1972)

to solve the differential equation for $\theta_{i,j}$. The differential equation is center differenced in the offshore (X) direction and forward differenced in the longshore (Y) direction. The finite difference scheme has greater weight on the forward differencing term to increase computational stability (Abbott, 1979) and is given as:

$$\begin{aligned} \theta_{i,j} = \sin^{-1} \{ & \frac{1}{k_{i,j}} [\tau (k \sin \theta_{i+1,j-1}) - (1-2\tau) (k \sin \theta_{i+1,j}) \\ & + \tau (k \sin \theta_{i+1,j+1}) - \frac{\Delta X}{2\Delta Y} (k \cos \theta_{i,j+1}) \\ & - (k \cos \theta_{i,j-1})] \} \end{aligned} \quad (4)$$

where:

$$\tau = \text{weighting factor} = 0.25$$

A first guess for the wave angle is calculated using Snell's law solution for straight and parallel bottom contours. The numeric scheme is iterated until $\theta_{i,j}$ is within 0.005 of the previous calculation. The 10 X 13 grid point system used by the SSSP is described by Figure 2.5. The initial differencing scheme used by the model is a simple forward stepping scheme (Fig. 2.6). The convention for the angle θ is illustrated in Figure 2.7. Theta is measured with respect to a ray drawn perpendicular to the beach. Therefore, a normally incident wave would have a Theta value of 180° . After the direction matrix has been specified, the subroutine HEIGH2 is called to calculate the height transformation as the wave moves down the grid (towards the shoreline).

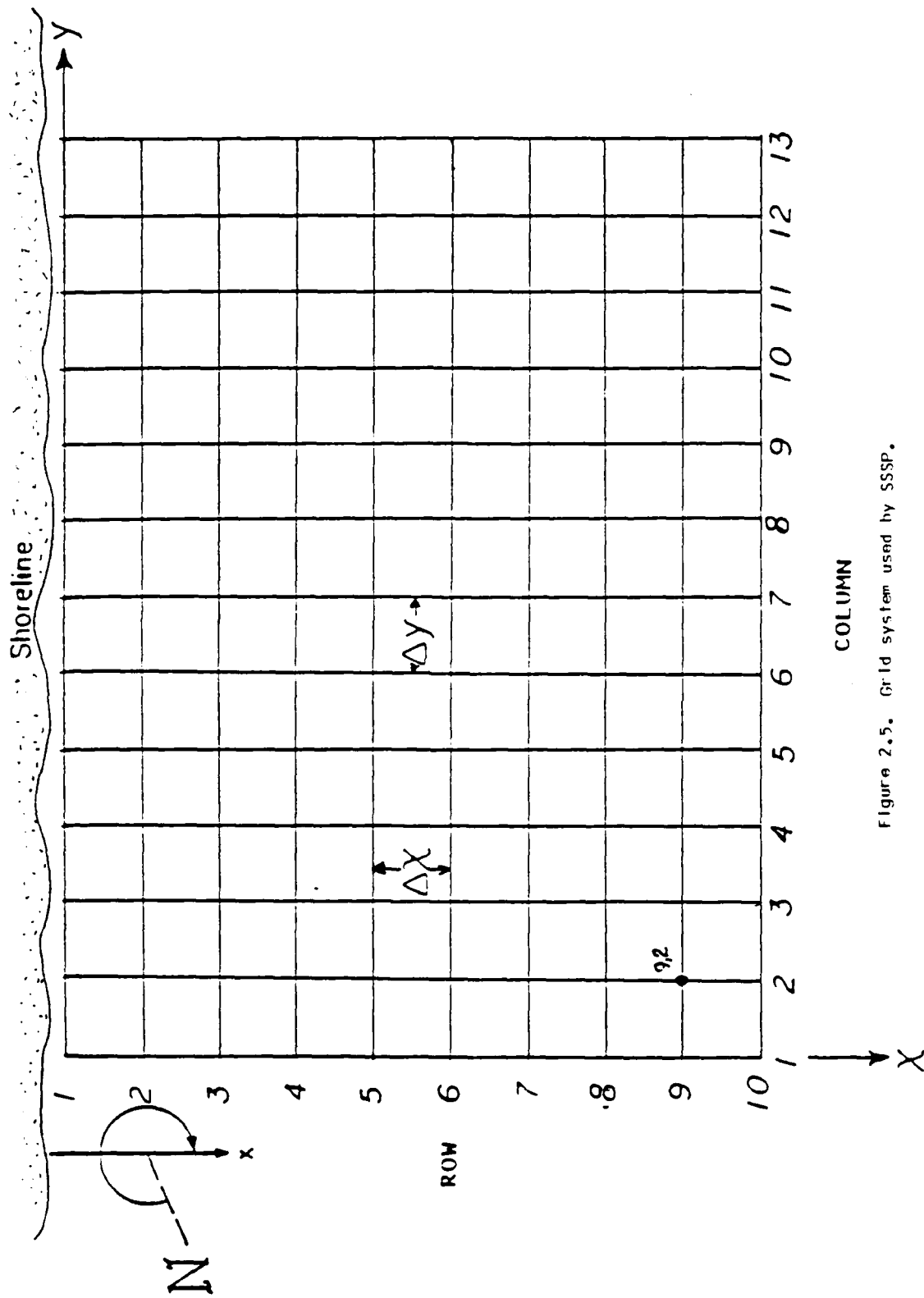


Figure 2.5. Grid system used by SSSP.

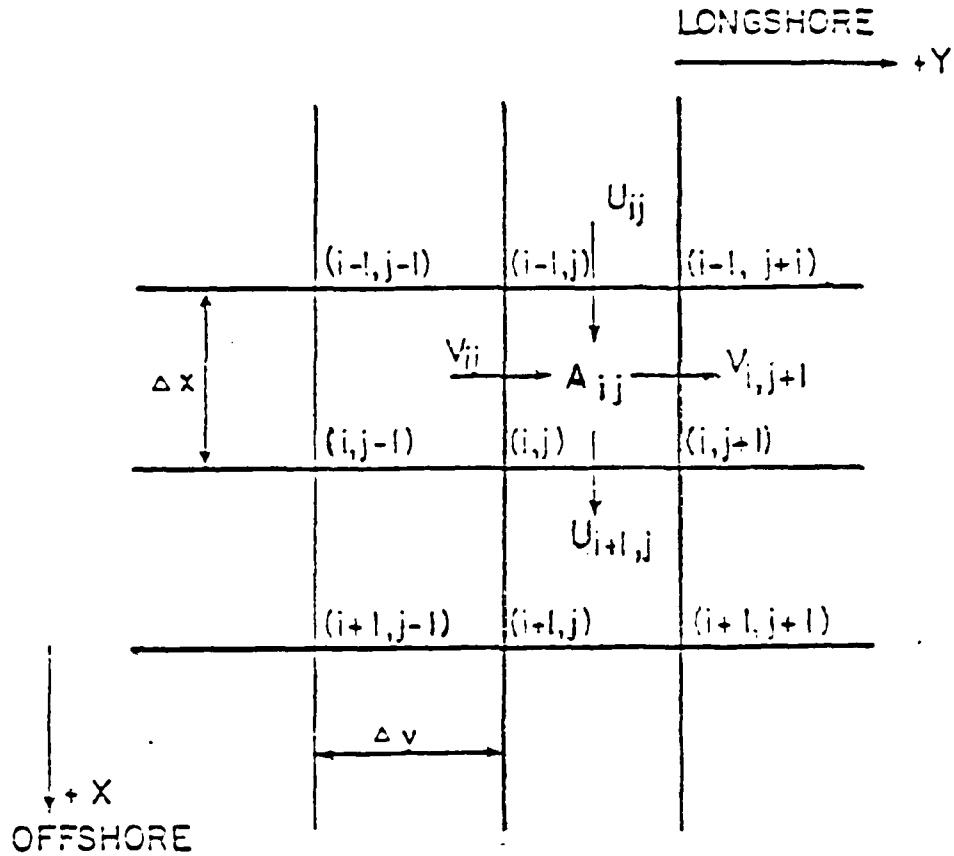


Figure 2.6. Numerical differencing scheme used by the OPEN water module.

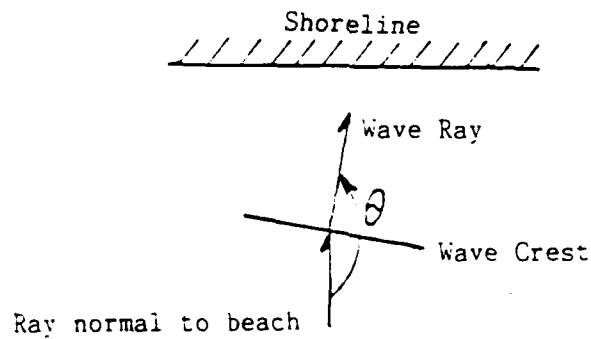


Figure 2.7. Theta convention used by the model.

2. Wave Height Transformation

This subroutine takes into account the wave direction (previously calculated), the wind generation, and the bottom dissipation. HEIGH2 employs the Phillips-Miles growth mechanism for the wind generation calculations. An initial energy field is developed for each grid point by assuming that energy is conserved over straight and parallel contours:

$$\frac{\partial}{\partial X} (E C_g \cos \theta) = 0 \quad (5)$$

where:

E = wave energy (joules)

C_g = group velocity (m sec⁻¹)

The initial energy field is derived by integrating (5) to yield:

$$E = E_o \frac{C_{g_o} \cos \theta_o}{C_g \cos \theta} \quad (6)$$

where the subscript (o) is the initial condition at the offshore boundary.

To simplify and increase the model's efficiency, Chen and Wang (1983) make four assumptions:

- a. Winds are steady
- b. Wave energy within a spectral band is restricted to that band (Allows superposition of wavelets).

c. Each frequency component can be described by a single mean direction, $\bar{\theta}$.

d. No wave-current interactions.

These four assumptions allow the steady state energy flux for each spectral energy band to be written as (Longuet-Higgins and Stewart, 1960; 1962):

$$\begin{aligned} \rho g \frac{d}{df} (S(f) C_g \cos \bar{\theta}) + \rho g \frac{d}{df} (S(f) C_g \sin \bar{\theta}) \\ = - \epsilon_d(f) + \epsilon_s(f) \end{aligned} \quad (7)$$

where:

- $S(f)$ = spectral energy flux
- ρ = density of fluid (kgm^{-3})
- $\epsilon_d(f)$ = energy dissipation due to bottom friction
- $\epsilon_s(f)$ = energy generation due to wind stress
- $\bar{\theta}$ = mean wave direction

The wind generation term ϵ_s is the sum of the linear and exponential contributions:

$$\epsilon_s = S_p - S_m \quad (8)$$

where:

$$S_p = \text{Phillips generation} = \rho g a$$

$$S_m = \text{Miles generation} = \rho g \beta [S(f)]$$

The energy generation term is based on the Phillips-Miles growth mechanisms. Starting with a flat ocean, wave growth is initially linear until larger waves are present, after which the growth is exponential. The linear growth term (Phillips, 1957) is based on random atmospheric pressure variations acting on a perturbed sea surface. The SSSP first calculates the pressure fluctuation term as a function of wavenumber and frequency:

$$P(k, \sigma) = \frac{6.23 \cdot 10^{-4} W^6}{\sigma^2} \left[\frac{\nu_2}{\nu_2 + (k \sin \delta)^2} \right] \left[\frac{\nu_1}{\nu_1 + (k \cos \delta - 1)^2} \right] \quad (9)$$

where:

$$W = \text{wind speed in knots}$$

$$\delta = \frac{\sigma}{W}$$

$$\nu_1 = 0.33 \cdot 1.28$$

$$\nu_2 = 0.52 \cdot 0.95$$

$$\delta = \text{angle between wind and wave}$$

After $P(k, \sigma)$ is calculated, the linear growth term, α , is determined by:

$$\alpha = \frac{4\pi^2 k c^3}{c_w g^3} P(k, \sigma) \quad (10)$$

where:

$$\rho_w = \text{density of water (kg m}^{-3}\text{)}$$

The exponential growth term becomes important after waves have formed (LaBlond and Mysak, 1978). When flow separation occurs in the lee of a wave crest, momentum is transferred to the wave because of the pressure differential resulting in exponential wave growth (Miles, 1957; 1959a,b; 1962):

$$\delta = \left(\frac{aS\sigma}{2\pi}\right) \left[\left(\frac{W}{C}\right) \cos \delta - b\right] \quad (11)$$

where:

$$a = \text{constant} = 5.0$$

$$S = \text{ratio of air to water density}$$

$$C = \text{wave celerity (m sec}^{-1}\text{)}$$

$$b = \text{constant} = 0.90$$

The Phillips-Miles wind wave generation has no mechanism for shutting off the wave growth. In nature, wind waves will grow as a function of wind speed, duration and fetch. But after growing to a certain size and steepness, the waves will become unstable and break. Therefore, it is necessary to have a limiting function so that the waves will only grow to a "fully arisen" sea. Several functions have been proposed to introduce an "equilibrium value", above which the wave growth stops. The SSSP uses a Pierson and Moskowitz (1964) fully arisen sea in deep water. The high frequency tail is described by a Phillips (1957) equilibrium condition,

modified by Kitaigorodskii et al. (1975) and Thornton (1977) for intermediate or shallow water:

$$S(f, \delta) = B g^2 f^{-5} H(\delta) \Gamma(W_n) \quad (12)$$

where:

$$H(\delta) = \frac{8}{3} \pi \cos^4 \delta \quad \text{accounts for angular spreading}$$

$$\Gamma(W_n) = \zeta^{-2}(W_n) \left[1 + \frac{2 W_n^2 \zeta(W_n)}{\sinh[2 W_n^2 \zeta(W_n)]} \right]^{-1}$$

$$W_n = \sigma \left(\frac{h}{g} \right)^{1/2}$$

$\zeta(W_n)$ meets the condition that $\zeta \tanh(W_n \zeta) = 1$

$\zeta(W_n) = 1$ in deep water and for $W_n < 1$, $\zeta(W_n) \sim 1/2 W_n^2$ and $S(f, \delta) = 1/2 q g h df^{-3} H(\delta)$ where q is on the order of 10^{-2} (SSSP uses a value of 0.073).

Bottom dissipation, ε_d , is calculated as the work done on the bottom due to the bed shear stress. Assuming the usual quadratic bed shear stress law, the wave energy dissipation for a particular spectral frequency

band is described by Hasselmann and Collins (1968):

$$\varepsilon_d(f) = \rho_w C_f |\vec{U}_b| U_b^2(f) \quad (13)$$

where:

$$C_f = \text{bed shear stress coefficient} = 0.01$$

$$|\vec{U}_b| = \text{total flow field bottom velocity}$$

$$U_b(f) = \text{wave induced water particle bottom velocity for a specific spectral component}$$

Using linear wave theory transfer functions to relate the surface elevation energy spectrum to the bottom velocity field, the frequency dependent dissipation function $\varepsilon_d(f)$ can be expressed as:

$$\varepsilon_d(f) = \rho C_f T(f) S(f) |\vec{U}_b| \quad (14)$$

where the transfer function $T(f) = [g^2 k^2 / \sigma^2 \cosh^2(kh)]$. The total wave induced bottom velocity $|\vec{U}_b|$ is calculated by integrating the spectral transfer function across the entire frequency spectrum:

$$|\vec{U}_b| = \left[\int_0^{\infty} T(f) S(f) df \right]^{1/2} \quad (15)$$

Bottom dissipation in the SSSP is only calculated when dealing with intermediate or shallow water waves. If deep water wave heights are being computed, the value ε_d is set equal to zero (Wang and Chen, 1983).

3. Longshore Currents

One of the most serious problems with the original model was the instability of the nearshore circulation calculations. As much as 23 hours of CPU time were required for the subroutine to converge to an answer. It was decided that a one dimensional longshore current model which assumes straight and parallel bottom contours would be substituted for the unstable two-dimensional model. This model uses a simple alongshore radiation stress balance to calculate the mean longshore current. Although no circulation information is derived, the new longshore current subroutine, LONSHOR, provides the longshore current velocity efficiently and accurately. The physics and details of the LONSHOR subroutine are outlined in Chapter II.

4. Surf Zone

The original SURFCON module made calls to the same wave direction (DIRECT) and wave height (HEIGH2) subroutines as the offshore module. One disadvantage of this scheme is that these subroutines are very computationally intensive, especially when considering the narrow width between grid points. A faster wave height model was needed.

The state of the art in breaker height models uses a probability density function to describe breaking wave heights (Thornton and Guza, 1983). Some limitations are imposed by using this new model, however. The model assumes that the beach has a local straight and parallel bottom contour. This bathymetric restriction allows longshore features such as sandbars to be modeled accurately, but offshore feature such as channels or canyons are smoothed out by a depth averaging subroutine. It is felt that this assumption is reasonable, in light of the fact that many beaches of

operational interest are of the "straight and parallel" type within the first two hundred meters from shore.

The above assumption means that a simple Snell's law calculation of the wave direction is possible. A short subroutine, called DIRECT2, is implemented to calculate the wave direction matrix. The use of the new height and direction modules, HEIGH3 and DIRECT2 have increased the efficiency of the SURFCON calculations immensely. The average run time for the surf zone model predicted wave heights has decreased from over four minutes to less than 30 seconds.

III. MODEL IMPROVEMENTS

A. OFFSHORE WAVE HEIGHT GROWTH

The current version of the SSSP, converted to run in HP BASIC on the HP-9845B/275 micro-computer, gives reasonable values for wave height growth for wind speeds of 15 knots or less (Devendorf, 1985). However, for higher wind speeds of 30 knots, the SSSP exhibits a growth rate that is significantly faster than the growth of the JONSWAP spectrum (Bishop, 1983), used for comparison in this analysis. The JONSWAP spectrum was chosen as a basis for comparison because the JONSWAP curves were experimentally derived from the limited fetch North Sea area. It is foreseen that the SSSP model may be applied to similar operational areas.

For 30 knot winds, the model's wave growth not only occurs too quickly, reaching a maximum value within 50 nautical miles, but the magnitude of the growth is too high (maximum wave height of 6.0 meters compared to a JONSWAP maximum of 4.2 meters. Before sensitivity tests were run on the wind generation portion of the model, the code was checked carefully to ensure that the equations were being implemented correctly.

To determine the sensitivity of the model wave growth, several runs were made with changes to the key growth parameters. These parameters include A, the Phillips linear growth term, Equation 9 (Phillips, 1957); B, the Miles exponential growth term, Equation 10 (Miles, 1957; 1959a,b; 1962), and R, a weighting factor set equal to 1.0 in the original model.

The first run was used as a standard to compare the modifications against. The inputs for the OPEN module were:

Grid Spacing X = Y = 10 NM

Wave Direction Theta = 180° (normal incidence)

Wind (W) = 30 and 15 kts @ 270°

Shoreline = 270°

Bandwidth (Df) = 0.01 Hz

Frequency bands = 0.05 - 0.14 Hz

The output for these "standard" model runs are shown as Figures 3.1 and 3.2. The overbuilding of the open water waves for W = 30 kts is evident when compared with the JONSWAP spectrum wave growth (Fig. 3.1). For a more moderate case where W = 15 kts, the model wave growth shows satisfactory agreement with the JONSWAP growth (Figure 3.2). To see the impact of changing the weighting factor, R, two runs were made setting R equal to 0.5 and 0.1 respectively. The predicted wave height with R equal to 1, 0.5 and 0.1. is shown in Figure 3.3. Setting R equal to 0.1 (chain dashed line) gives a good fit for high wind speeds but underbuilds the wave field for lighter winds (Fig. 3.4). Clearly, a simple change of the weighting factor R will not resolve the problem.

The Miles exponential growth term, B, is in the denominator of the energy calculation so its value was increased to determine the growth retarding effect it would have. Two runs were made with B doubled (chain dotted line) and with B increased by a factor of 10 (not shown), depicted by Figure 3.5. The result of increasing the exponential growth term is to flatten out the upper portion of the growth curve which is not the correction that needs to be applied.

JONSWAP VS SSSP SIGNIFICANT WAVE HEIGHT
WIND = 30 KTS

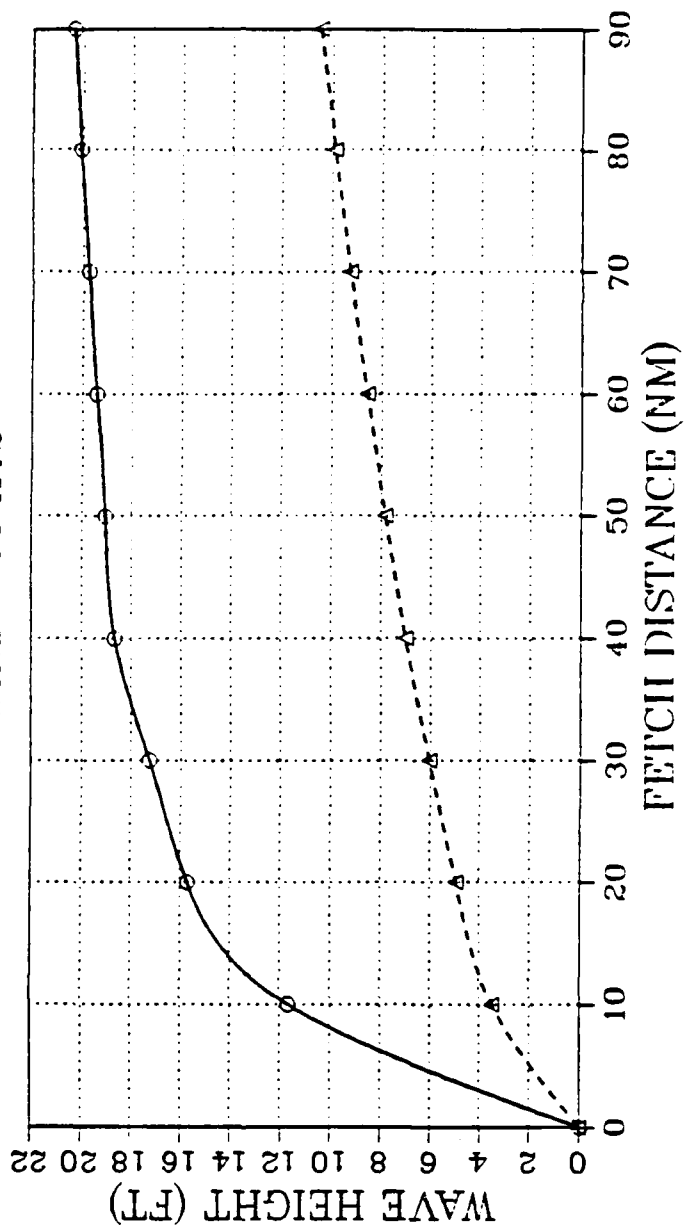


Figure 3.1. Model output (solid) versus JONSWAP curve (dashed) for W = 30 kts. The SSSP substantially over develops wind waves.

JONSWAP VS SSSP SIGNIFICANT WAVE HEIGHT
 WIND = 15 KTS

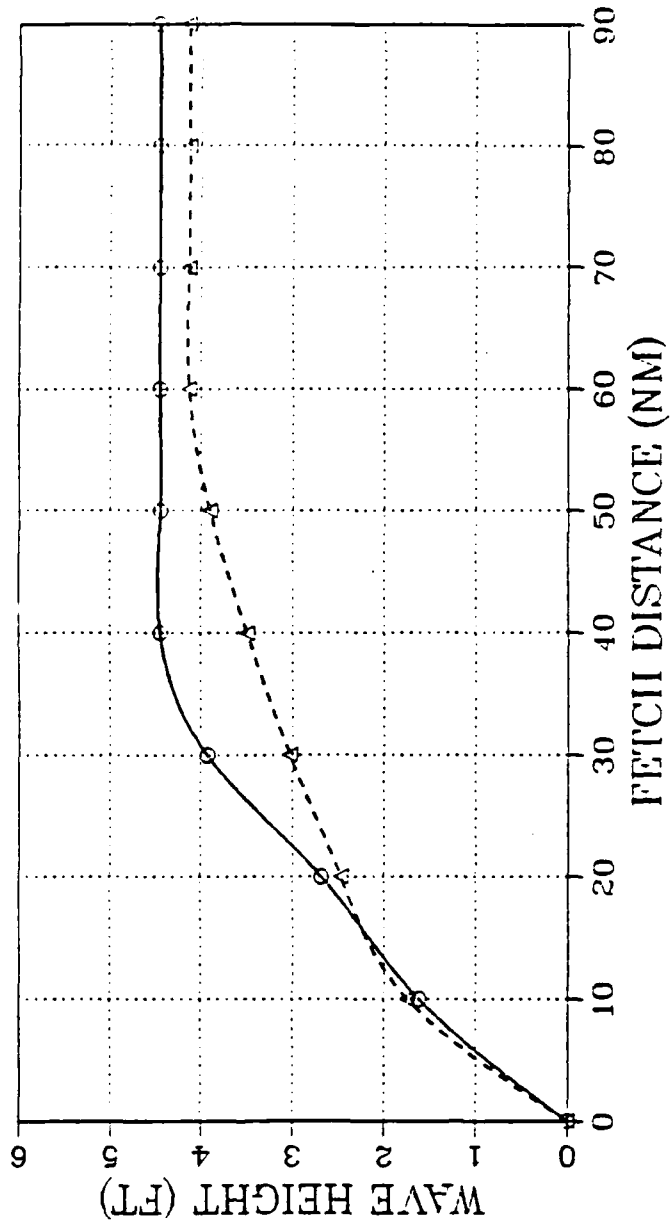


Figure 3.2. Model output (solid) versus JONSWAP curve (dashed) for W = 15 kts. For low wind speeds, there is good agreement between JONSWAP and SSSP.

JONSWAP VS SSSP SIGNIFICANT WAVE HEIGHT
 SENSITIVITY TEST $R = 0.1$ AND 0.5 $W = 30$ KTS

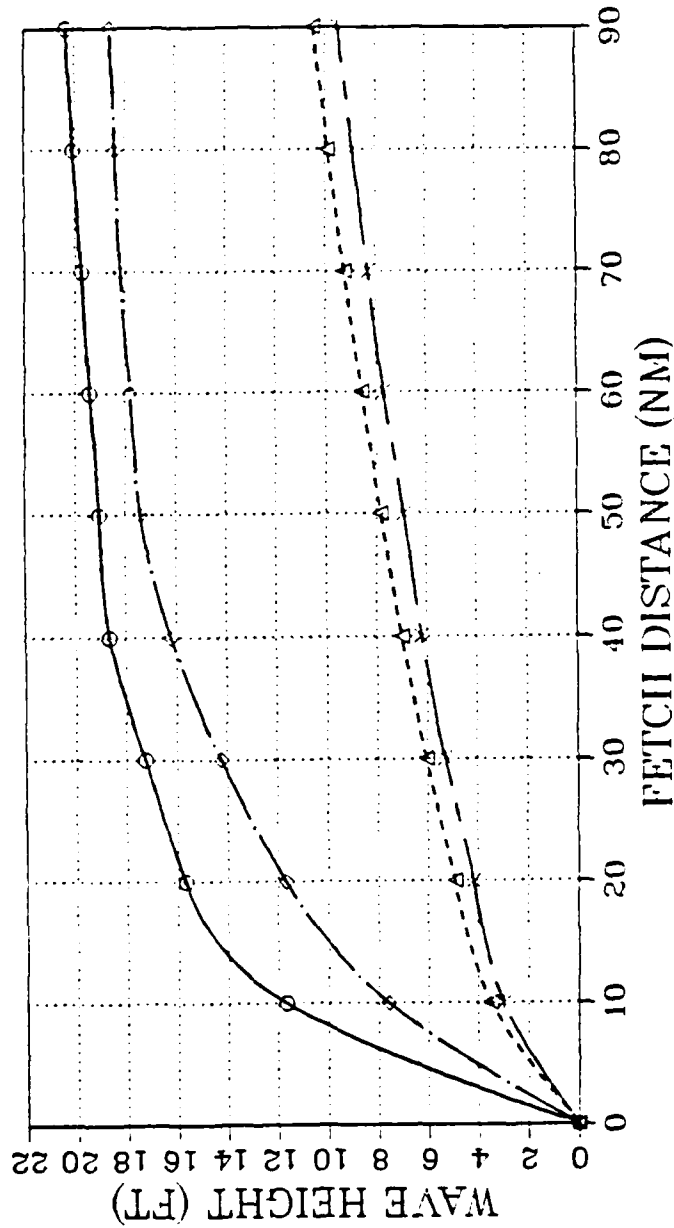


Figure 3.3. Sensitivity test; $R = 0.5$ (chain-dot) and 0.1 (chain-dash) for $W = 30$ kts. R is a weighting term which is set equal to 1.0 in the original SSSP model. The unchanged SSSP model (solid) and JONSWAP (dashed) are also shown.

JONSWAP VS SSSP SIGNIFICANT WAVE HEIGHT
 SENSITIVITY TEST $R = 0.1$ $W = 15$ KTS

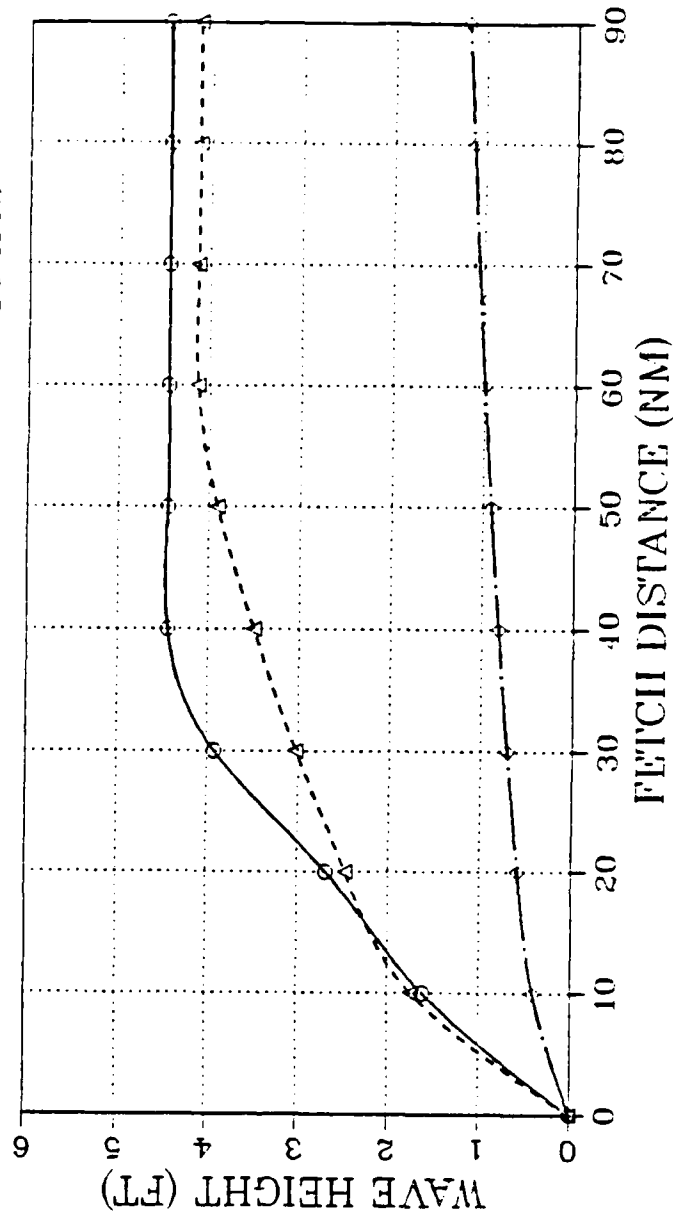


Figure 3.4. Sensitivity test; $R = 0.1$ (chain-dot) for $W = 15$ kts. Since each is multiplied by R , a reduced R value will decrease the low wind speed case as well as the high. The unchanged SSSP model (solid) and JONSWAP (dashed) are also shown.

Because the model's rapid growth appears to occur in the linear region of the growth curve, the Phillips linear term, A, was analyzed closely to see if a simple constant multiple would bring the wave growth in line with the JONSWAP curves. A constant multiple of 0.125 is applied to the A term (Fig. 3.6). This method gives a better fit to the JONSWAP curve for high wind speeds, although the SSSP still over builds the wave heights. To test this multiple at lower wind speeds, a model run was made for a wind speed of 15 knots, for a bandwidth of 0.05 Hz and frequencies of 0.05, 0.10, 0.15, and 0.20. The results of the model run are compared with the equivalent JONSWAP curve and the curve from the existing model (Fig. 3.7). The fit, while not exact, is reasonable, suggesting that the A term is responsible for the overbuilding of the model wave heights.

The actual cause of the overbuilding of wind waves by the SSSP is unknown. Several ad hoc "fixes" to the model are suggested with the recommendation that further research on this problem be conducted. A simple constant multiple of the linear growth term, on the order of 0.10 to 0.15 is one recommended empirically derived modification to the wind generation calculation. Another possible modification is to have the weighting function, R, decrease as the wind increases, to act as a damper on the over generation. At present, the SSSP wave generation routine remains in its original form. It is felt that the model is adequate for low wind speed generation. Operational planners should be cautioned about the high wind speed generation problems.

B. WAVE REFRACTION MODULE

To test the SSSP model's stability during the wave height prediction in the coastal zone, a sinusoidally varying bottom was explicitly entered using

JONSWAP VS SSSP SIGNIFICANT WAVE HEIGHT
 SENSITIVITY TEST $B = 2B_0$ $W = 30$ KTS

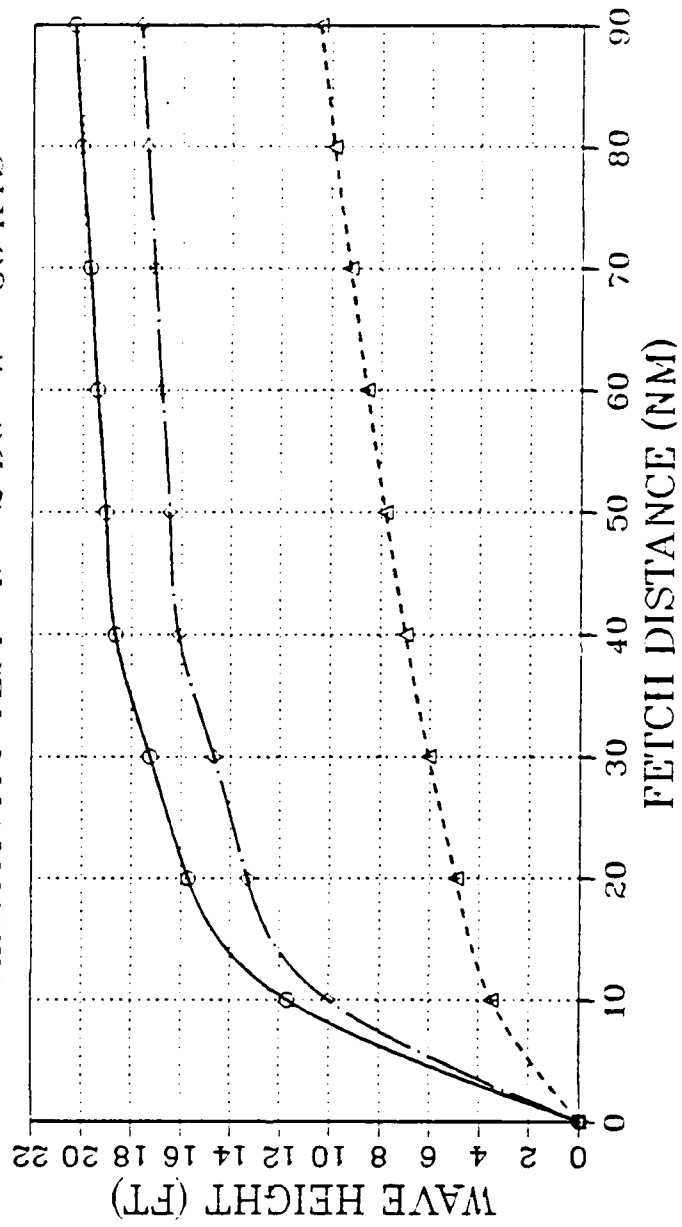


Figure 3.5. Sensitivity test; $B = 2B_0$ for $W = 30$ kts (chain-dot). B is the exponential growth term. Increasing the B value only tends to flatten out the upper part of the curve. The unchanged SSSP model (solid) and JONSWAP (dashed) are also shown.

JONSWAP VS SSSP SIGNIFICANT WAVE HEIGHT
 SENSITIVITY TEST $A = 0.125 A_0$ $W = 30$ KTS

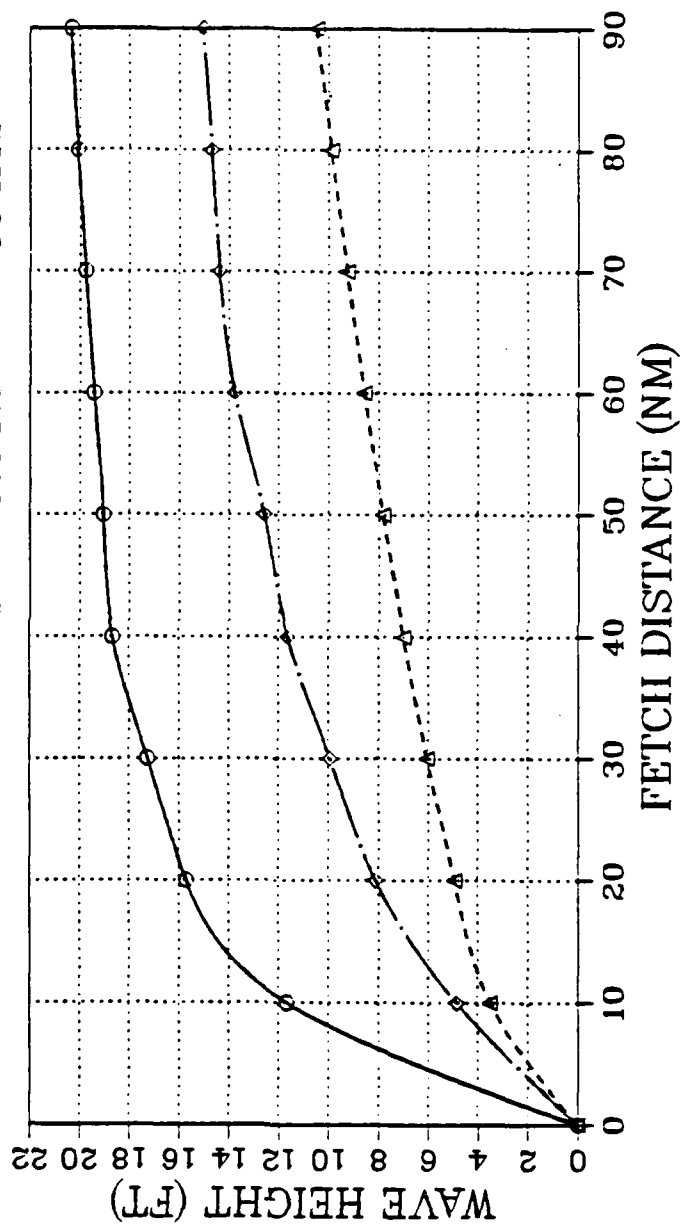


Figure 3.6. Sensitivity test; A term reduced by constant multiple of 0.125 (chain-dot) for $W = 30$ kts. The unchanged SSSP model (solid) and JONSWAP (dashed) are also shown.

JONSWAP VS SSSP SIGNIFICANT WAVE HEIGHT
 SENSITIVITY TEST $A = 0.125 A_0$ $W = 15$ KTS

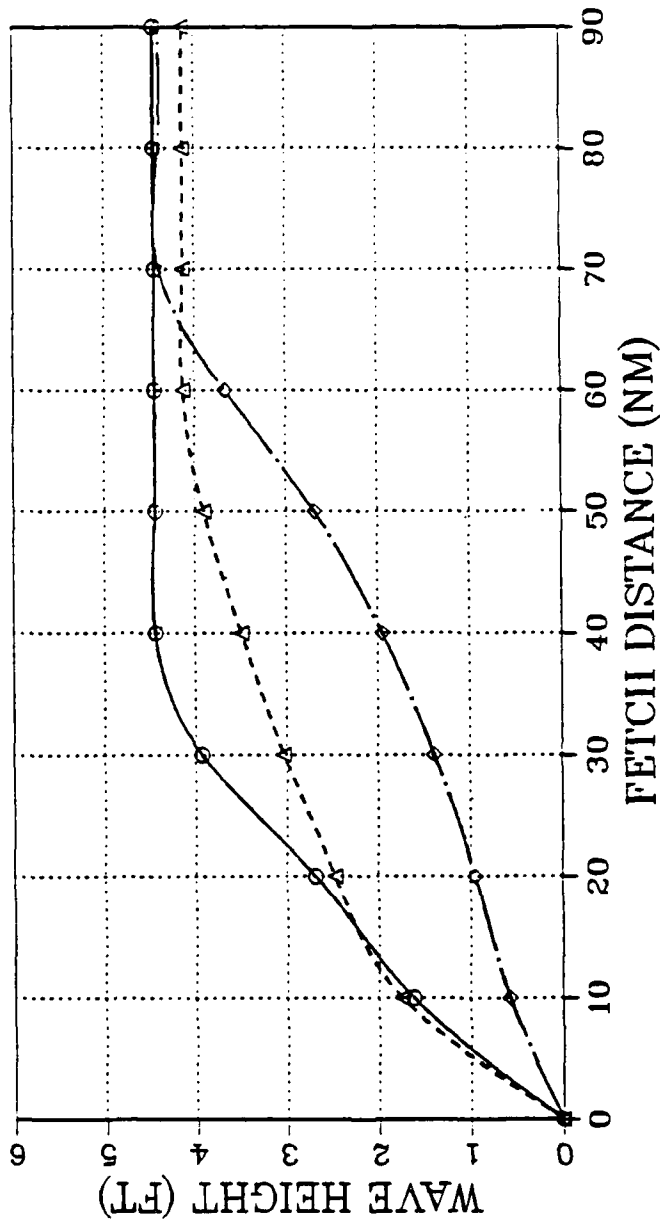


Figure 3.7. Sensitivity test; $A = 0.125 A_0$ (chain-dot) for $W = 15$ kts. The unchanged SSSP model (solid) and JONSWAP (dashed) are also shown.

the following equation:

$$h_{(x,y)} = 0.025X + \epsilon h_b \left(\frac{X}{X_b}\right) \left(1 - \left(\frac{X}{X_b}\right)\right) \cos\left(\frac{2\pi Y}{L_y}\right) \quad (16)$$

where:

ϵ = bottom perturbation term (0.2)

h_b = breaker depth (2.5 m)

X_b = offshore distance to breaker line
(100 m)

L_y = wave length of bottom perturbation (240 m)

This equation provides a smoothly varying bottom profile in both the X (offshore) and Y (longshore) directions. To check that the bottom profile was being accepted correctly by the model, and that the calculated results were reasonable, approximately 25 model runs were completed with varying input parameters. Selected cases are presented herein for discussion. In the cases presented, the offshore waves are normally incident to the shoreline. Obliquely incident model runs were made with Theta ranging from +10 to -10 degrees from normal, for comparison with the normally incident case.

1. Model Experiments

The input parameters in the model are: significant wave height, H_s (1 m); wave period, T (12 s); offshore boundary depth, h (12 m); artificial viscosity, τ (0.0); and bottom perturbation term, ϵ (0.2). The beach faces 270° and the normally incident wave rays come from 270° . This gives a Theta value of 180° according to the model convention shown in Figure 2.7.

The model results for wave heights and directions are shown in Figures 3.8-3.15. The longshore depth profiles for locations inside ($X=3$) and outside ($X=8$) the surf zone are chosen to examine the wave refraction. Grid point $X = 3$ implies a distance of 40 meters offshore, well inside the breaker line, while $X = 8$ is 140 meters offshore and outside the breaker line. The depth profile presented in Figure 3.8 shows that the depth varies sinusoidally in the longshore direction. The beach profile along grid point $Y = 3$ is shown as Figure 3.9. As shown, the depths are slightly deeper than the plane beach inside 100 meters (breaker position), and shallower outside 100 meters.

As waves enter the surf zone, their increase in height is a function of water depth. For the points outside the breakers, the largest waves are expected to occur where the water depth is the shallowest due to shoaling. As can be seen from Figure 3.10, the peak waves (dashed) are towards the edges of the domain, but they do not coincide with the minimum in depths at 0 and 240 meters. This anomaly is a result of the boundary conditions of the model. Also note the asymmetric peaks at 40 and 200 meters. This implies errors in wave height prediction due, in part, to the wave direction calculations. These errors will be addressed later in this discussion.

Wave direction is calculated in terms of Theta. An angle greater than 180 tends to turn the wave ray to the left while Theta less than 180 turns the ray to the right (See arrows in Figure 3.11). The model at least quantitatively predicts the wave refraction pattern correctly for all cases, consistently turning the rays to "attack" the shallower water depths outside the breaker line. The model's boundary conditions force $\theta_1 = \theta_2$ and $\theta_{n-1} = \theta_n$ where θ is the wave direction at the n^{th} long shore grid point. This

LONGSHORE DEPTH PROFILE (EPS = 0.02)

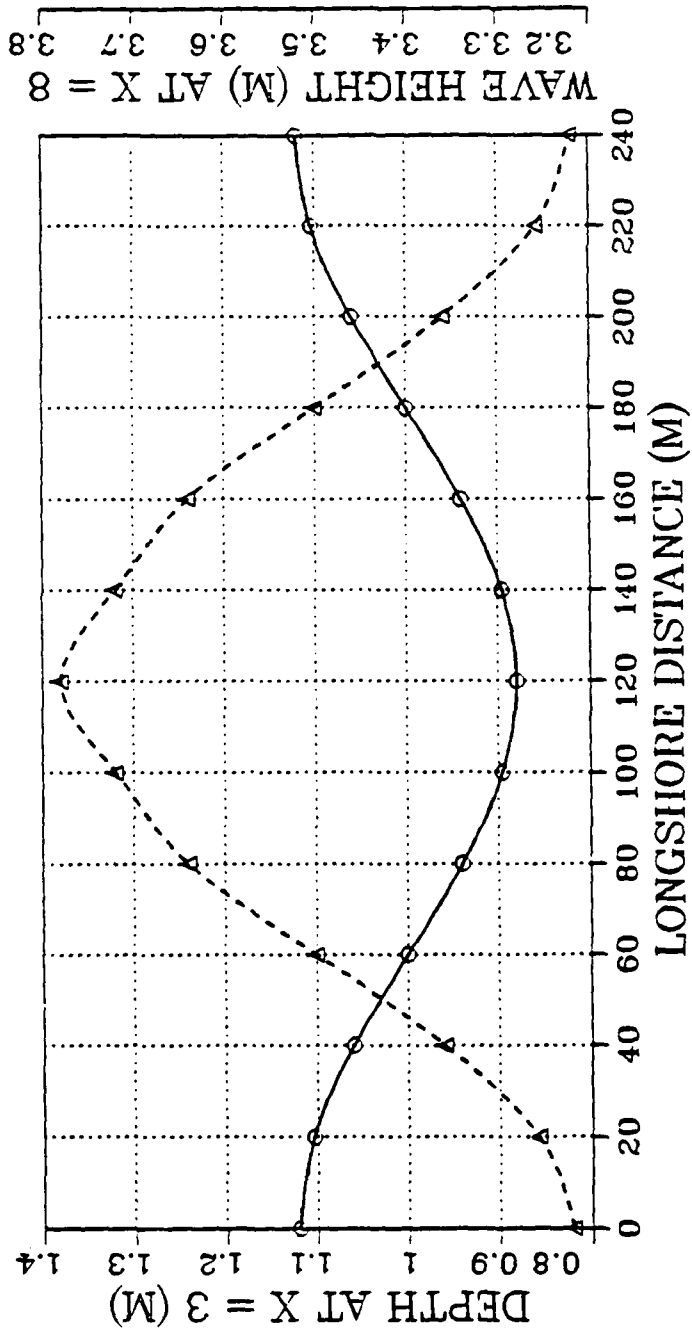


Figure 3.8. Longshore depth profile for $X = 3$ (solid) and $X = 8$ (dashed). The sinusoidally varying bottom profile was used as a depth field for testing the SSSP.

OFFSHORE DEPTH PROFILE (EPS = 0.02)

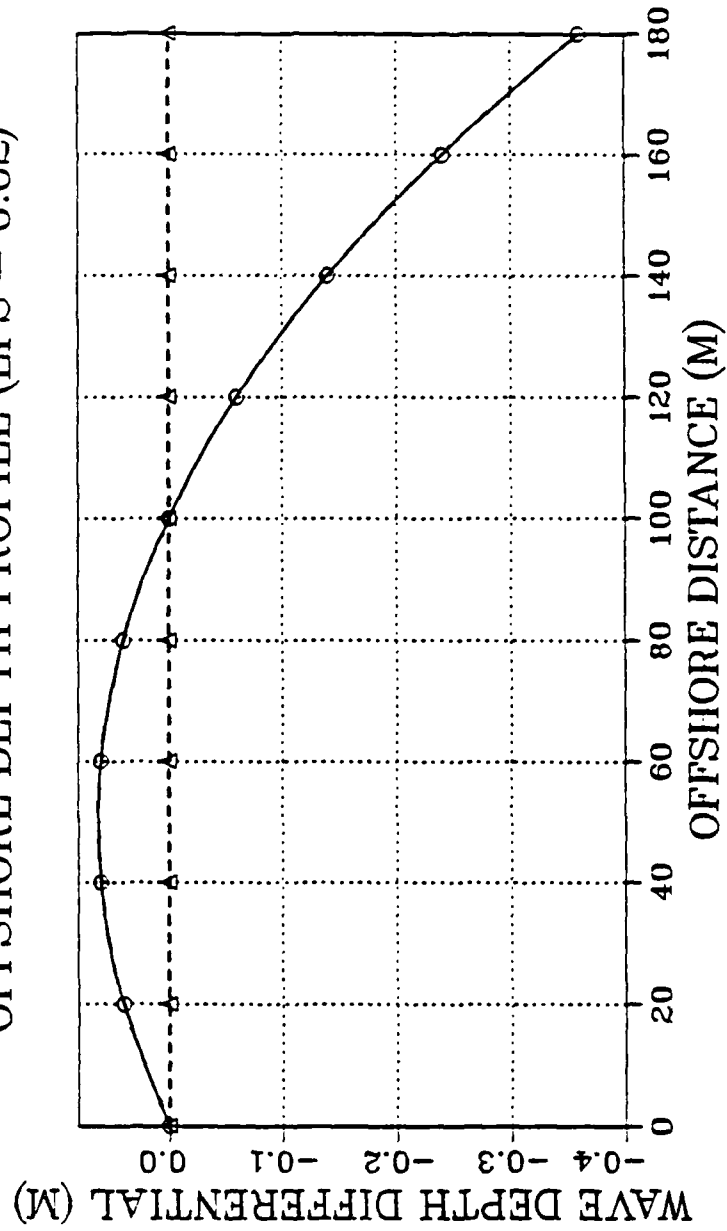


Figure 3.9. Offshore depth profile for $Y = 3$ (solid). Depths are deeper/shallower than a plane beach profile of slope 0.025 (dashed).

WAVE HEIGHT FIELD ($\Theta = 180$)

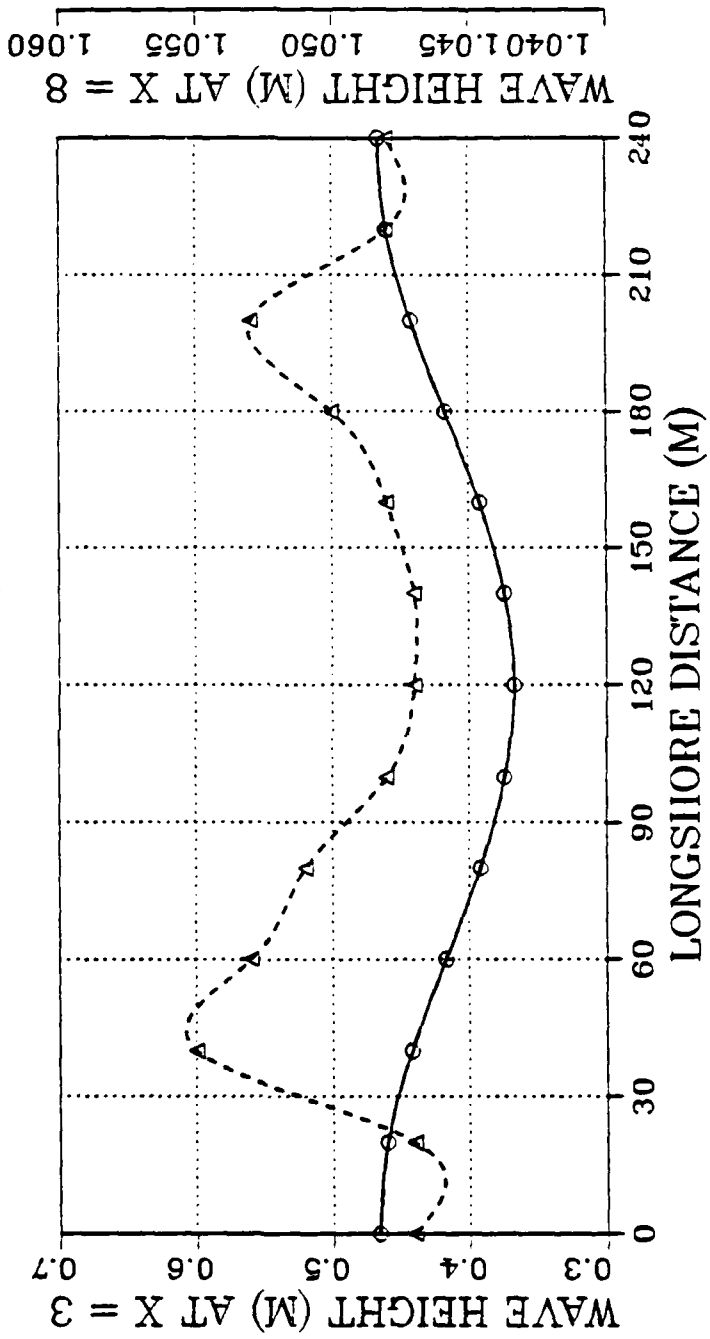


Figure 3.10. Wave heights at $X = 3$ (solid) and $X = 8$ (dashed). Note asymmetric peaks at 40 and 200 meters. Wave heights inside the breaker line are related to the bottom depth only.

WAVE DIRECTION FIELD ($\theta = 180$)

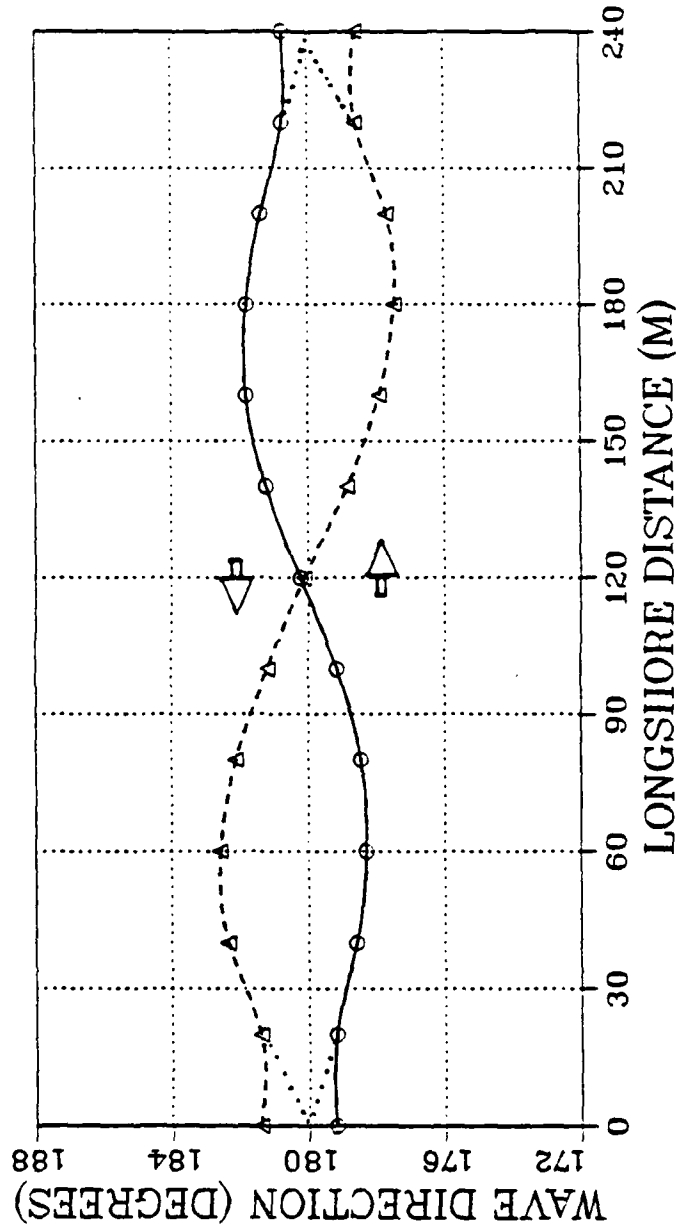


Figure 3.11. Wave Directions at $X = 3$ (solid) and $X = 8$ (dashed). Arrows indicate the directions the wave rays point with respect to a ray normal to the beach. Dotted lines at the boundaries are the expected behavior of the wave rays.

accounts for the departures of the wave direction at the edges of the domain. The dotted lines are the interpretation of how the wave direction patterns should behave. In the middle of the domain, where both cases exhibit a nodal point, the wave direction passes through 180 or normal to the beach as expected.

The final test conducted compared the effect of Tau on the wave direction calculations. Tau is an artificial viscosity parameter which is intended to be a smoothing term for the calculation of wave angle. Changing Tau from 0.00 to 0.25 had a negligible effect on the wave height calculations, but the difference in direction increased with decreasing distance from shore. The case where $X = 8$ is plotted in Figure 3.12. The introduction of the Tau term (dashed) decreases the magnitude of the wave angle, but the maximum (minimum) values are not exactly in phase with the Tau = 0.00 case. The maximums are shifted slightly toward the edges of the domain. This is the expected behavior of the smoothing term.

The dissipative model exhibits unexplained behavior inside the breaker line as depicted by Figures 3.13 - 3.15. At $X = 5$ (Fig. 3.13), the Tau model reduces the magnitude of the wave direction field. At $X = 4$ (Fig. 3.14), spurious asymmetry appears in the direction calculations with the Tau term applied. Furthermore, at $X = 3$ (Fig. 3.15), the effect of Tau is to increase the magnitude of the wave direction. This apparent angular deviation has no effect on the model's wave height calculations because, inside the breaker line, wave height becomes a function of depth only. However, this instability does effect the longshore current calculations, which are sensitive to local wave direction inside the surf zone.

WAVE DIRECTION FIELD ($\theta = 180$)
 $\tau = 0.0$ AND 0.25 AT $X = 8$

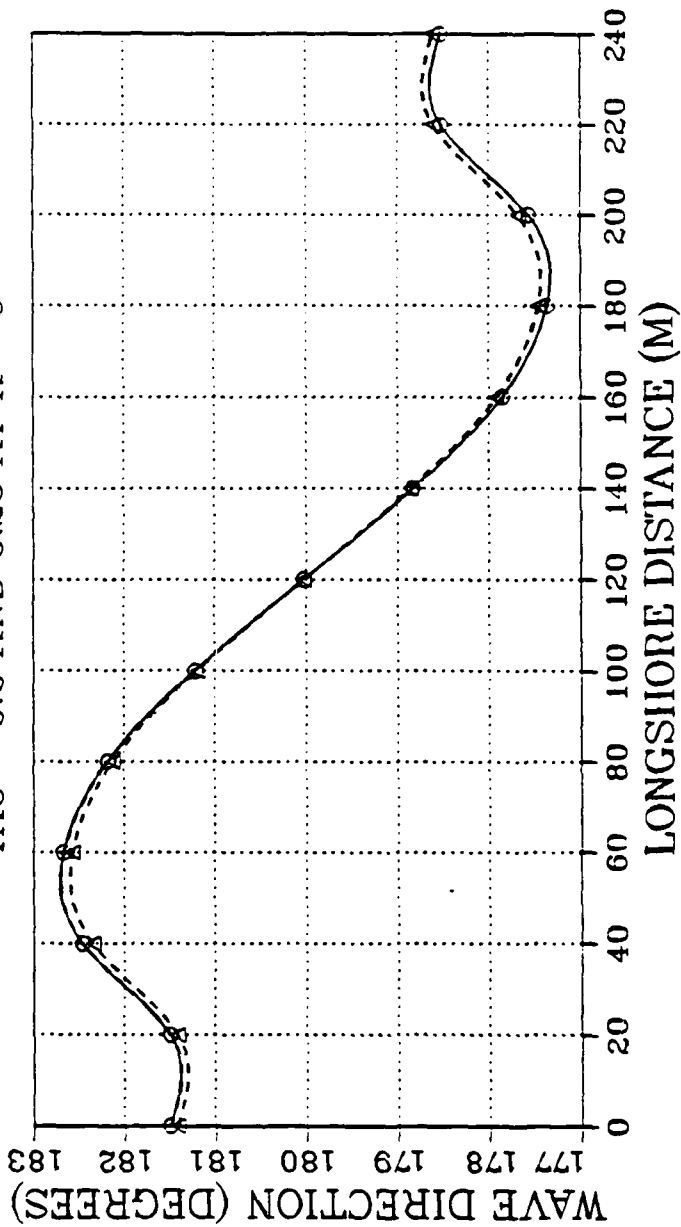


Figure 3.12. Wave Directions at $X = 8$ for $\tau = 0.0$ (solid) and 0.25 (dashed). The condition that $\theta = 180$ is a function of the original boundary conditions.

WAVE DIRECTION FIELD ($\theta_{\text{IETA}} = 180$)
 $\tau = 0.0$ AND 0.25 AT $X = 5$

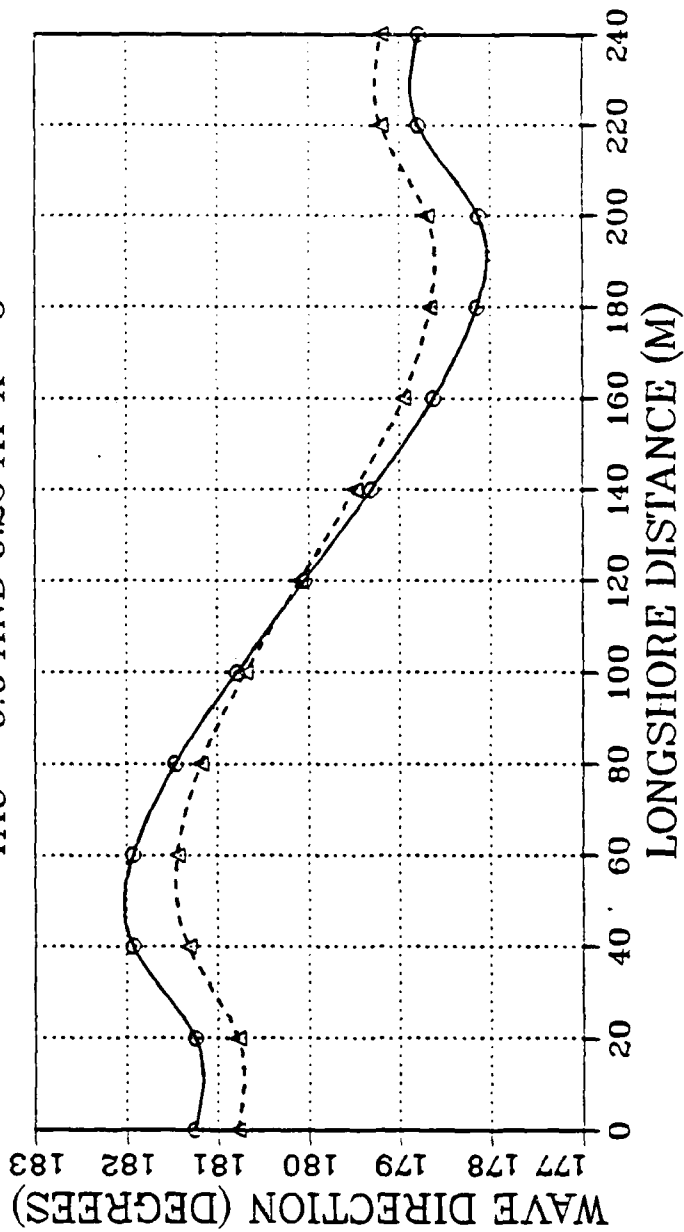


Figure 3.13. Wave Directions at $X = 5$ for $\tau = 0.0$ (solid) and 0.25 (dashed). The expected modifying behavior of τ is exhibited.

WAVE DIRECTION FIELD ($\eta = 180$)
 $\tau = 0.0$ AND 0.25 AT $X = 4$

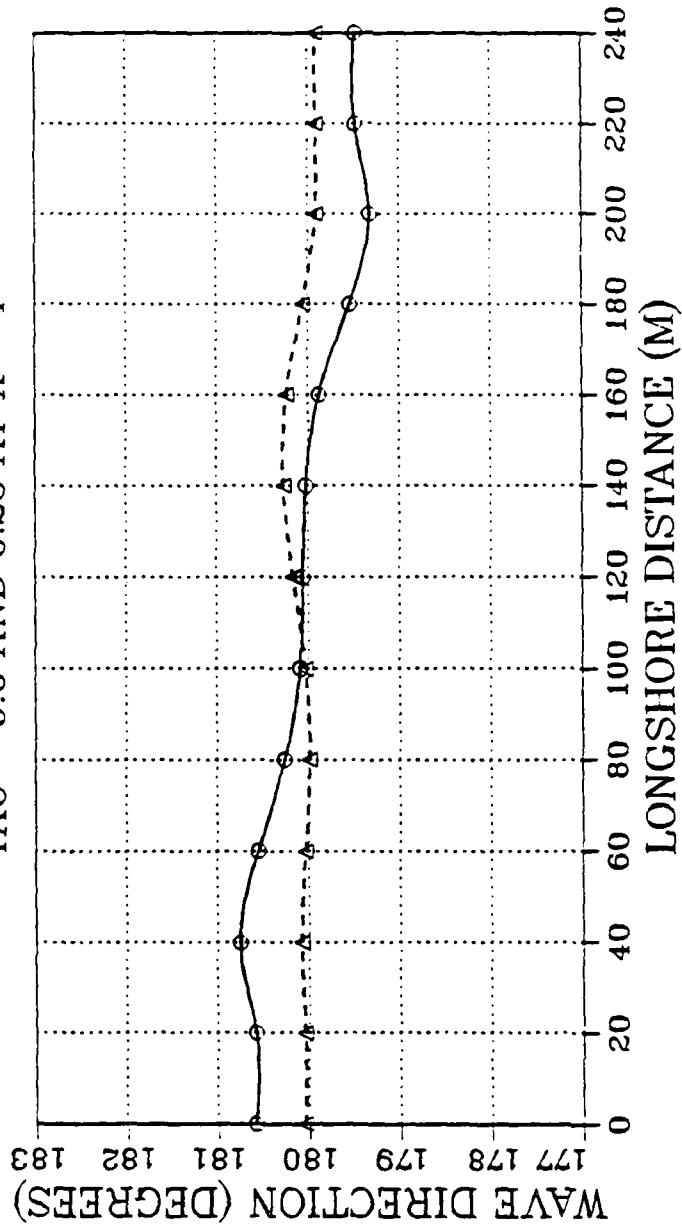


Figure 3.14. Wave Directions at $X = 4$ for $\tau = 0.0$ (solid) and 0.25 (dashed). As the wave approaches the shoreline, the τ modification shows irregular behavior.

WAVE DIRECTION FIELD ($\eta = 180$)
 $\tau = 0.0$ AND 0.25 AT $X = 3$

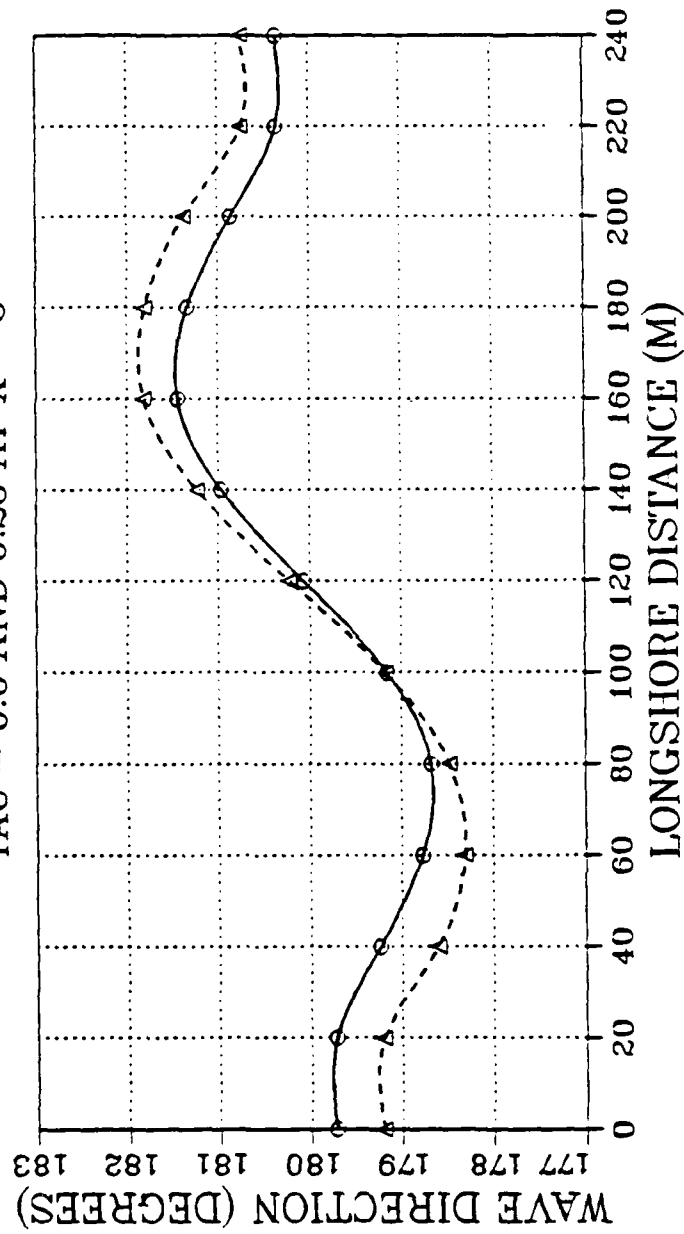


Figure 3.15. Wave Directions at $X = 3$ for $\tau = 0.0$ (solid) and 0.25 (dashed). Contrary to its intent, close to the shoreline, τ actually increases the magnitude of the wave direction.

Another indication of a numeric error in the wave direction calculation was noted in the exact center ($Y = 7$) of the domain. Since the depth profiles exhibit a maximum (minimum) value at the domain center, theory suggests that the waves remain normally incident at these nodal points. Therefore, the Theta value should be 180 degrees at the center of the domain. The model output, both with and without Tau, exhibits a monotonically increasing error as seen in Figure 3.16.

2. Improvement of the Numerical Scheme

In an effort to eliminate the numerical instability in the wave direction module, the finite differencing scheme was analyzed to see if an improvement could be made. The original scheme, pictured in Figure 2.6, uses a simple centered and forward differencing method and is fairly robust in the longshore (Y) direction but is less so in the offshore (X) direction. To increase the accuracy of the numerical scheme, the method pictured in Figure 3.17 was substituted in the DIRECT subroutine for the original scheme. This particular method is a well accepted technique which has proven to be stable and free of damping (Haltiner and Williams, 1980).

Several model runs were made to test the new technique. Using the standard input parameters and setting Tau equal to 0, the first result was a gain in accuracy of the wave direction calculations. The domain's central directions were exactly 180° (to three significant figures), as seen in Figure 3.18, and the refraction angles were symmetric about the center of the domain as expected due to the symmetrically varying bathymetry (Figure 3.19).

A second result of the implementation of the improved numerical technique is the stabilizing effect on the wave height calculations. The

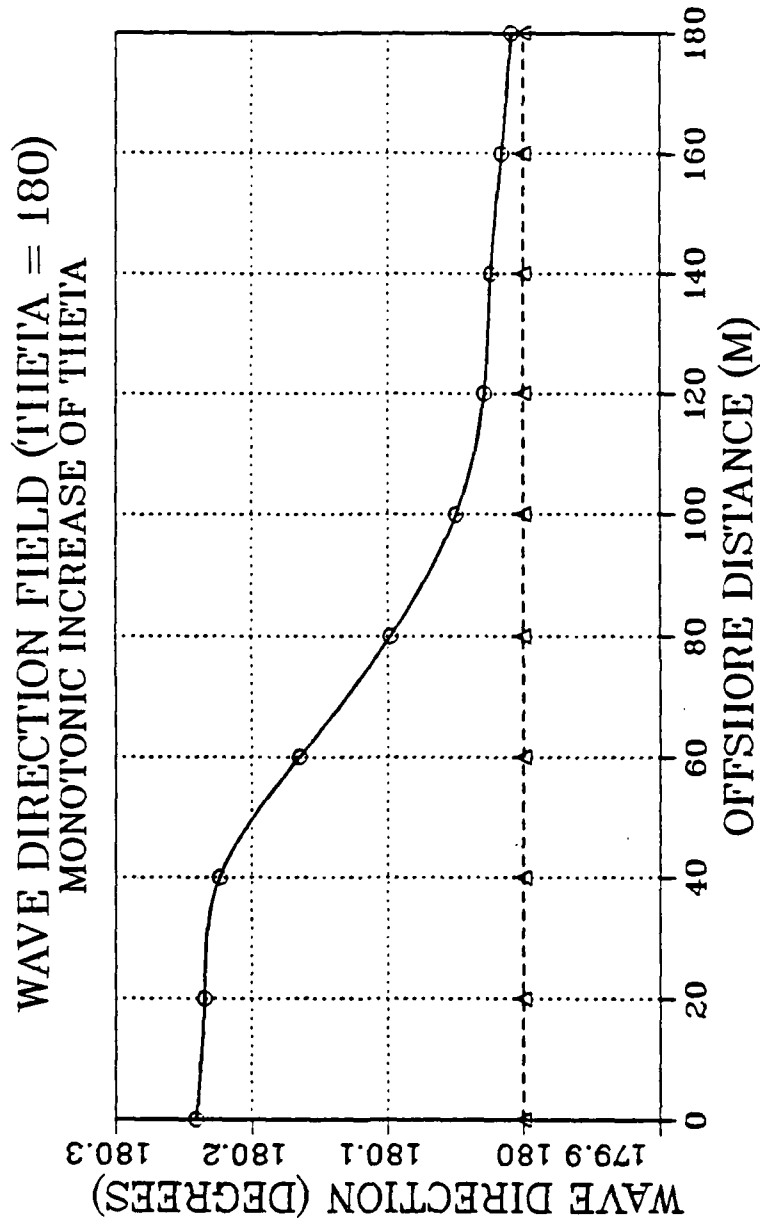


Figure 3.16. Monotonic increase of Theta (solid) versus the expected value of 180° at beach center.

OLD SCHEME

$$F2a = K_{i,j+1} \cos \theta_{i,j+1}$$

$$F2b = K_{i,j-1} \cos \theta_{i,j-1}$$

$$F2 = \frac{Dx}{2 Dy (F2a - F2b)}$$

NEW SCHEME

$$F2a = (K_{i,j+1} \cos \theta_{i,j+1}) + (K_{i+1,j+1} \cos \theta_{i+1,j+1})$$

$$F2b = (K_{i,j-1} \cos \theta_{i,j-1}) + (K_{i+1,j-1} \cos \theta_{i+1,j-1})$$

$$F2 = \frac{0.5 Dx}{2 Dy (F2a - F2b)}$$

where: F2 = difference form for the on-offshore direction

K = wave number at the i,jth grid point

θ = wave direction at the i,jth grid point

Figure 3.17. A more robust differencing scheme was substituted for the original numeric scheme seen in Figure 2.6.

WAVE DIRECTION FIELD ($\theta = 180$)
 DIFFERENCE BETWEEN θ AND 180 DEGREES

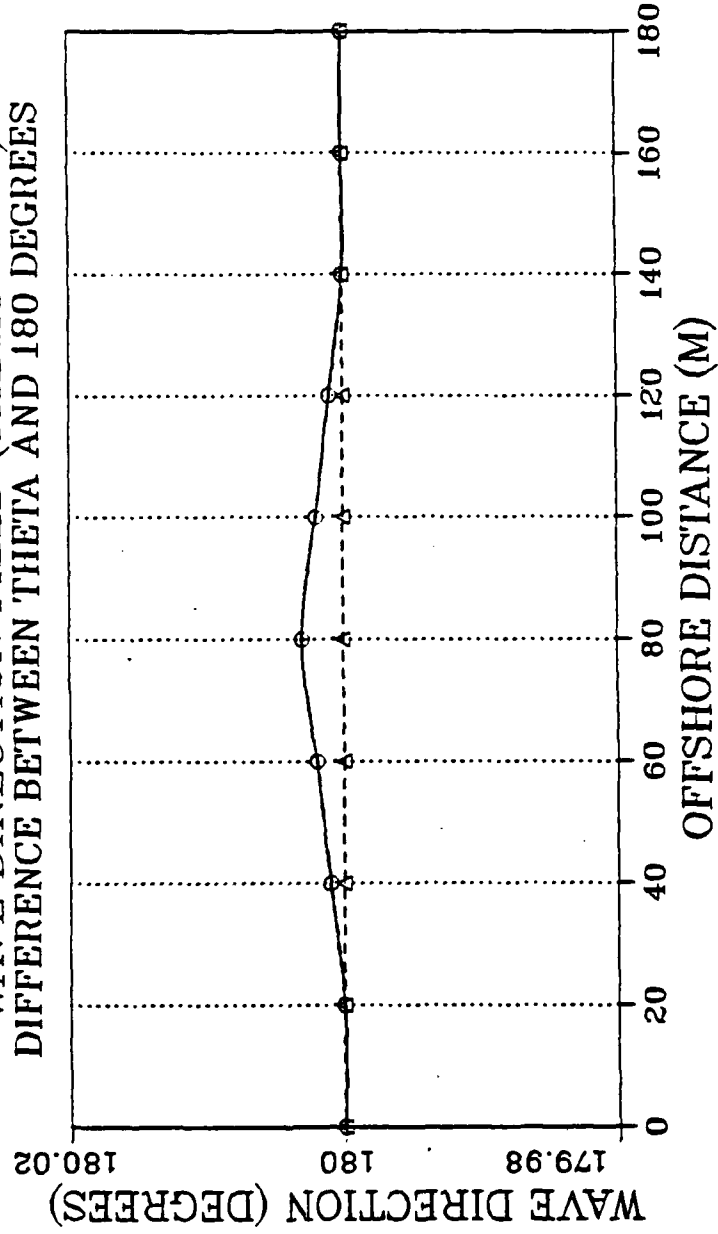


Figure 3.18. Increased stability in Theta calculations resulting from the new numeric scheme (compare with Figure 24). The expected value of 180.000 is achieved with the new scheme.

WAVE DIRECTION FIELD (THETA = 180)

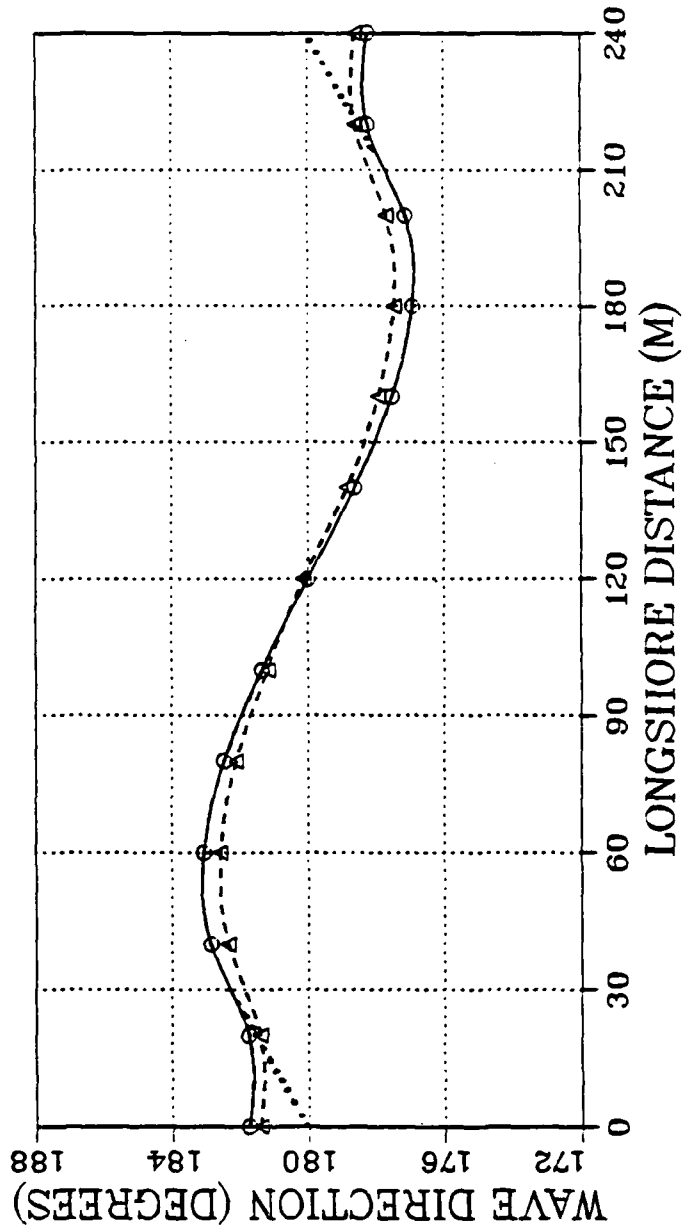


Figure 3.19. Wave Directions for $\tau = 0.0$ at $X = 8$ (solid) using the new numeric scheme compared with the old scheme (dashed). Dotted lines show expected behavior at the boundaries.

previous asymmetric wave heights are now symmetric with respect to height and peak location (Fig. 3.20).

3. Boundary Conditions

The SSSP model imposes no flux boundary conditions on the refraction and wave height calculations so that the left and right boundaries are specified as follows:

$$Q(M,1) = Q(M,2)$$

$$Q(M,N) = Q(M,N-1)$$

where: Q = the quantity being calculated

M = offshore row number (10 to 1)

N = the last longshore column (13)

The offshore row is completely specified by the initial conditions. The calculations then proceed from offshore to onshore and from left to right on the grid.

No flux boundary conditions account for the unusual behavior of the wave height and direction curves at the edges of the domain. To satisfy the condition of well-posedness for the applied model, cyclic boundary conditions are substituted such that:

$$Q(M,1) = Q(M,N-1) \quad (17)$$

$$Q(M,N) = Q(M,2)$$

A plot of wave height versus longshore distance at $X = 8$ using the same inputs as the previous case is presented in Figure 3.21. Note the shift of the peaks toward the edges of the domain as well as the abrupt increase in the magnitude of the wave height. These numerical results now match quite well with theory which requires that the wave rays turn toward the

shallowest water, implying that the largest wave heights should occur at the edges of the domain.

The wave direction calculations also show improvement. Close agreement between the cyclic boundary condition values and the expected values (dotted) is shown in Figure 3.22. Additionally, the average value on the boundary segment agrees closely with the exact value (solid circles).

4. Results

Based on the results of many model experiments, the new model appears to offer an increase in stability and computational accuracy. The improved wave direction subroutine consistently turns the wave rays in the correct direction. The magnitude of the direction changes is qualitatively correct. The wave height subroutine works well both inside and outside the surf zone. Wave heights are highest at the shoal and lowest at the trench.

One drawback to the original wave height subroutine is the computational speed. When running the program to generate an energy spectrum for sea and swell, the model takes approximately 45 minutes per frequency band. Even the monochromatic surf module is slow (4.5 - 5 minutes) because of the number of iterations required to converge to the preassigned criterion.

Least acceptable of all is the Nearshore Circulation module which proved to be unstable as well as requiring as much as 23 hours to asymptotically approach an answer. To provide fast, accurate longshore current information, a one dimensional model is substituted for the two dimensional circulation model. While some potential rip current information will not be provided by this simple model, the one dimensional model has the

WAVE HEIGHT FIELD ($\theta = 180$)

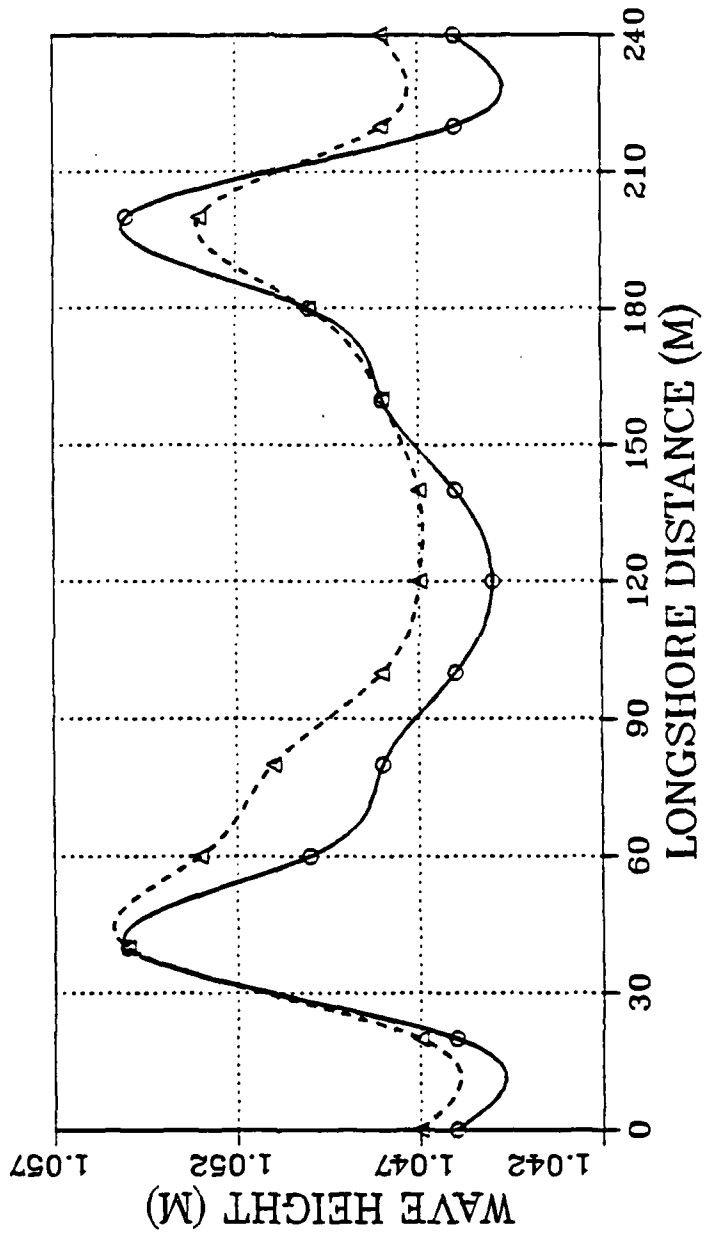


Figure 3.20. Wave heights at $X = 8$ using new numeric scheme (solid). Note expected wave height symmetry compared to original heights (dashed).

WAVE HEIGHT FIELD ($\Theta = 130$)

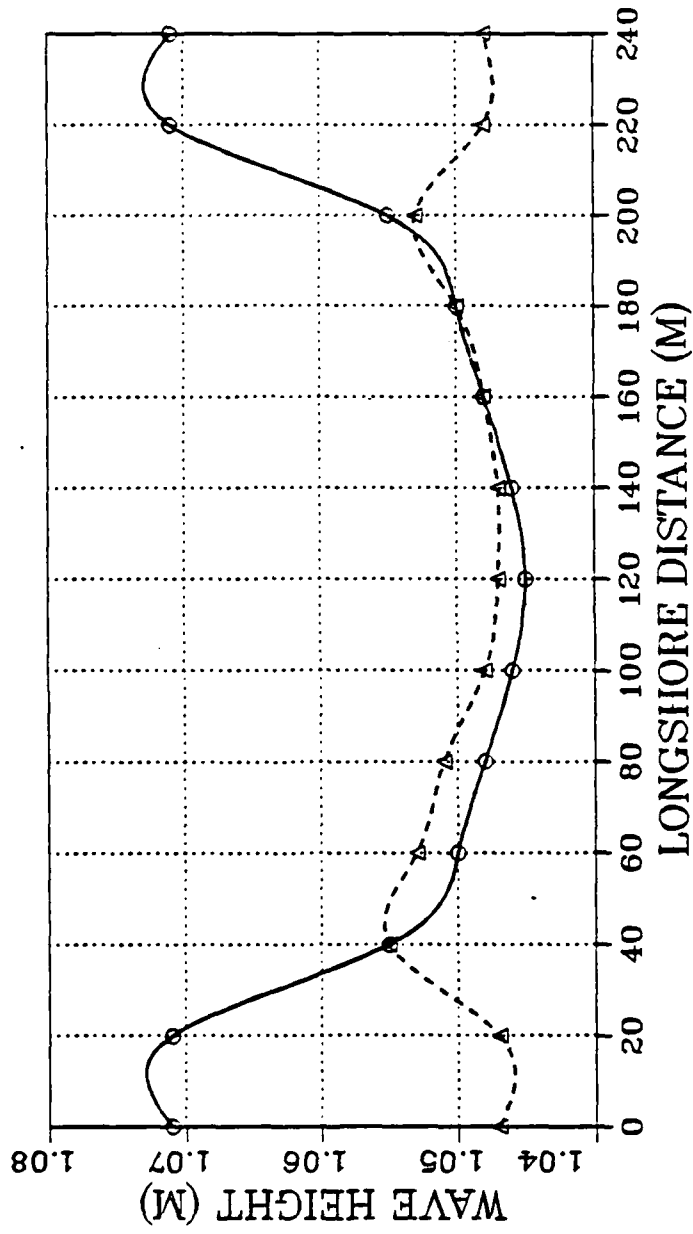


Figure 3.21. Wave heights at $X = 8$ with cyclic boundary conditions imposed (solid) compared with the wave height field using the old boundary conditions (dashed). The wave peaks have shifted to the edges of the domain as suggested by theory.

WAVE DIRECTION FIELD ($\theta = 180$)

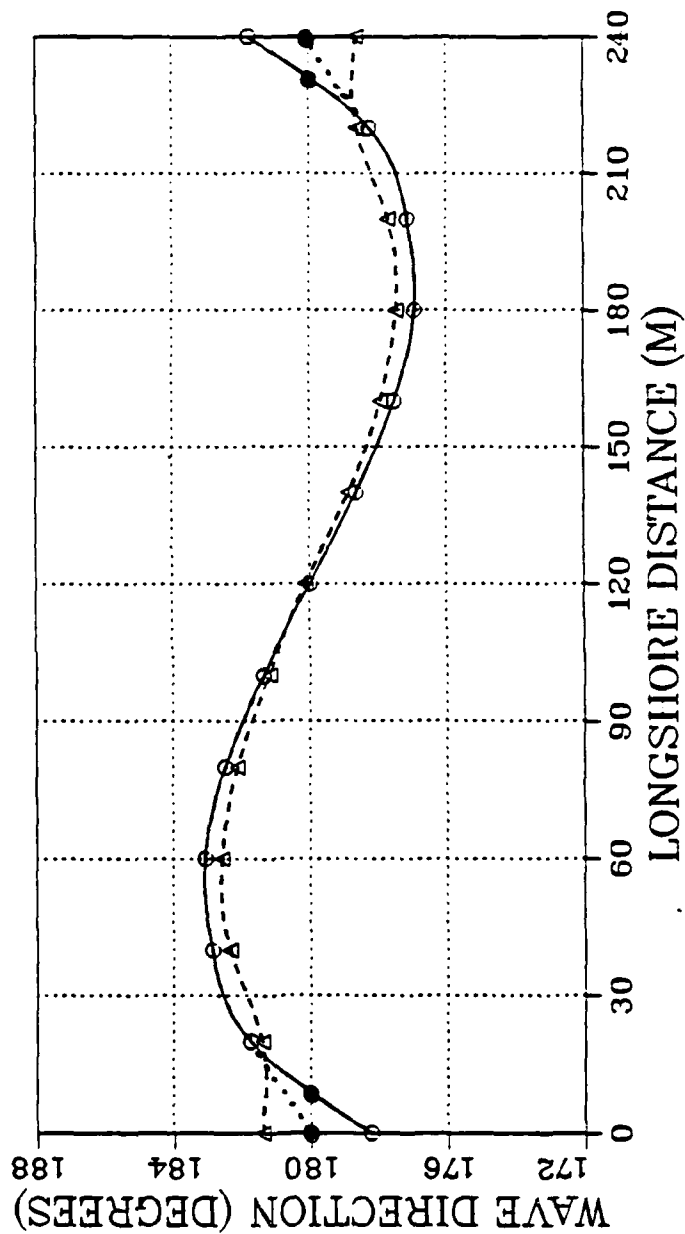


Figure 3.22. Wave Directions at $X = 8$ with cyclic boundary conditions imposed (solid) compared with original direction calculations (dashed). Note close agreement with expected behavior (dotted).

advantage of being fast, accurate and able to provide the most important input, the longshore current distribution.

A state of the art, one-dimensional wave height model is used as input to the longshore current model. The new wave height and longshore current subroutines are described below.

C. ONE DIMENSIONAL WAVE HEIGHT CALCULATION

To increase the SSSP's computational efficiency while maintaining reasonable accuracy, a one dimensional random wave height model was substituted for the original two dimensional monochromatic model. This model characterizes the transformation of the wave height probability density function (pdf) from offshore to the shoreline (Thornton and Guza, 1983). The model assumes that the waves are narrow banded in frequency and direction such that the waves are specified by a single mean frequency \bar{f} and mean direction $\bar{\theta}$, that the bottom contours are straight and parallel, and that the wave conditions are stationary. This probabilistic approach to the wave breaking problem was originally suggested by Collins (1970) and Battjes (1972). The form that is used here is based on integrating the energy flux balance equation. The calculated wave heights are a function of the shoaling conditions of the integral path from offshore to the shoreline (Battjes and Janssen, 1978).

For straight and parallel contours, the energy flux is balanced by wave breaking and the frictional dissipation:

$$\frac{\partial (E C_g \cos \theta)}{\partial X} = \langle \epsilon_b \rangle + \langle \epsilon_f \rangle \quad (18)$$

where:

$\langle \epsilon_b \rangle$ = dissipation due to wave breaking

$\langle \epsilon_f \rangle$ = frictional dissipation

In the domain of interest, it has been shown that the frictional dissipation is less than 3% of the dissipation due to breaking waves (Thornton and Guza, 1983) and will be neglected.

The waves in the new model are described by the Rayleigh wave height distribution:

$$p(H) = \frac{2H}{H_{rms}} e^{-\left(\frac{H}{H_{rms}}\right)^2} \quad (19)$$

where:

H_{rms} = root mean square wave height

where H_{rms} is the root mean square wave height. This distribution takes into account the fact that there is a distribution of wave heights throughout the entire field for a given frequency. Previous random wave models truncated the Rayleigh distribution in various ways. Recent observations have found that even after the waves break, the Rayleigh distribution is still valid (Thornton and Guza, 1983). Therefore, in the improved model, the waves are everywhere Rayleigh distributed. The probability of a wave breaking $p_b(H)$ is described by a simple weighting of the Rayleigh distribution:

$$p_b(H) = W(H) p(H)$$

The weighting function, $W(H)$, which makes larger waves at a given depth more likely to break, is given by (Thornton and Guza, 1983):

$$W(H) = \left[\frac{H_{rms}}{\gamma h} \right]^4 \quad (20)$$

where:

γ = adjustable parameter based on field data

The model assumes that breaking waves are similar to periodic bores (LeMehaute', 1962) as depicted in Figure 3.23. The bore dissipation per unit area is calculated:

$$\epsilon_{bore} = \frac{1}{4} \rho g \frac{(h_2 - h_1)^3}{h_1 h_2} Q \cong \frac{1}{4} \rho g \frac{(BH)^3}{h^2} Q \quad (21)$$

where:

Q = volume discharge across bore

B = breaker coefficient (described from data)

The volume discharge parameter is described for a linear periodic bore (Hwang and Divoky, 1970) by:

$$Q = Ch/L \quad (22)$$

where C is the wave celerity. Using linear wave theory, the wave energy

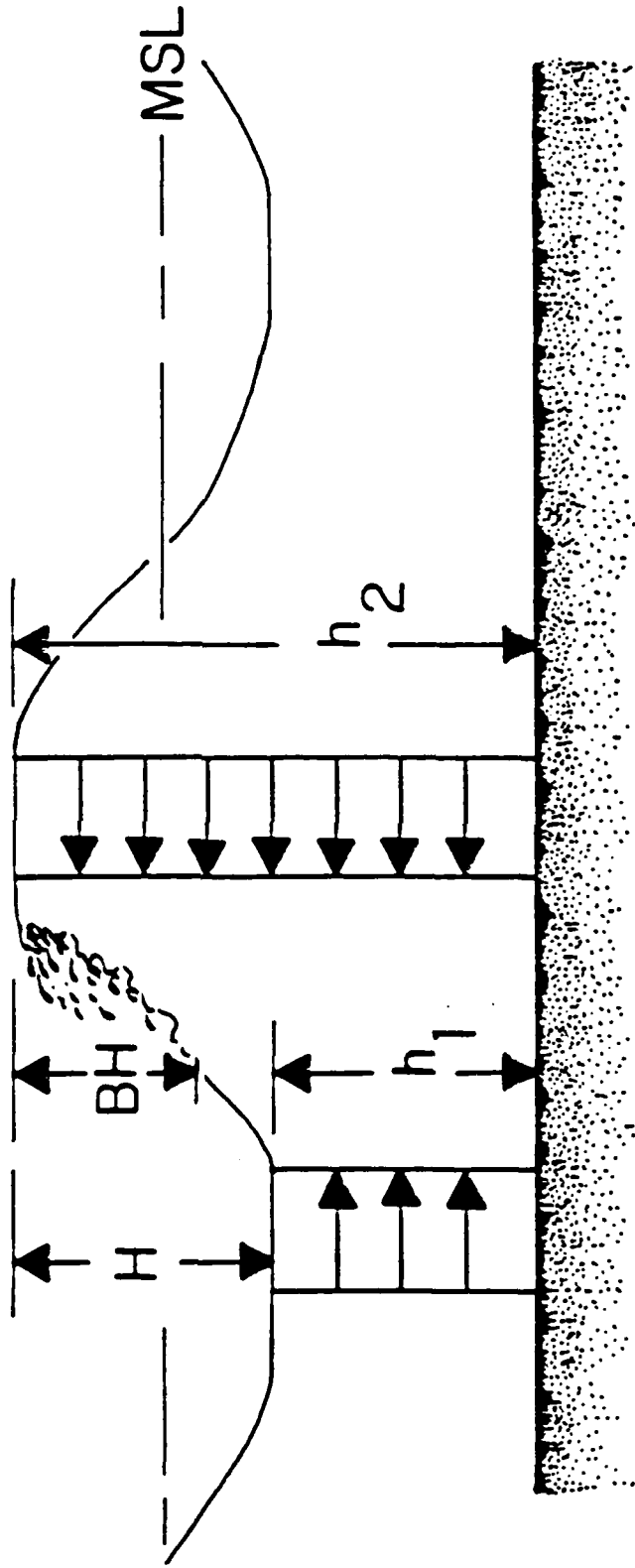


Figure 3.23. Periodic bore used to describe spilling breakers (after Thornton and Guza, 1983). B is the breaker coefficient which describes how much of the wave is breaking at any given time.

and group velocities are given by:

$$E = \rho g \int_0^{\infty} H^2 p(H) dH = \frac{1}{8} \rho g H_{rms}^2 \quad (23)$$

and,

$$C_{gx} = \frac{C}{2} \left[1 + \frac{2kh}{\sinh 2kh} \right] \cos \bar{\theta} \quad (24)$$

After integration and the substitution of the probability density function, Equation 21 leads to:

$$\langle \epsilon_b \rangle = \frac{3}{16} \sqrt{\pi} \rho g \frac{\bar{f} B^3}{\gamma^4 h^5} H_{rms}^7 \quad (25)$$

where:

$$\bar{f} = \text{mean frequency}$$

This equation for the bore dissipation can be tuned to the data by varying the breaker coefficient B, or the adjustable parameter γ . Substituting the bore dissipation function (25), the energy flux equation (23) is given by:

$$\frac{d}{dx} \left(\frac{1}{8} \rho g H_{rms}^2 C_g \cos \bar{\theta} \right) = \frac{3}{16} \sqrt{\pi} \rho g \frac{\bar{f} B^3}{\gamma^4 h^5} H_{rms}^7 \quad (26)$$

For shallow water, the group velocity C_g is approximately equal to the wave celerity C which equals $(gh)^{1/2}$. Equation (26) was chosen to be used in the wave height module because, although a more complicated expression

gave a slightly better fit to the data, Equation (26) provides an analytical solution which allows a detailed study of the model's behavior. The analytical solution is obtained for normally incident waves impinging on a plane sloping beach and is used to compare the accuracy of the numerical model. The analytical solution is solved by integrating (26) for the wave height (Thornton and Guza, 1983):

$$H_{rms} = a^{1/5} h^{9/10} \left[1 - h^{23/4} \left(\frac{1}{h_o^{23/4}} - \frac{a}{y_o^{5/2}} \right) \right]^{-1/5} \quad (27)$$

where:

$$a = \frac{23}{15} \left(\frac{g}{\pi} \right)^{1/2} \frac{\gamma^4 \tan \beta}{B^3 \bar{f}}$$

$$\tan \beta = \text{slope of beach}$$

$$y_o = H_o^2 h_o^{1/2}$$

The numerical model uses a modified Euler integration scheme to integrate the energy flux equation. A weighted predictor/ corrector loop is used to increase accuracy and stability as the water depth becomes shallow. The basic calculation is a forward stepping scheme with a variable grid size:

$$E Cg_x \Big|_2 = E Cg_x \Big|_1 + \frac{1}{2} (\langle \epsilon_b \rangle \Big|_2 + \langle \epsilon_b \rangle \Big|_1) \Delta X \quad (28)$$

Well outside the surf zone the wave height changes are very slight with distance as the bore dissipation is essentially zero, and are relatively insensitive to the grid size. However, once the waves start to break, the bore dissipation increases rapidly, modifying the wave heights. To increase

the resolution, the mesh size decreases by a factor of four when the bore dissipation reaches a value of 0.01. This flag value was arrived at by a series of model tests under different initial conditions.

The model was tested against the analytical solution for a variety of initial values. The initial conditions insured that shallow water criteria were met so that the shallow water approximation of $C_g = (gh)^{1/2}$, rather than the explicit Equation (24), could be used. The first test used a shallow steepness offshore wave ($H_o/L_o = 0.01$) having a height of 1.0 meter normally impinging on a plane beach with a slope of 0.04. The period of the wave was 10 seconds. The numerical and the analytical solutions are compared in Figure 3.24. Agreement is very close through most of the offshore grid points. As the water depth gets very shallow, the step size is again reduced to insure the solution converges for the last few grid points.

For a steep wave case ($H_o/L_o = 0.02$), an incident wave of 2.5 meters was used as the offshore input (Fig. 3.24). The wave period, beach slope and normal incidence all remained the same. The numeric and analytic solutions are again in good agreement, although the numeric solution slightly underpredicts the wave height as it did in the case where H_o equals 1.0 m. It is of interest to note that the high wave steepness case shows no growth in wave height due to shoaling prior to breaking. The wave heights decay monotonically toward the shoreline.

Having satisfactorily compared the model results with the analytic solution, further improvements to the model's computational efficiency were made. Since the model is one dimensional, the depth variations in the longshore direction are averaged out. Sand bars and other longshore features are taken into account but offshore trenches and channels are smoothed out

WAVE HEIGHT FIELD ($\theta = 180$)
 NUMERICAL VS ANALYTICAL SOLUTIONS

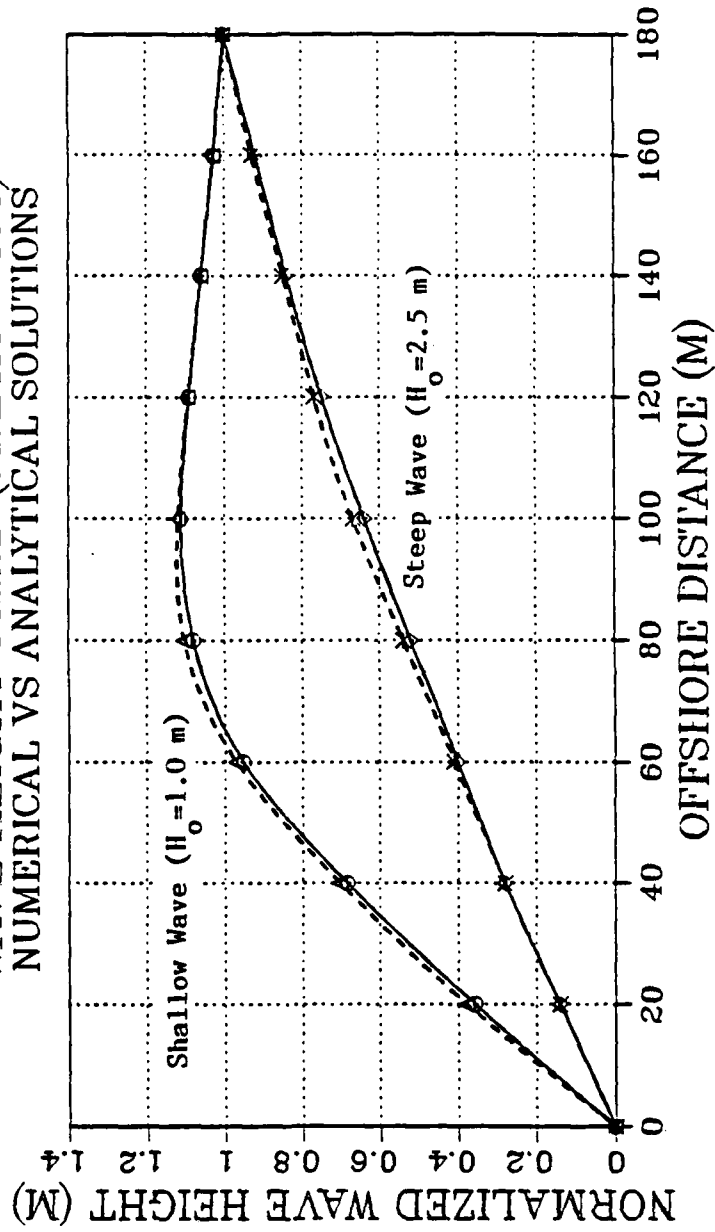


Figure 3.24. Numeric (solid) versus analytic (dashed) wave height solutions for low ($H_0 = 1.0$ meter) and steep ($H_0 = 2.5$ meter) incident wave cases.

by this process. The new height module, with this simplification, runs six times faster than the original module.

The new wave height subroutine has many advantages. It uses a simple but robust probabilistic approach to the wave height problem. It allows variable bathymetry in the offshore direction and obliquely impinging wave fronts. It is fast, accurate, and the governing equations can easily be fine tuned by varying the parameters.

D. LONGSHORE CURRENT CALCULATION

The original longshore current model (Chen and Wang, 1983) used a two dimensional momentum flux balance which was numerically intensive. The model converged very slowly (over 23 hours of CPU time in some cases), and the calculations exhibited unstable behavior (Devendorf, 1985). To provide the necessary longshore current information to an operational planner, a simple one dimensional model was substituted for the original two dimensional subroutine. The model was designed to work with the one dimensional wave height model discussed in the previous section. The random wave probability model is used as input for the longshore current calculations. A narrow banded wave distribution is assumed so that the wave frequencies can be approximated by a mean frequency \bar{f} and direction $\bar{\theta}$. The longshore momentum equation is a balance between the mean wave momentum flux divergence and the longshore component of the bed shear stress (Thornton and Guza, 1985):

$$\frac{\partial S_{yx}}{\partial x} = -\tau_y^b \quad (29)$$

where:

S_{yx} = time and depth averaged covariance
between unsteady velocity components

τ_y^b = bed shear stress in longshore direction

S_{yx} is made up of two terms which are assumed to be statistically independent. The first term is the radiation stress term (\tilde{S}_{yx}) which is the wave induced momentum flux. The second term (S_{yx}') is the depth integrated turbulent Reynold's stress, often parameterized in terms of an eddy viscosity term.

Monochromatic current models require the eddy viscosity term to smooth out the discontinuity in the current field at the breaker line. Since no waves break outside the surf zone in a monochromatic model, there is no current generated. However, there is a jump discontinuity at the breaker line which requires smoothing by the eddy viscosity term. In the random wave model, there is no clearly defined breaker line. Some waves break offshore and, as the beach is approached, more waves break until, in the inner surf zone, almost all waves are breaking (Thornton and Guza, 1985). The smooth transition of energy dissipation reduces the requirement for the eddy viscosity term, which simplifies the velocity calculation.

The radiation shear stress \tilde{S}_{yx} is described by (Longuet-Higgins and Stewart, 1964):

$$\tilde{S}_{yx} = E C_g \cos \bar{\theta} \frac{\sin \bar{\theta}}{C} \quad (30)$$

Snell's law requires that:

$$\frac{\sin \bar{\theta}}{C} = \text{constant} = \frac{\sin \bar{\theta}_o}{C_o} \quad (31)$$

so that when (30) is differentiated the result is:

$$\frac{d}{dX} \bar{S}_{yx} = \frac{\sin \bar{\theta}_o}{C_o} \frac{d}{dX} (E C_g \cos \bar{\theta}) = \frac{\sin \bar{\theta}_b}{C_o} \langle \epsilon_b \rangle \quad (32)$$

This implies that the shear stress is balanced by the bore dissipation for breaking waves on a straight and parallel beach.

The bed shear stress is given as:

$$\tau_y^b = \rho C_f \overline{|\vec{U}|} V \quad (33)$$

where:

$|\vec{U}|$ = instantaneous total bottom velocity

V = longshore current velocity

The bed stress is linearized by assuming small angles of wave incidence and weak longshore currents (Thornton, 1970; Longuet-Higgins, 1970):

$$\tau_y^b = \rho C_f \overline{|\vec{U}|} V \quad (34)$$

Using shallow water wave theory, the bottom velocity is computed by:

$$\overline{|\vec{U}|} = \frac{1}{2} \left(\frac{g}{h}\right)^{1/2} \left[\frac{\sqrt{\pi}}{2} H_{rms}\right]^2 \frac{2}{\pi} \quad (35)$$

Making the appropriate substitutions into the longshore momentum relation and solving for V:

$$V = \frac{3}{4} \frac{B^3 \bar{f} g^{1/2}}{C_f \gamma^4} \frac{\sin \bar{\theta}}{C_o} \frac{H_{rms}^6}{h^{9/2}} \quad (36)$$

The numerical scheme is compared to the analytical solution, which is obtained by simply substituting the expression for H_{rms} (Equation 27) into the velocity calculation (Equation 36). The numerical and the analytical solutions for the shallow and steep wave cases studied above are compared in Figures 3.25 and 3.26. The numerical solution of V slightly underpredicts the current velocity compared with the analytic solution. This is due in part to the introduction of a small error in H_{rms} which was discussed in the previous section. The value of H_{rms} is raised to the sixth power in Equation (36) which means that V may be sensitive to small errors in H_{rms} . However, the magnitude of the error for V is on the order of 0.05 and 0.07 m/sec which may be neglected.

The initial runs of the updated wave height and longshore current subroutines are presented and the reworked SURFCON module is discussed in the next section.

E. IMPROVEMENTS TO THE SURFCON MODULE

During the reprogramming effort, a major consideration was maintaining the integrity of the original model, while incorporating modular improvements. The new height, direction and current subroutines were coded under new names, leaving the old subroutines intact. To maintain consistency, the control module, SURFCON, was renamed OLDSURFCON and a new module, NEWSURFCON, was written to make use of the new

WAVE CURRENT FIELD ($\theta = 170$)
 NUMERICAL VS ANALYTICAL SOLUTIONS

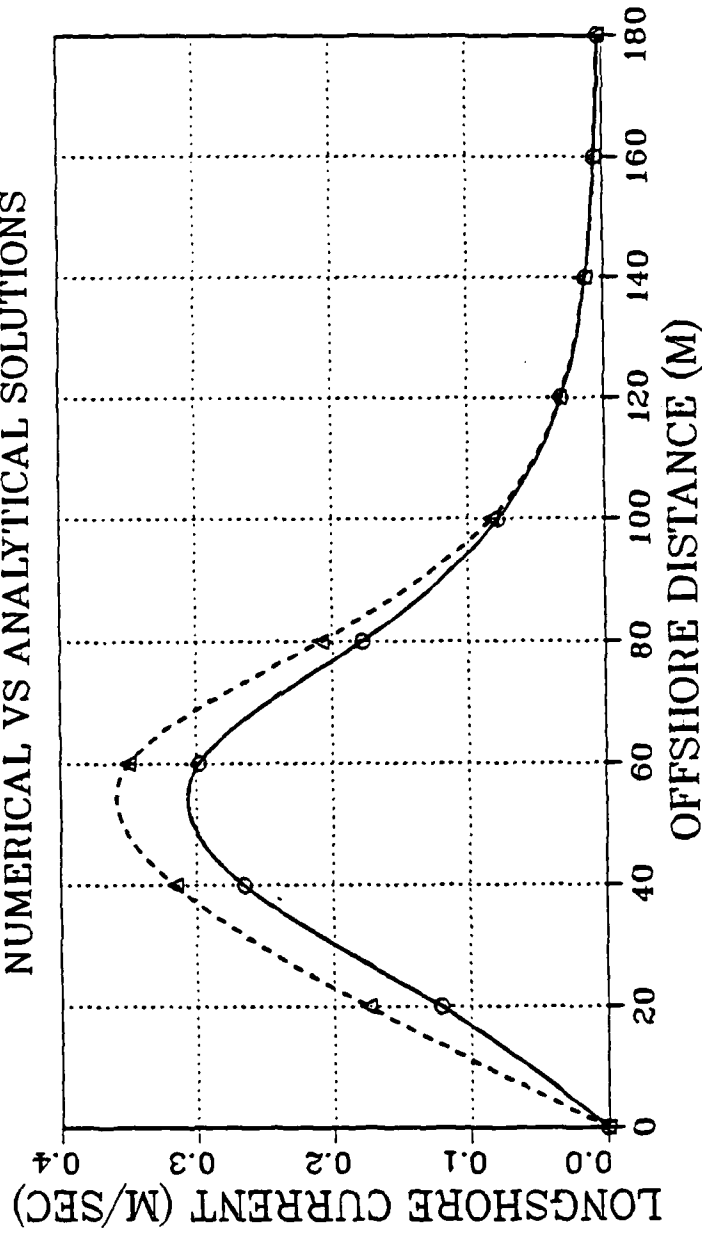


Figure 3.25. Numeric (solid) versus analytical (dashed) longshore current solutions for $H_0 = 1.0$ meter. Numerical values are slightly lower because the wave height values are raised to the seventh power in the velocity calculation.

WAVE CURRENT FIELD ($\theta = 170$)
 NUMERICAL VS ANALYTICAL SOLUTIONS

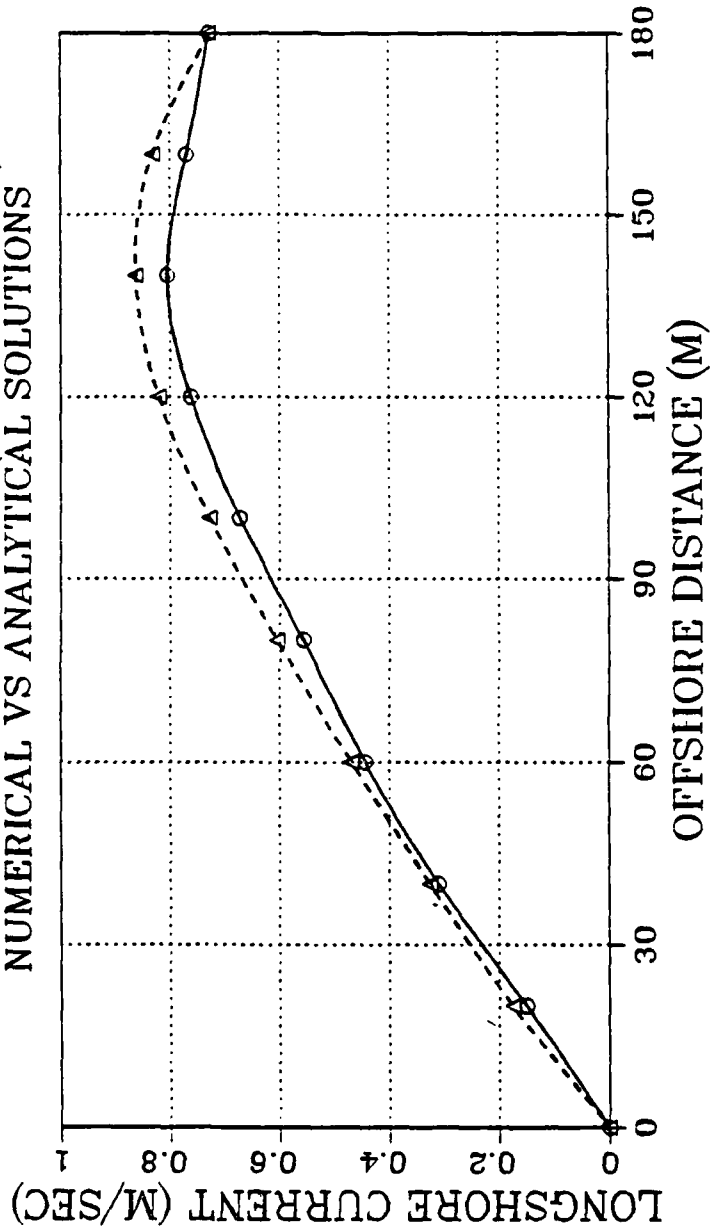


Figure 3.26. Numeric (solid) versus analytical (dashed) longshore current solutions for $H_0 = 2.5$ meter.

subroutines. The advantage of this approach is that the model can be changed from the new to the old version simply by changing the main program "CALL NEWSURFCON" to "CALL OLDSURFCON".

The NEWSURFCON module is basically the same as the old module with some exceptions. The wavenumber k , celerity C and group speed C_g are initially calculated. Then the new wave direction and height subroutines are called, which return direction, height and longshore current matrices.

The first major change incorporated in this new module is the way the breaker line is defined. In the old module, a quadratic equation was solved for the location of the first breaker line. Since the new breaker heights are calculated using a weighted probability density function, $p_b(H) = W(H) p(H)$, there is, by definition, no specific spot where all waves are said to be breaking. The weighting function, $W(H)$, as defined in Equation (37), gives a measure of the percent of breaking waves (Thornton and Guza, 1983):

$$W(H) = \left[\frac{H_{rms}}{h\gamma} \right]^4 = \int_0^{\infty} p_b(H) d(H) \quad (37)$$

To specify a "breaker line", the model first differentiates between steep waves, which show no wave growth due to shoaling towards the shore, and shallow waves, which increase in wave height until they break. The critical wave steepness, determined from Equation (27), is $H_o/L_o = 0.02$. A wave with a steepness greater than this criteria is considered steep while a wave with steepness less than 0.02 is considered shallow. For steep waves, a decision must be made as to what percentage of waves having broken constitutes the surf line. After some rather ad hoc experimentation, a value of 0.33 was chosen as a reasonable, which in effect defines a "significant

breaker height". That is, once 33 percent of the waves are breaking, the model chooses that point along the grid as the first breaker line. This test is actually conducted in the wave height subroutine. As the model moves down the column, the parameter $W(H)$ is tested at each grid point to see if it greater than or equal to 0.33. Once this value is reached, the breaker height, breaker depth, and distance from shore are returned to the NEWSURPCON module. For shallow waves, the model selects the maximum wave height as the breaker line. These two methods give good estimates of the observed breaker line, as discussed in Chapter 5.

Once the initial breaker height is defined in this manner, the number of additional lines are computed by dividing the initial breaker distance by the wave length corresponding to the average surf zone depth. If there are one or more wave lengths between the initial breaker line and the beach, the number of breaker lines are incremented accordingly. No additional calculations are performed on these interior breaker lines, if present. The breaker type is calculated based on the value of the surf parameter, Eta , which is a function of the beach slope and the deep water wave steepness (Battjes, 1974):

$$\xi = \frac{\tan \beta}{(H_o/L_o)^{1/2}} = \frac{\tan \beta}{(2\pi (\frac{H_o}{gT^2}))^{1/2}} \quad (38)$$

If Eta is less than or equal to 0.4, the breaker type is defined as spilling. Eta values between 0.4 and 2.0 are defined as plunging and values greater than 2.0 are called collapsing or surging waves.

The next calculation performed by NEWSURFCON is the "Effective surf" computation. Effective surf is a measure of surf intensity and is used by operational planners to provide a criterion for the feasibility of conducting amphibious landing operations using specific kinds of equipment. Effective surf, expressed as a wave height in feet, is a modification of significant breaker height, taking into account the total beach and surf conditions. It is important to note that effective surf is simply a planning parameter, and not a direct correspondence to the significant breaker height. Most commonly, H_{eff} is larger than H_s , but in some cases, especially when the H_s is small and the breaking waves are all spilling, H_{eff} can be smaller than H_s .

The calculation of effective surf uses a simple "look-up table" method which is outlined in the Joint Surf Manual (COMNAVSURFPAC/COMNAVSURFLANT Inst. 3840.1, 1976). The calculations of effective surf are retained from the original model with only minor modifications. Originally, the effective surf was retained as a wave height matrix. However, H_{eff} is simply a single number for a specific beach, based on significant wave height and direction, period, wind speed and direction, and percentage of spilling waves. The new module calculates a single number for H_{eff} and outputs all the H_{eff} parameters as specified by the Joint Surf Manual. Other information of use to the planner is printed at the same time. The new calculation also allows for a wind input (speed and direction) which was not available previously.

The final operation in NEWSURFCON is the limitation of the wave heights to the maximum stable wave height for a given depth and period. This

maximum wave height is given as (Wang and Chen, 1983):

$$H_{\max} = 0.067 \tanh(kh) \left(\frac{2\pi}{k}\right) \quad (39)$$

Each generated wave height is compared against this maximum value and is reset to H_{\max} if it exceeds the limiting wave height. The wave height, direction, current and effective surf matrices are then sent to OUTSURF for formatted output to either the screen or to a designated printer.

F. DEVELOPMENT OF AN OPERATIONAL USERS GUIDE

A simple users guide was written for the new version of the SSSP (Gill, 1985). Several guidelines were adhered to during its development. The manual assumes some familiarity with the HP-9845/275 and a working knowledge of oceanographic terms. The manual is tutorial in nature. It is divided into two parts, for the two main modules OPEN and SURFCON. The manual explains each input request and appropriate examples are included where necessary. An effort was made to keep the manual brief and user friendly. The model, being extensively menu driven, is straight-forward enough to require little documentation, after it has been used once or twice. The BASIC code is extensively documented throughout. Where appropriate, the old program lines are left in place (commented to prevent execution), with the replacement lines documented to point out the reason for the specific change.

IV. DISCUSSION

A. SENSITIVITY TEST OF BREAKER PARAMETERS

As discussed in Chapter III, the computation of H_{rms} , using the Rayleigh probability density function model, depends on two breaker parameters, Gamma and B. Gamma is an adjustable coefficient of $O(1)$ which appears to be strongly related to the beach slope (Sallenger and Holman, 1985). B is the breaker coefficient which represents the percentage of foam on the face of the breaking wave (i.e., the intensity of the breaking wave). This parameter is expected to be less than or equal to 1.0, since a B value of 1.0 corresponds to a fully developed bore (a wave that has fully broken from crest to trough). Values of B greater than 1.0 imply that the bore dissipation function underestimates the wave dissipation due to breaking (Thornton and Guza, 1983).

To verify the validity of the model assumptions, 24 wave data sets were studied to gain an understanding of the interaction of the B and Gamma values as used in the model. These data sets are summarized in Table 4.1. The data were digitized and appropriate Gamma values chosen, based on the slope of H_{rms}/h inside the surf zone. The Gamma values ranged from 0.39 to 0.60 and, for each data set, the specific Gamma value was held constant while the B values were varied. A curve fitting routine was used to optimize the B parameter for a given Gamma. As B was varied, the new model curve was compared with the real data points, and a sum of the square of the errors was generated. The B values were iterated until the error sum was minimized. Plots of the model output versus the data points were generated for each case.

A total of 24 data sets were tested against the model (See Table 4.1). In every case, the model accurately predicts the wave heights described by the data points. The first ten data sets are from a laboratory study of energy saturation of irregular waves during shoaling (Vincent, in press). These wave tank tests were conducted with a plane bottom slope of 1:30, with various frequency and incident wave heights. The experiments can be divided up into two groups based on wave steepness. The low steepness cases ($H_o/L_o < 0.02$) are represented by Case 1638 (Fig. 4.1). The Gamma value of 0.60 was derived from the slope of H_{rms}/h as described above. Using the curve fitting routine, an optimum B value of 0.82 was chosen. Note the good fit of the model curve (solid) compared with the data points (circles). The high steepness cases are represented by Case 1148 (Fig. 4.2). Gamma was set equal to 0.60 and a B value of 1.2 was obtained. As before, there is good agreement between the model curve and the data points.

To determine the optimized model's behavior when used with more difficult bathymetry, data from several wave tank experiments with offshore bars were tested (Battjes and Stive, in press). Case 5 (Fig. 4.3) has a simple offshore bar with a mean bottom slope of 1:25. Gamma was estimated to be .45 and a B value of 1.2 was obtained. Although the presence of the offshore bar (Fig. 4.4) radically changes the wave height data profile, the optimized model curve again faithfully predicts the wave heights. Wave tank test case 15 (Fig. 4.5) has a very complex bathymetry (Fig. 4.6). The model divides the on/offshore distance into 10 grid points with the intermediate depths calculated by straight linear interpolation. Therefore,

TABLE 4.1. SURF PARAMETERS

CASE	H _o (cm)	L _o (cm)	H _o /L _o	B	SLOPE	GAMMA	ETA	FREQ
1509	7.8	961.0	0.0081	1.55	0.0333	0.60	0.3699	0.403
1526	9.8	961.0	0.0102	1.05	0.0333	0.60	0.3300	0.403
1638	15.7	961.0	0.0163	0.81	0.0333	0.60	0.2608	0.403
1604	12.4	961.0	0.0129	0.82	0.0333	0.60	0.2934	0.403
1623	14.5	961.0	0.0151	0.88	0.0333	0.60	0.2713	0.403
1058	8.6	199.3	0.0432	0.62	0.0333	0.60	0.1604	0.885
1116	11.1	268.1	0.0414	0.67	0.0333	0.60	0.1638	0.763
1132	14.1	263.9	0.0534	0.67	0.0333	0.60	0.1442	0.769
1148	14.6	345.6	0.0422	0.72	0.0333	0.60	0.1622	0.672
1206	16.0	345.6	0.0463	0.70	0.0333	0.60	0.1549	0.672
Case 5	12.1	832.4	0.0145	1.30	0.0400	0.45	0.3318	0.433
Case 10	13.6	389.5	0.0349	0.65	0.0250	0.47	0.1338	0.633
Case 15	13.2	503.0	0.0262	0.84	0.0480	0.55	0.2963	0.557
Feb 2	37.0	39321.6	0.0009	0.80	0.0590	0.46	1.9234	0.063
Feb 3	49.0	31850.5	0.0015	0.90	0.0440	0.48	1.1218	0.070
Feb 4	52.0	31850.5	0.0016	1.10	0.0380	0.45	0.9405	0.070
Feb 5	41.0	25652.1	0.0016	1.10	0.0350	0.43	0.8755	0.078
Feb 6	26.0	19267.6	0.0013	1.00	0.0330	0.34	0.8983	0.090
Nov 4	35.0	39321.6	0.0009	1.50	0.0260	0.40	0.8715	0.063
Nov 10	56.0	51592.5	0.0011	1.70	0.0200	0.37	0.6071	0.055
Nov 12	88.0	26322.7	0.0033	1.30	0.0260	0.43	0.4497	0.077
Nov 17	38.0	32780.4	0.0012	1.50	0.0240	0.40	0.7049	0.069
Nov 18	49.0	32780.4	0.0015	1.50	0.0220	0.39	0.5690	0.069
Nov 20	50.0	39321.6	0.0013	1.60	0.0200	0.39	0.5609	0.063

MODEL OUTPUT VS WAVE TANK DATA
CASE 1638 B = 0.81 GAMA = .60

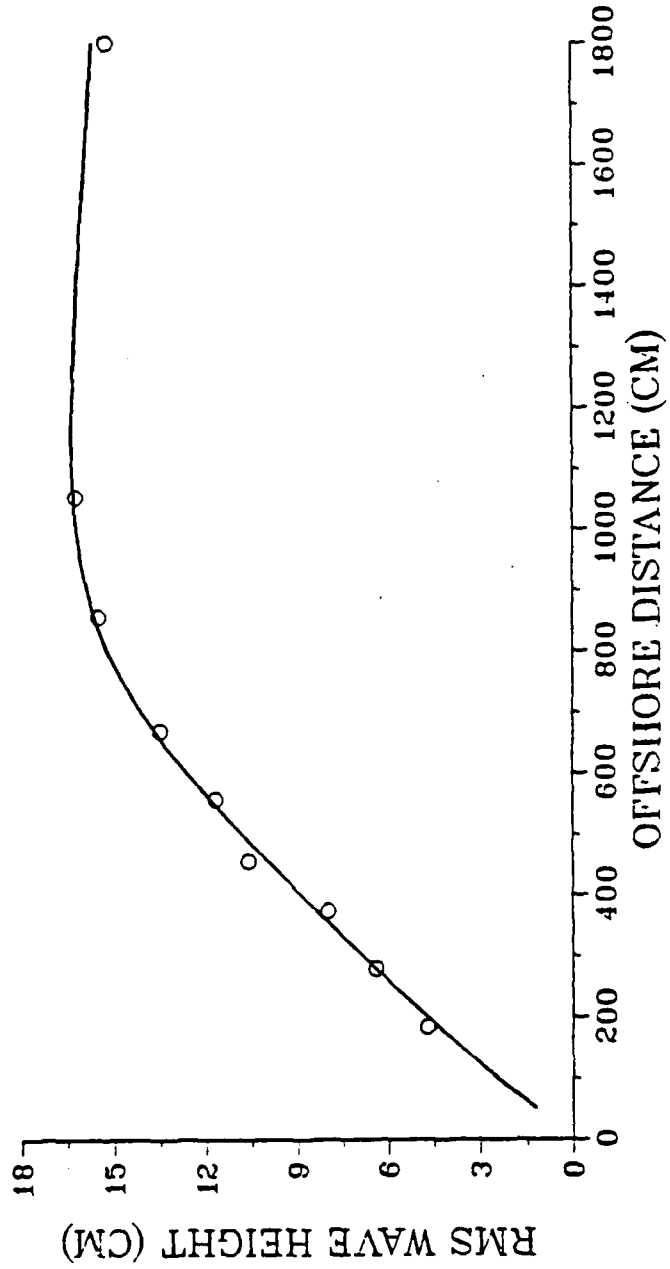


Figure 4.1. Optimized model output for Case 1638 (Vincent, 1985).

MODEL OUTPUT VS WAVE TANK DATA
CASE 1148 B = 0.72 GAMA = .60

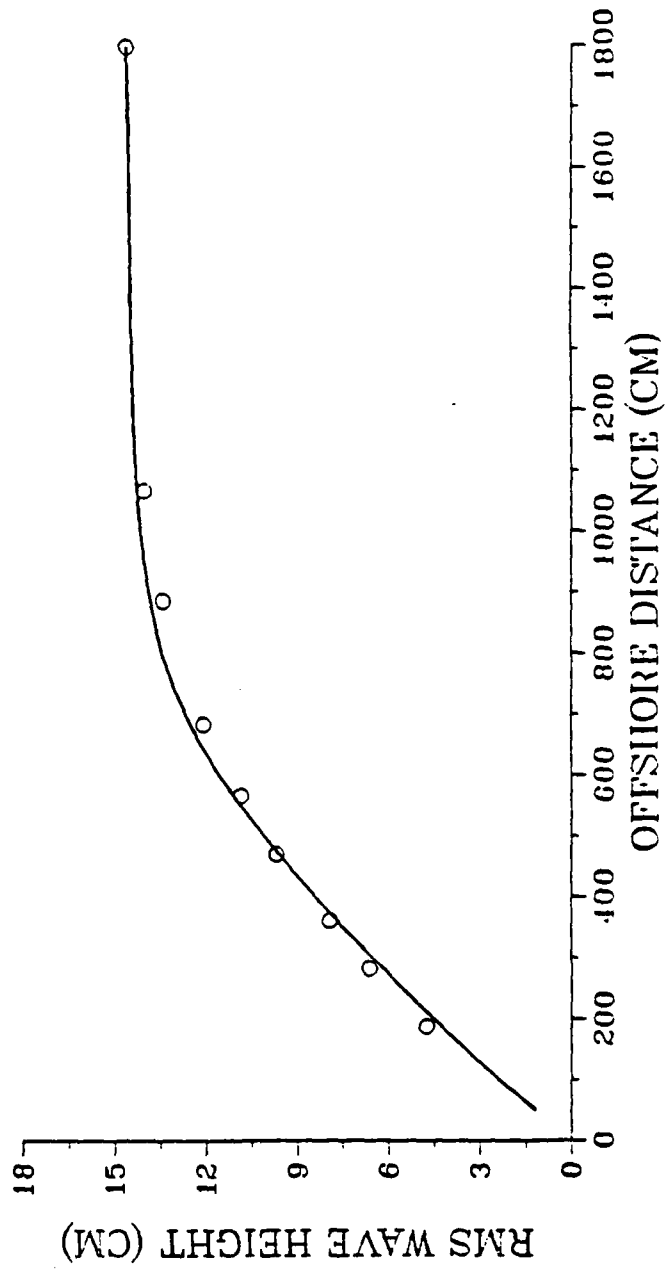


Figure 4.2. Optimized model output for Case 1148 (Vincent, 1985).

MODEL OUTPUT VS WAVE TANK DATA
CASE 5 B = 1.3 GAMA = .45

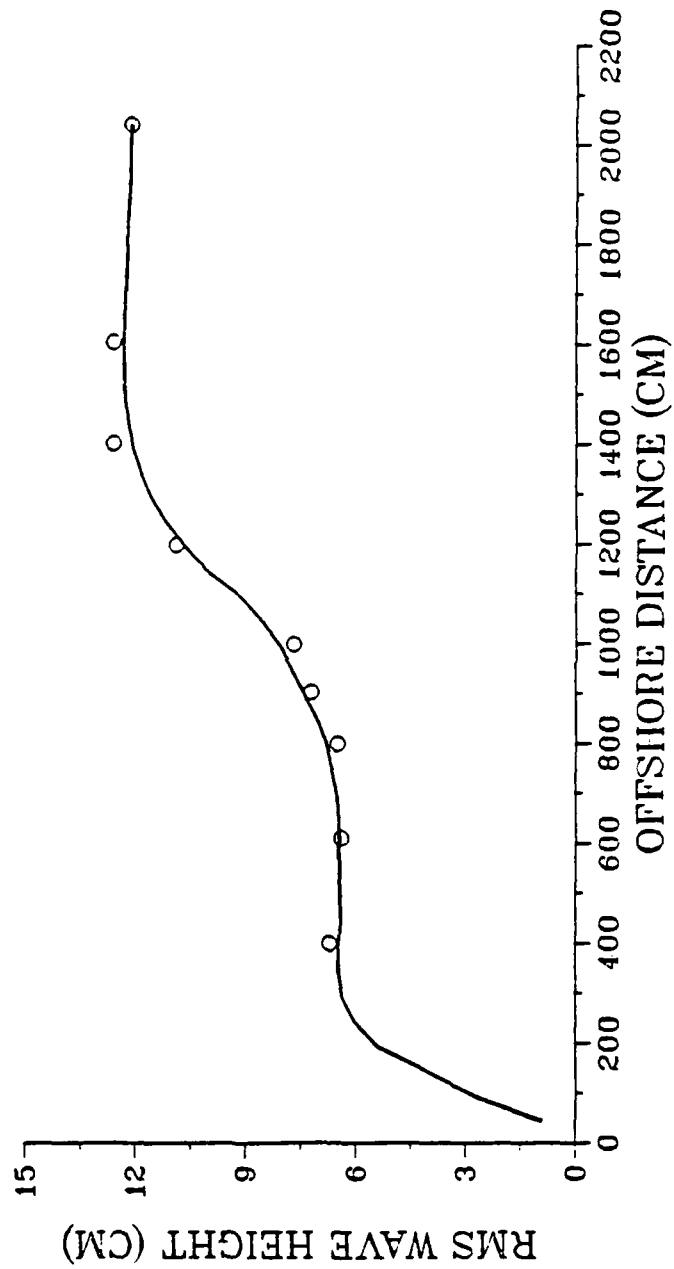


Figure 4.3. Optimized model output for Case 5 (Battjes and Stive, 1985).

Case 5. Bottom Topography

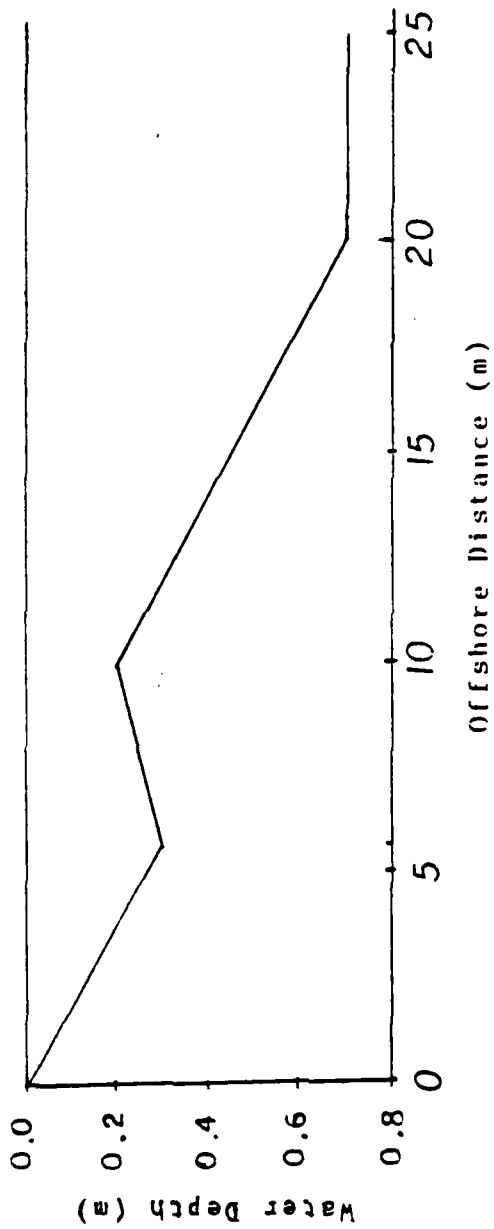


Figure 4.4. Case 5 wave tank bathymetry. (Battjes and Stive, 1985).

MODEL OUTPUT VS WAVE TANK DATA
CASE 15 B = 0.84 GAMA = .55

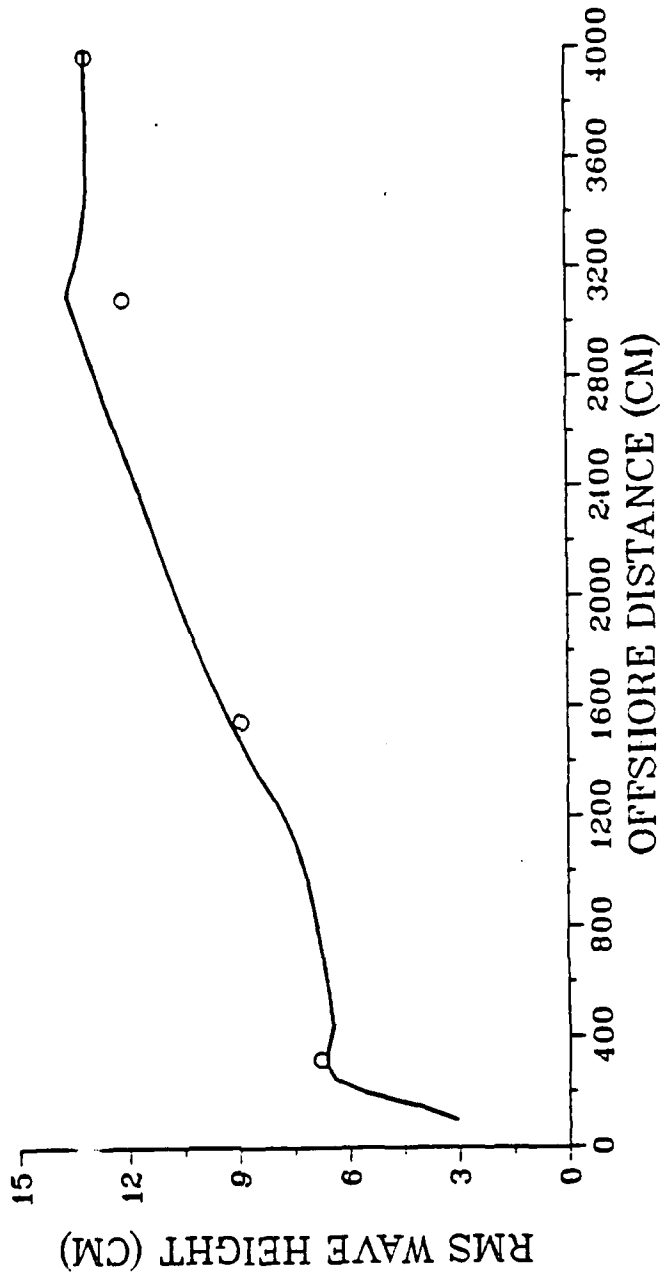


Figure 4.5. Optimized model output for Case 15 (Battjes and Stive, 1985).

Case 15. Bottom Topography

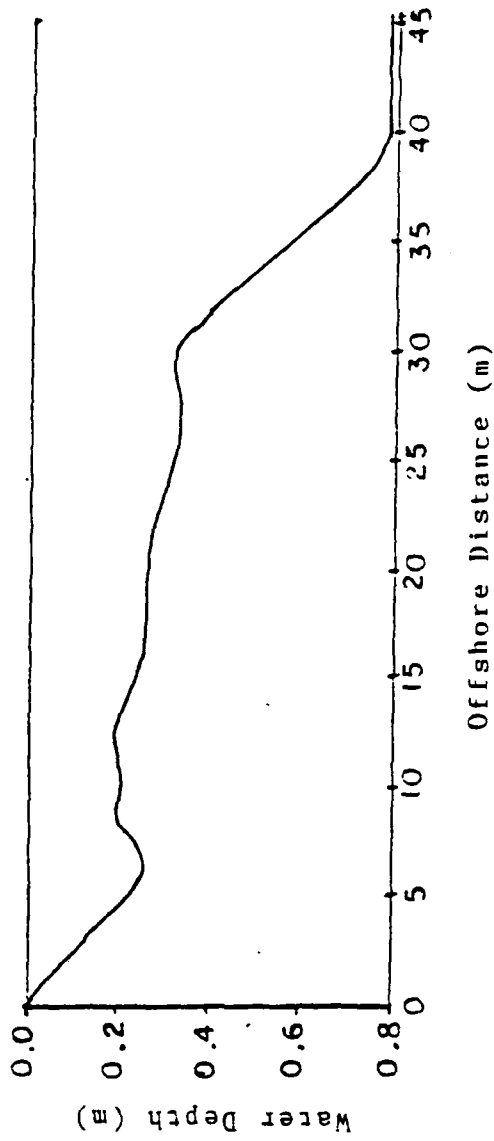


Figure 4.6. Case 15 wave tank bathymetry. (Battjes and Stive, 1985).

complex bathymetry, such as that in Case 15, was smoothed out to a certain degree. Even with that limitation in mind, the optimized model curve appears to accurately estimate the recorded wave heights. The model results will be tested against field data in the next chapter.

It is evident that the random wave model, with the appropriate choice of the surf parameters, Gamma and B, will accurately forecast wave heights throughout the domain. A sensitivity test for the choice of parameters was conducted on three representative cases 1638, 1148, and 5. Case 5 (Battjes and Stive, in press) was chosen for discussion here because of its more interesting bottom profile. It was felt that this barred profile was representative of many real beaches and would provide a more rigorous test than a simple plane bottom. Using a Gamma value of 0.45, the optimum B value of 1.3 was changed to 1.7, 1.5, 1.1 and 0.9 (Fig. 4.7). B values less than optimal tend to over-estimate the wave heights and vice-versa. It is of interest to note that changes in B of 22-33 percent only results in an increase in the model error of about 10-12%. This was confirmed in a study of Torrey Pines, California wave data by Thornton and Guza (1983). They found that a variation of +/- 25% about the optimum B value resulted in an increased model error of less than 10% (Fig. 4.8).

It was found that the model demonstrated a similar sensitivity to changes in the Gamma value. A change of about +/- 20% to the optimum Gamma value of 0.45 resulted in an increased model error of 8-10% (Fig. 4.9). Sensitivity tests were conducted on high and low steepness plane beach cases (1638 and 1148) with similar results. In the next section, techniques and rationale for choosing B and Gamma values, based on initial conditions, are discussed. It is important to bear in mind the above sensitivity analysis.

MODEL OUTPUT VS WAVE TANK DATA
CASE 5 B = 1.3 GAMA = .45

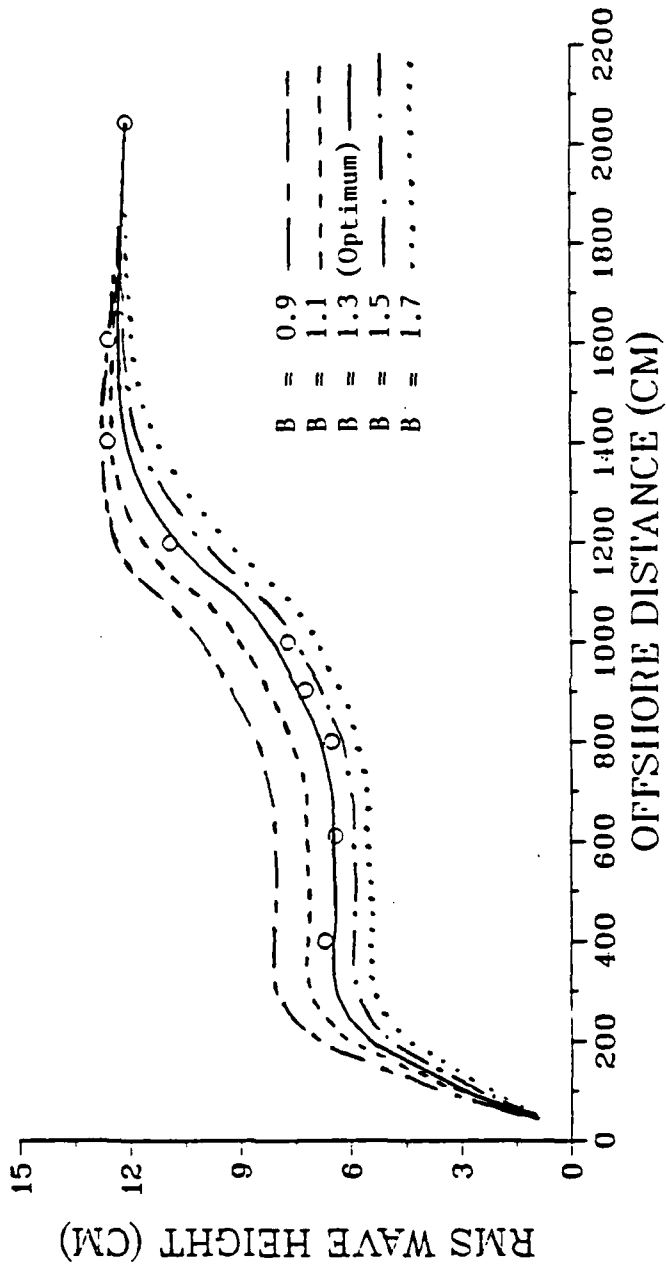


Figure 4.7. Sensitivity test; G = 0.45; B varies from 0.9 to 1.7. about the optimum B value of 1.3.

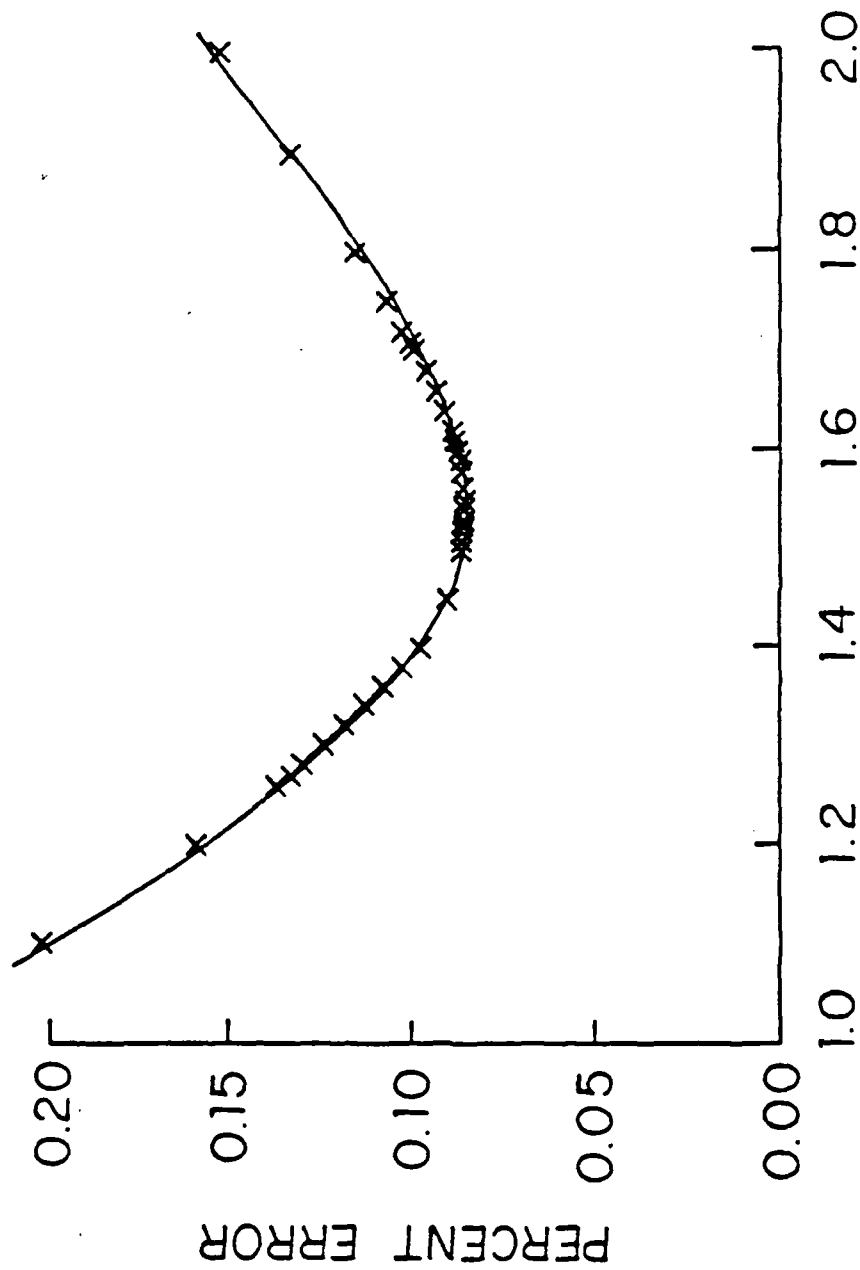


Figure 4.8. Error percentage only increases about 10% as B is varied by 25-30% (Thornton and Guza, 1983).

MODEL OUTPUT VS WAVE TANK DATA

CASE 5 B = 1.3 GAMMA = .45

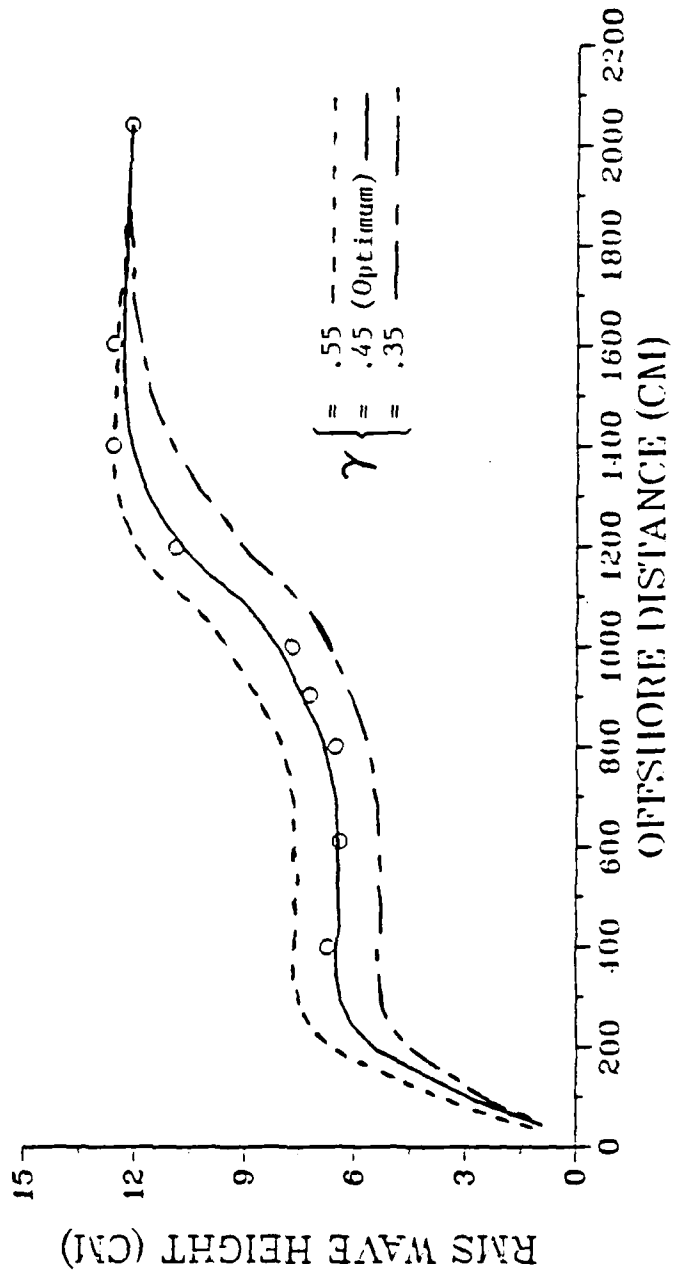


Figure 4.9. Sensitivity test; B = 1.3; Gamma varies from 0.35 to 0.55 about the optimum Gamma value of 0.45. The model appears to be slightly more sensitive to fluctuations in Gamma than in B.

The model appears to be fairly robust with respect to small changes in the surf parameters. Therefore, slight errors in the choice of these values should not degrade the final performance of the model to a great extent.

B. CHOOSING THE BREAKER PARAMETERS

The two breaker parameters, B and Gamma, are multiplicative constants in the H_{rms} wave height calculation (see Equation 27). They could therefore be combined as a single bulk modulus coefficient, or kept as two separate parameters. It was felt that keeping the two terms separate would better serve the requirements of the model.

Some work has already been done on the problem of choosing the breaker parameters. A recent study by Sallenger and Holman (1985) has determined a functional relationship between Gamma and the average beach slope based solely on field observations inside the surf zone. This relationship is given by:

$$\gamma = 3.2 \tan \beta + 0.3 \quad (40)$$

Using the 24 wave data sets, the chosen Gamma values are plotted against beach slope (Fig. 4.10). The solid line is a straight linear regression of the data points while the dashed line is the Holman/Sallenger function. There seems to be a general agreement in the slope of the line although the intercept is slightly different. Gamma is also plotted against wave steepness (Fig. 4.11) but the plot is less linearly correlated. As an initial trial, the Holman/Sallenger functional relationship will be adopted as the model's convention for choosing the Gamma value. The average slope is defined here

GAMMA VERSUS SLOPE

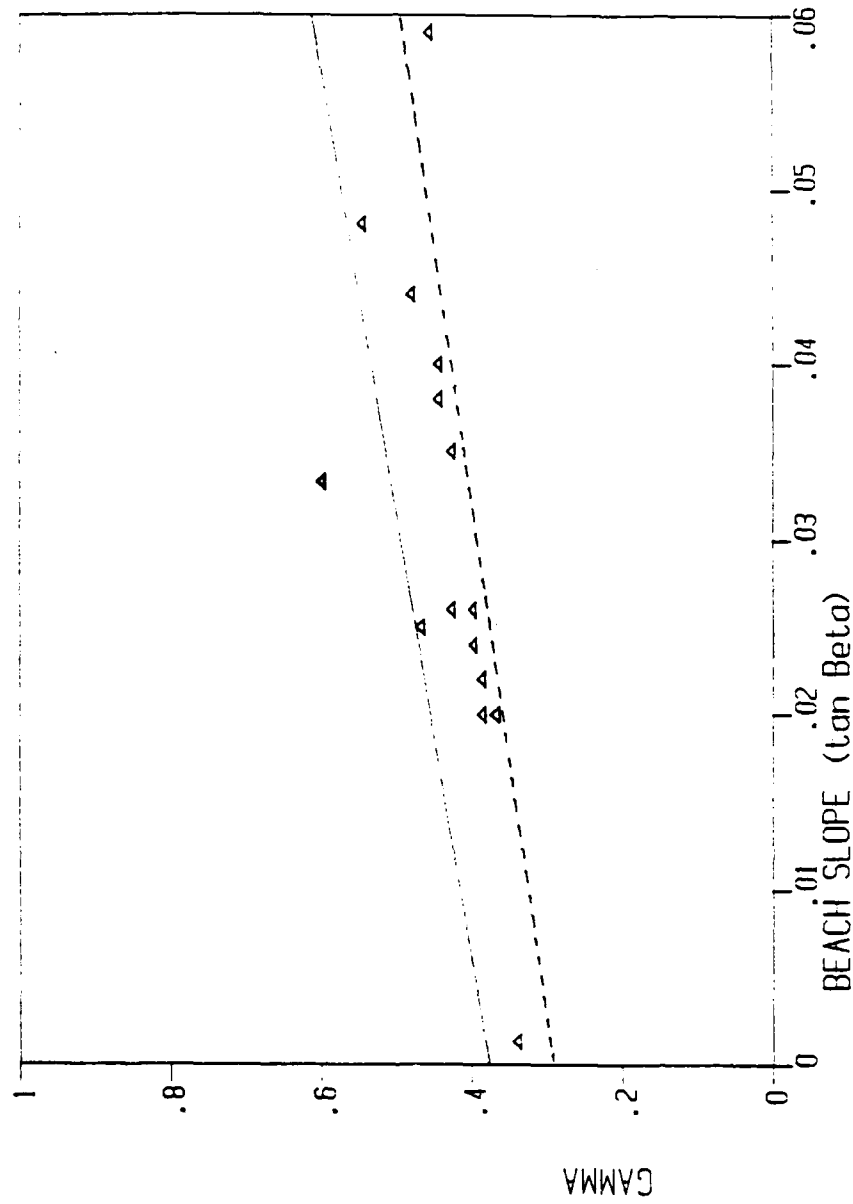


Figure 4.10. Gamma versus beach slope. Solid line is a linear regression fit to the data. Note that the single point above the solid line is heavily weighted since it represents 10 cases. Dashed line is the linear relation suggested Sallenger and Holman (1985).

AD-A161 023

TEST AND EVALUATION OF AN IMPROVED SEA SHELL AND SURF
PROGRAM(U) NAVAL POSTGRADUATE SCHOOL MONTEREY CA
M J GILL SEP 85

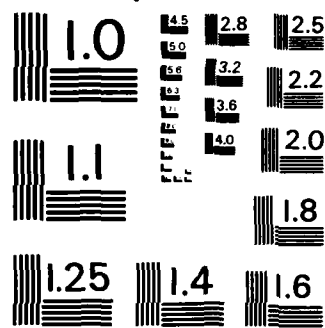
2/2

UNCLASSIFIED

F/G 8/3

NL

							END						
							FILMED						
							DTIC						



MICROCOPY RESOLUTION TEST CHART
NATIONAL BUREAU OF STANDARDS-1963-A

GAMMA VERSUS STEEPNESS

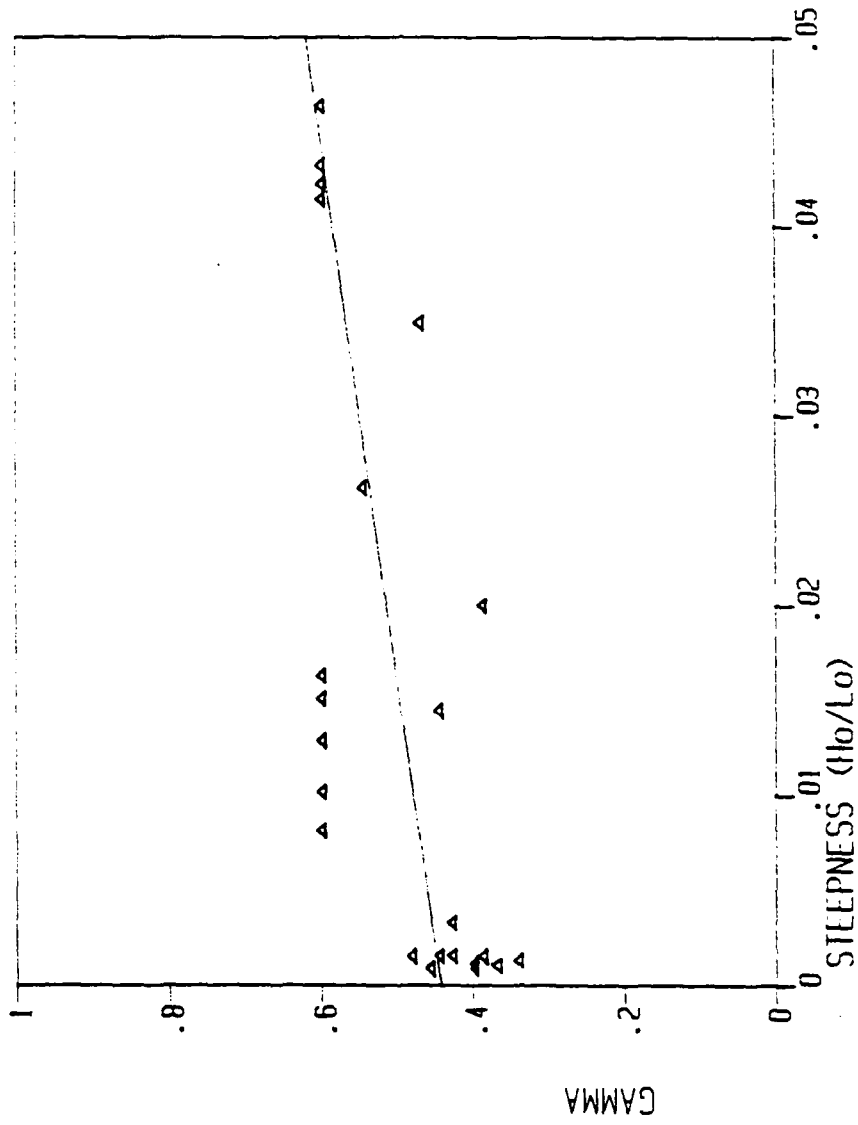


Figure 4.11. Gamma versus incident wave steepness.

as the depth at the outermost grid point divided by the offshore grid distance.

Choosing a proper predictor for the B value proved to be more difficult. Since B represents a measure of breaker intensity, it is felt that it would be related to incident wave steepness which has previously been shown to be related to breaker type (Battjes, 1972). The optimum B values for the 24 wave sets are plotted against steepness in Figure 4.12 and against beach slope in Figure 4.13. The wave steepness in this case was defined as the incident wave height divided by the deep water wave length (H_o/L_o). Although there is a considerable scatter, B appears correlated with wave steepness and less with beach slope.

Several other parameters were considered as predictors for B. The B and Gamma values were compared with the surf parameter, $\text{Eta} = \tan \beta / (H_o/L_o)^{1/2}$. Additionally, the Bulk Modulus (B^3/Gamma^4) was plotted against beach slope and wave steepness. Since, from Figures 4.11 and 4.12, B appears to be related to both beach slope and wave steepness, it was hoped that Eta, which is a measure of the expected breaker intensity, would offer a predictor for B. The plot of B versus Eta (Fig. 4.14) shows an interesting pattern. B appears to increase almost linearly as Eta increases to about 0.6 and then decreases in an exponential fashion to an asymptotic B value of 0.8. This behavior appears reasonable. As the surf parameter increases, indicating a transition from spilling to plunging waves, the B value (amount of wave face that is breaking), should increase.

The maximum value that B should reach, according to theory, is 1.0. Studies have shown, however, that in many cases, the optimum B value is on the order of 1.4 (Thornton and Guza, 1983). The maximum B value

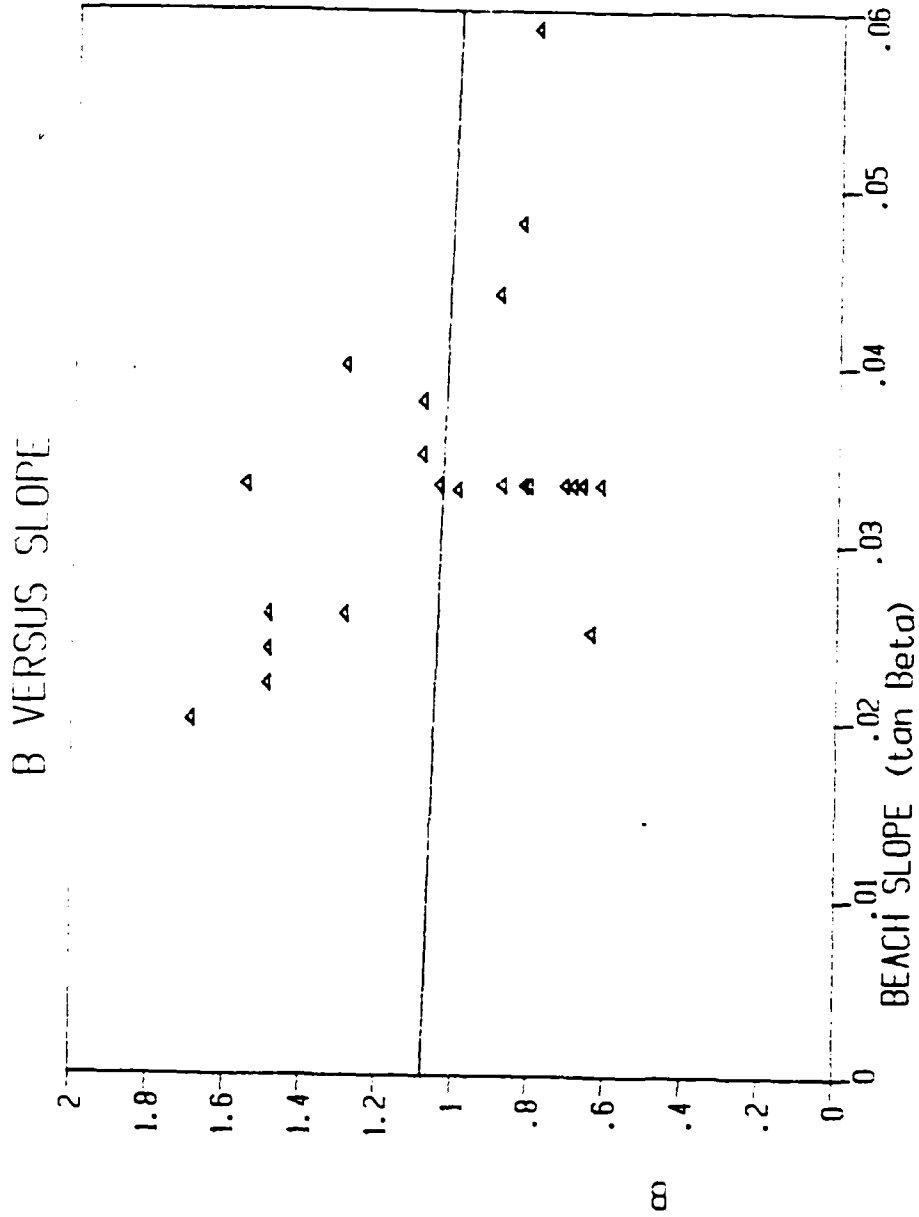


Figure 4.12. B versus beach slope. B is only weakly characterized by slope.

B VERSUS STEEPNESS

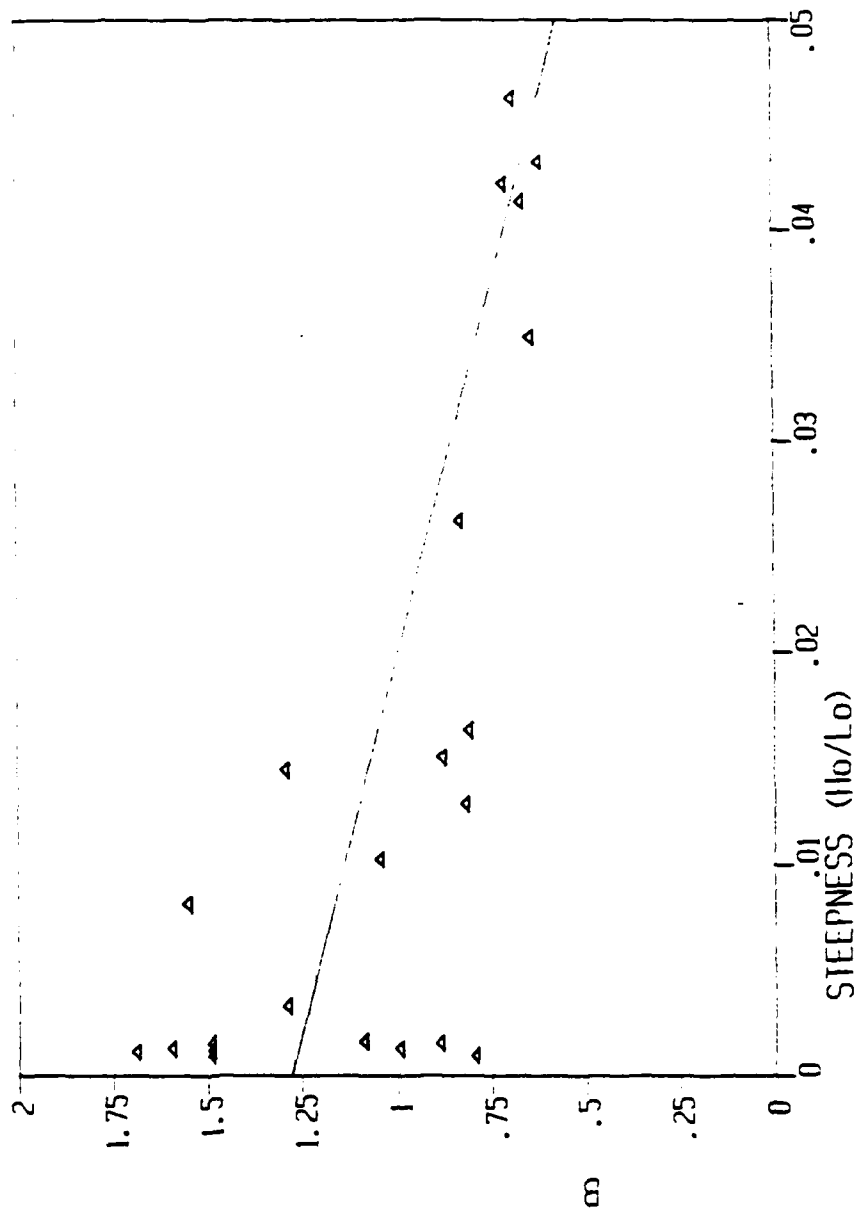


Figure 4.13. B appears to be a function of incident wave steepness.

B VERSUS ETA

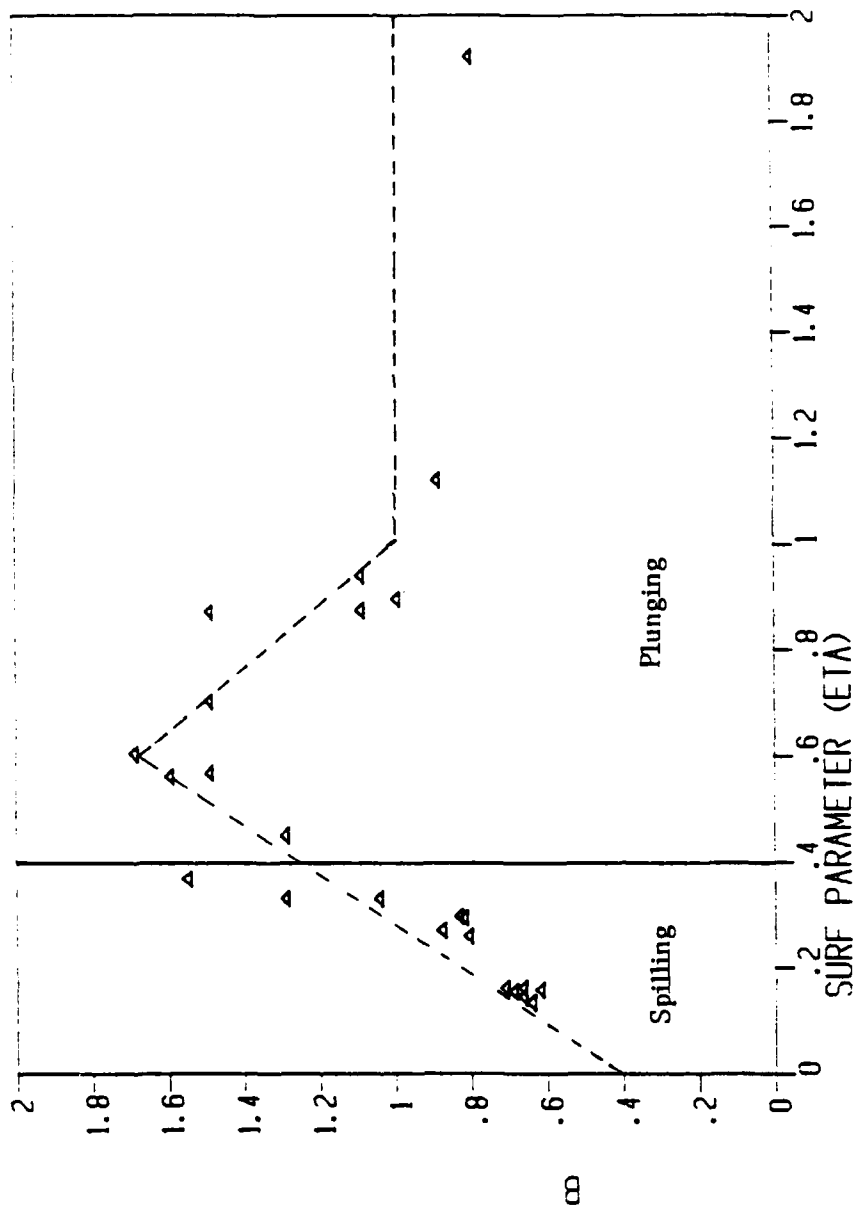


Figure 4.14. B versus the surf parameter Eta. B is strongly related to Eta which is to be expected. Both B and Eta are measures of the intensity of the wave breaking. Dashed line depicts piecewise function used by the model to define B.

GAMMA VERSUS ETA

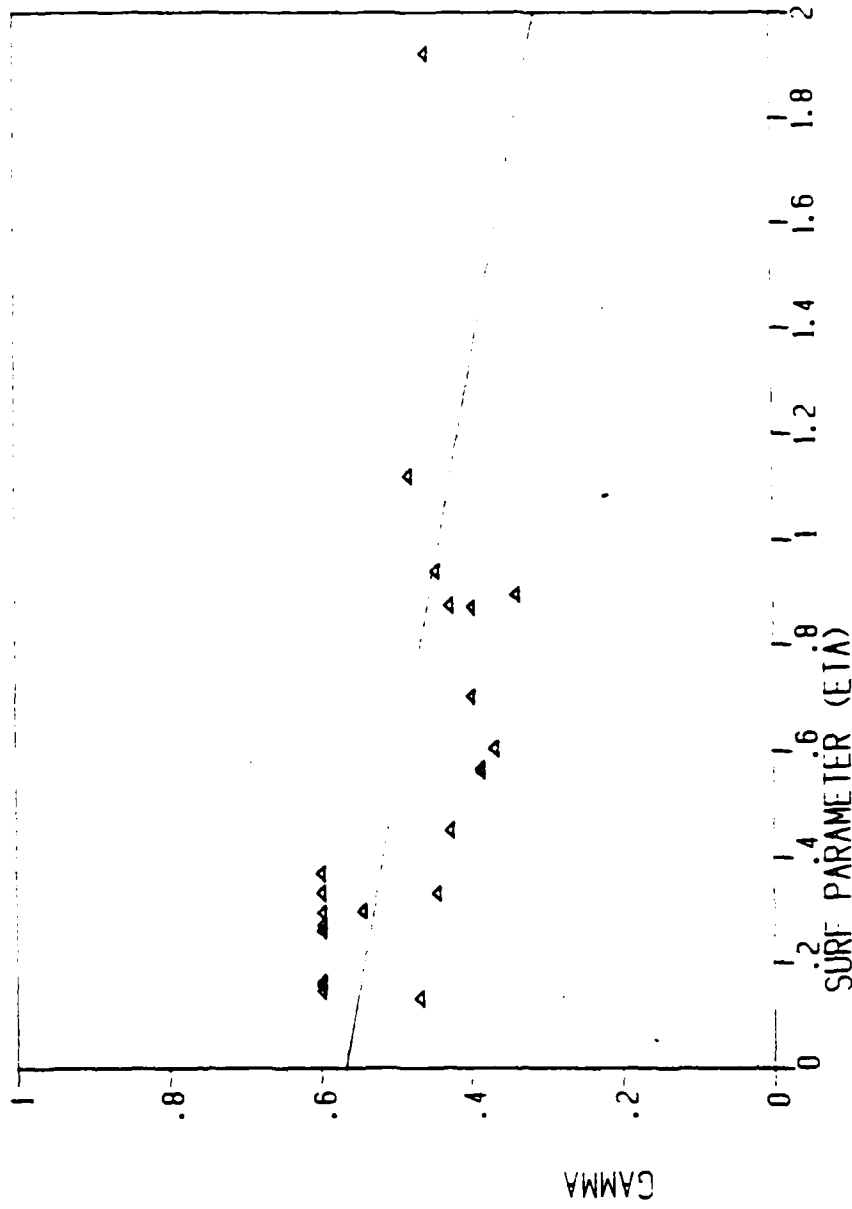


Figure 4.15. Gamma versus Eta.

occurs when Eta is about 0.6, indicating that the breakers are mixed spilling and plunging. As Eta continues to increase, the B values fall more into line with theory and approach the expected value of 1.0, as the waves become fully plunging.

To simplify and expedite the model development, the following piecewise continuous function is used to determine the B term (Fig. 4.14):

$$\begin{aligned} B &= 2.167 \text{ Eta} + 0.4 & \text{Eta} \leq 0.6 & \quad (41) \\ B &= -1.70 \text{ Eta} + 2.7 & 0.6 < \text{Eta} \leq 1.0 & \\ B &= 1.0 & \text{Eta} > 1.0 & \end{aligned}$$

This choice is somewhat ad hoc and is based primarily on the data sets discussed above. Future refinements in the techniques for predicting the breaker parameters may substantially improve the use of this model operationally. Using equations (40) and (41) as predictors for Gamma and B, the SURFCON module is essentially complete. The next chapter will discuss testing the model against two well-documented natural beach data sets, to get a feeling for how the improved model behaves against actual data.

C. MOTIVATION FOR THE RANDOM WAVE MODEL SUBSTITUTION

As discussed in Chapters 3 and 4, the primary motivation for substituting the one dimensional random wave model for the two dimensional model was to increase computational efficiency and accuracy. The improved model calculates longshore current information quickly and accurately. Significant wave height predictions compare well with actual data sets, as will be discussed in Chapter 5. There is, however, a potential for loss of detailed

information by using the one dimensional model. Nearshore circulation and longshore variation in wave heights are smoothed out by the one dimensional approach.

The surf model (both old and new versions) uses a single wave height input to define the offshore boundary condition. This implies that variations in the interior wave heights and directions are due only to variations in bathymetry. Because the model uses a very small grid (only 13 longshore grid points), very accurate bathymetry must be entered. It is questionable whether the operational planner would have access to bathymetric data of the required accuracy to define a two dimensional bathymetry.

Many beaches which would potentially be used for amphibious operations are shallow, almost planar in nature. Other common landing beaches are barred, but rather uniform in the longshore direction. Therefore, for many operationally relevant beaches, the assumption of straight and parallel contours, and the use of a one dimensional model, appears justified. The "mean beach" surf information provided by the model will adequately represent the conditions over a standard 500 yard landing beach. If a wider beach needs to be characterized, the improved model would be run several times, entering the required information for each beach segment.

V. TEST AND EVALUATION OF THE IMPROVED MODEL

A. WAVE HEIGHT AND BREAKER LOCATION

The improved version of the SSSP was tested against one wave tank experiment and two sets of beach surf data to see if the model would choose reasonable Gamma and B parameter values, based on the predictors discussed in Chapter 4. The predicted wave heights and surf characteristics are compared with the observed values.

Case 5 (Battjes and Stive, 1985), discussed in the preceding chapter, was chosen as the wave tank experiment with which to test the finished model. This case was chosen because of its barred beach bathymetry. The model selected values of 0.41 and 0.963 for Gamma and B. The optimum values, from Table 4.1, are 0.45 and 1.30. The model wave height fit to the observed data points is still quite reasonable (Fig. 5.1). The solid line represents the model output and the circles are the observed data.

Two Southern California beach data sets were used for further tests. Data collected at Santa Barbara's Leadbetter Beach during February, 1980 and Torrey Pines during November, 1978 (Thornton and Guza, 1983), were used as the primary tests of the performance of SSSP.

The first Santa Barbara test used data collected on 3 February, 1980. The average beach slope was 0.047 and the incident waves were 0.55 meters (rms) with a period of 14.3 seconds. The observed breaker height was measured at 0.70 meters, approximately 40 meters from the beach (dashed line). The wave angle was 7.8 degrees from normal. The SSSP predicted a

MODEL OUTPUT VS WAVE TANK DATA
CASE 5 B = 0.963 GAMMA = .41

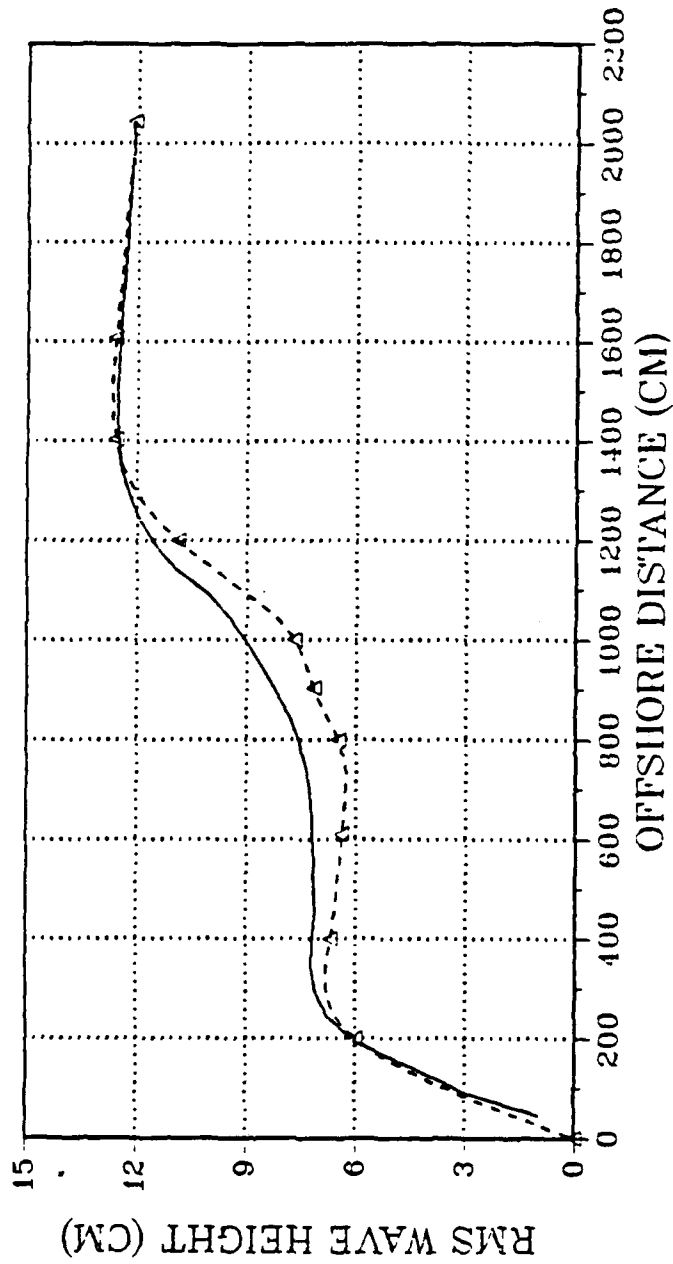


Figure 5.1. Comparison between the model output (solid) and the observed wave tank data (dashed). C_f for all cases is 0.009.

rms breaker height of 0.68 meters (solid line), 40.0 meters from the beach (Fig. 5.2). The model under predicted the observed heights less than 4 percent.

Similar results are obtained for Leadbetter Beach data obtained on 4 and 5 February, 1980. On 4 February, the incident wave height was 0.56 meters with a period of 14.3 seconds. The wave angle was 9 degrees from normal. The observed breaker height was 0.67 meters, 50 meters from the beach. The model predicted 0.65 meters, 40 meters from the shore (Fig. 5.3).

On 5 February, the incident wave was 0.45 meters with a period of 12.8 seconds. The wave angle was 8.4 degrees from normal. Observed breakers were 0.60 meters, about 36 meters from the beach. SSSP predicted 0.55 meter breakers, 33 meters from the shore (Fig. 5.4).

Torrey Pines beach data acquired on 4 and 10 November, 1978 is compared with model results in Figures 5.5 and 5.6. The beach has a shallow slope of 0.022 which accounted for a wide surf zone of about 160 meters. On 4 November, the incident waves were about 0.35 meters with a period of 14.3 seconds and normal incidence. The observed breaker height was 0.47 meters about 110 meters from the shore. SSSP predicted 0.48 meter breakers at a distance of 106 meters from the beach. The model correctly forecast the wave height and surf zone width (Fig. 5.5).

A similar result is seen for the November 10 Torrey Pines Case. The incident wave is 0.68 meters with a period of 15.9 seconds and normal incidence. Observed breakers were 0.72 meters, approximately 130 meters from the shoreline. The model predicted breaker heights of 0.75 meters, 140 meters from the beach (Fig. 5.6). As for the November 4 case, the model

MODEL OUTPUT VS OBSERVED DATA
3 FEB 1980 B = 1.00 GAMMA = .45

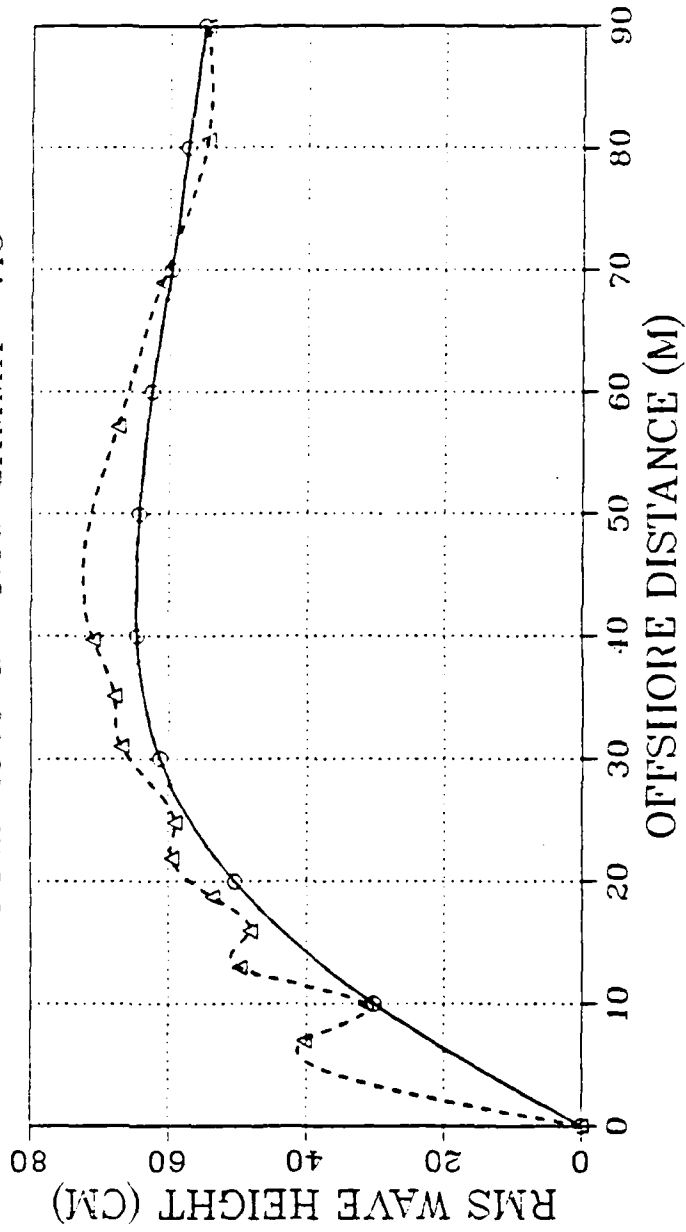


Figure 5.2. Comparison between the model output (solid) and the observed data from Santa Barbara on 3 Feb., 1980 (dashed).

MODEL OUTPUT VS OBSERVED DATA
 4 FEB 1980 B = 1.00 GAMMA = .45

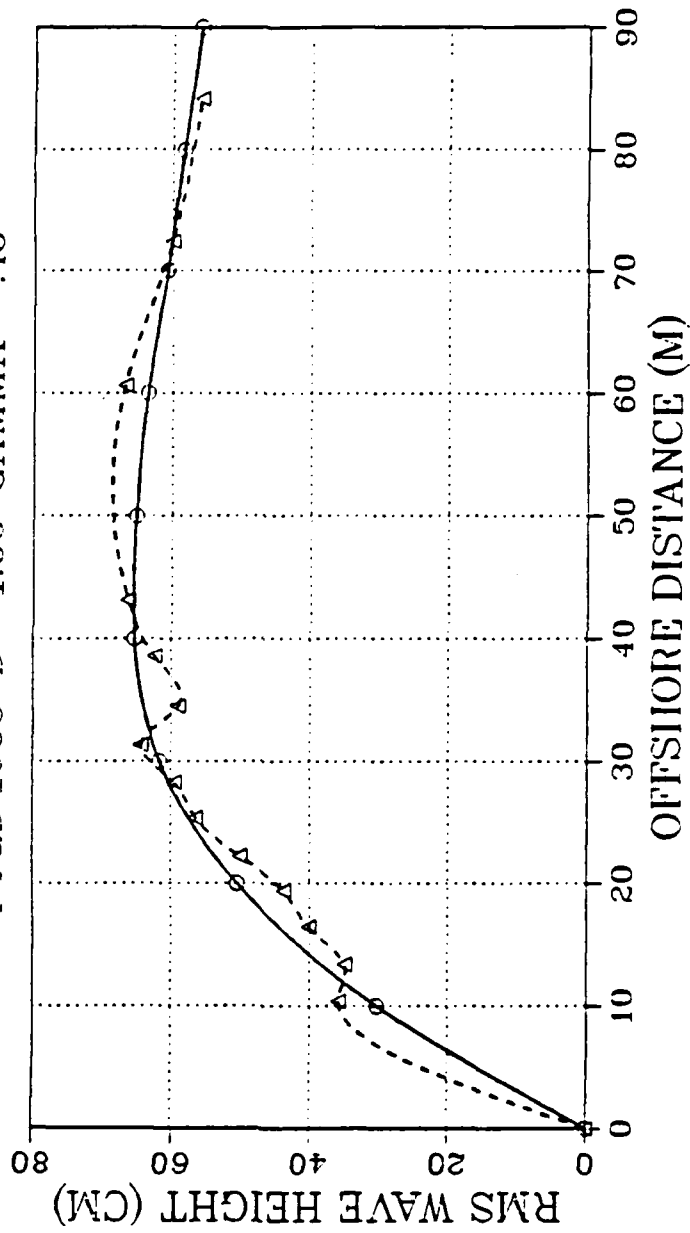


Figure 5.3. Comparison between the model output (solid) and the observed data from Santa Barbara on 4 Feb., 1980 (dashed).

MODEL OUTPUT VS OBSERVED DATA
5 FEB 1980 B = 1.00 GAMMA = .45

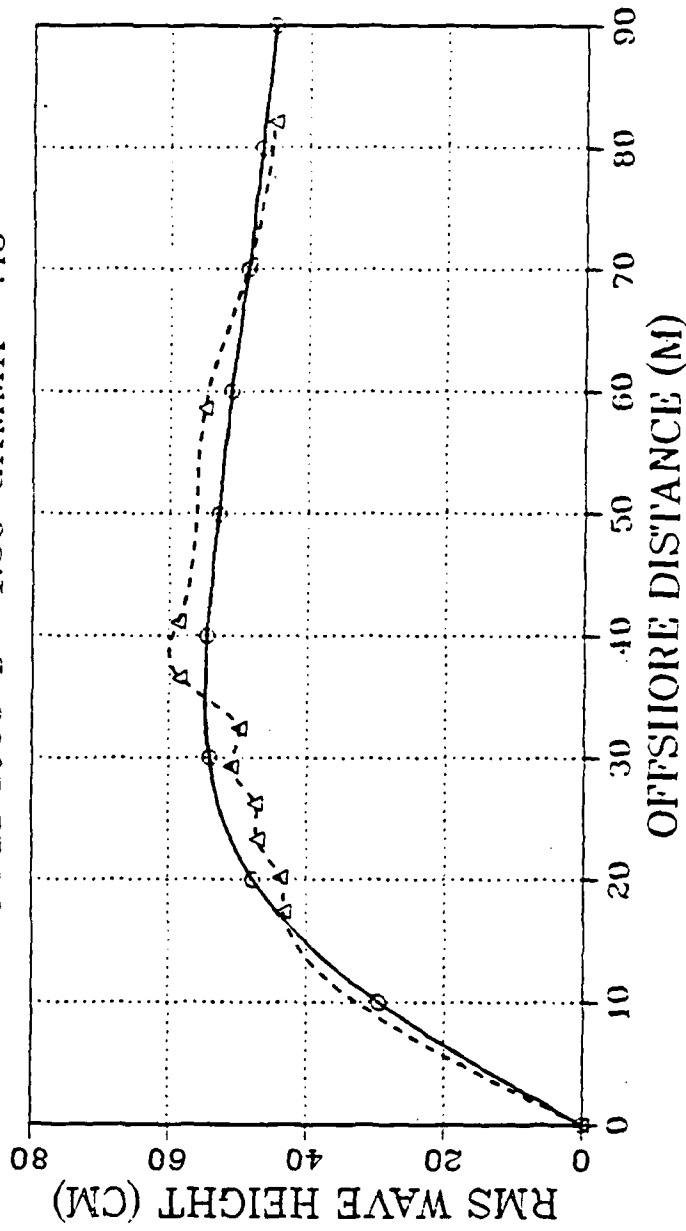


Figure 5.4. Comparison between the model output (solid) and the observed data from Santa Barbara on 5 Feb., 1980 (dashed).

MODEL OUTPUT VS OBSERVED DATA
4 NOV 1978 $B = 1.63$ $GAMMA = .376$

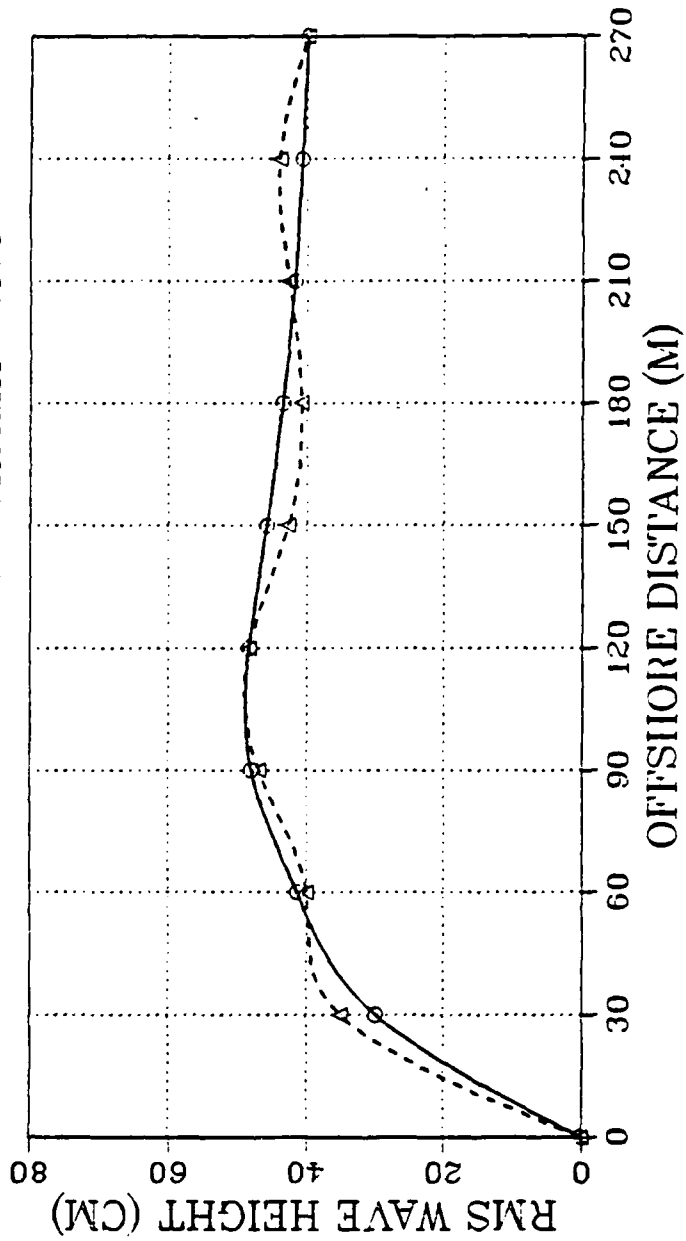


Figure 5.5. Comparison between the model output (solid) and the observed data from Torrey Pines on 4 Nov., 1978 (dashed).

MODEL OUTPUT VS OBSERVED DATA
10 NOV 1978 B = 1.57 GAMMA = .376

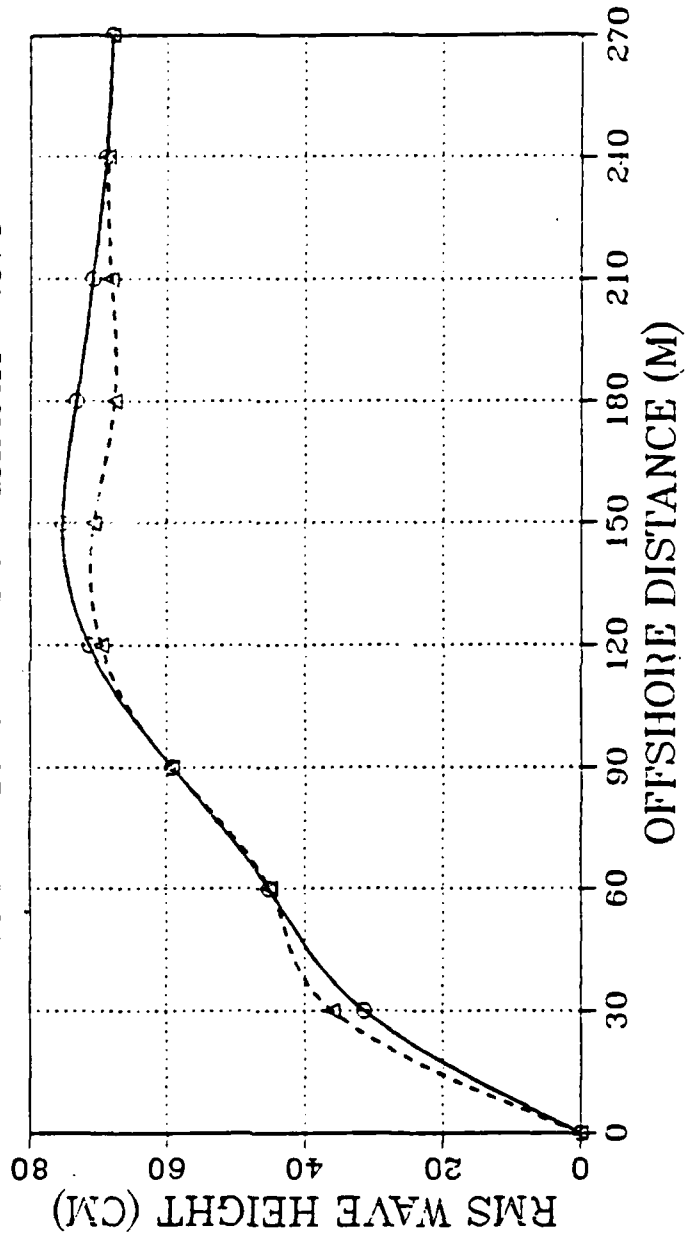


Figure 5.6. Comparison between the model output (solid) and the observed data from Torrey Pines on 10 Nov., 1978 (dashed).

worked quite well for wave height prediction and the location of the breaker line.

Based on the tests of the SSSP against various data sets, it appears that the new version is an improvement over the original model. The old version consistently underpredicted the wave heights and was very inaccurate at estimating the location of the breaker line (Devendorf, 1985). The new version appears to be quite good at predicting the breaker height and gives better estimates of the breaker line. Table 5.1 is a comparison between the optimum values of the two breaker parameters and the values chosen by the model. The technique for choosing Gamma and B is convenient, although improvements will need to be made in this area.

B. LONGSHORE CURRENT DISTRIBUTION

Longshore currents are the result of waves impinging at an oblique angle to the shoreline. All the wave tank tests, as well as the Torrey Pines cases, had normally incident waves. The Santa Barbara Leadbetter Beach data is the only comprehensive field data on longshore currents acquired to date. There exists no laboratory data for longshore currents generated by obliquely incident, random waves. The same three data sets (February 3,4,5) were chosen as study cases because they had a variety of incident wave heights and wave angles. For the February 3 case (Fig. 5.7), the maximum observed current (dashed) was 0.48 m/sec at a distance of 22 meters from the shoreline. The bed shear stress coefficient, C_f , was set equal to 0.009 for all cases. This value was derived experimentally by Thornton and Guza (1985). The SSSP prediction (solid) for longshore current was a maximum of 0.5 m/sec, 25 meters from the beach (solid line).

TABLE 5.1. COMPARISON OF BREAKER PARAMETERS

Case	Optimized		Model Generated	
	Gamma	B	Gamma	B
Case 5	0.45	1.30	0.41	0.96
Feb. 3	0.48	0.90	0.45	1.00
Feb. 4	0.45	1.10	0.47	1.00
Feb. 5	0.43	1.10	0.47	1.00
Nov. 4	0.40	1.50	0.37	1.68
Nov. 10	0.37	1.70	0.38	1.57

For the February 4 case (Fig. 5.8), the maximum observed current was .48 m/sec, 25 meters from shore; the model prediction was .44 m/sec at 20 meters from the beach. The Feb 5 case (Fig. 5.9) shows an observed current maximum of .36 m/sec at 20 meters from the beach. The model predicted .36 m/sec at 20 meters from the shoreline.

The model not only predicts the maximum current velocity reasonably well, but the current distribution within the surf zone shows good agreement with the data. The model seems to underpredict the current velocity seaward of the maximum current, but, in general, the model does quite a good job of longshore current prediction.

The other Leadbetter Beach cases showed similar results. In all cases, the model gives reasonable maximum current locations and speeds as well as current distributions within the surf zones. These findings were also confirmed by Thornton and Guza (1985) in a study in which the random wave model's wave height and longshore current predictions are rigorously tested against the Leadbetter Beach data.

MODEL OUTPUT VS OBSERVED DATA
5 FEB 1980 B = 1.00 GAMMA = .45

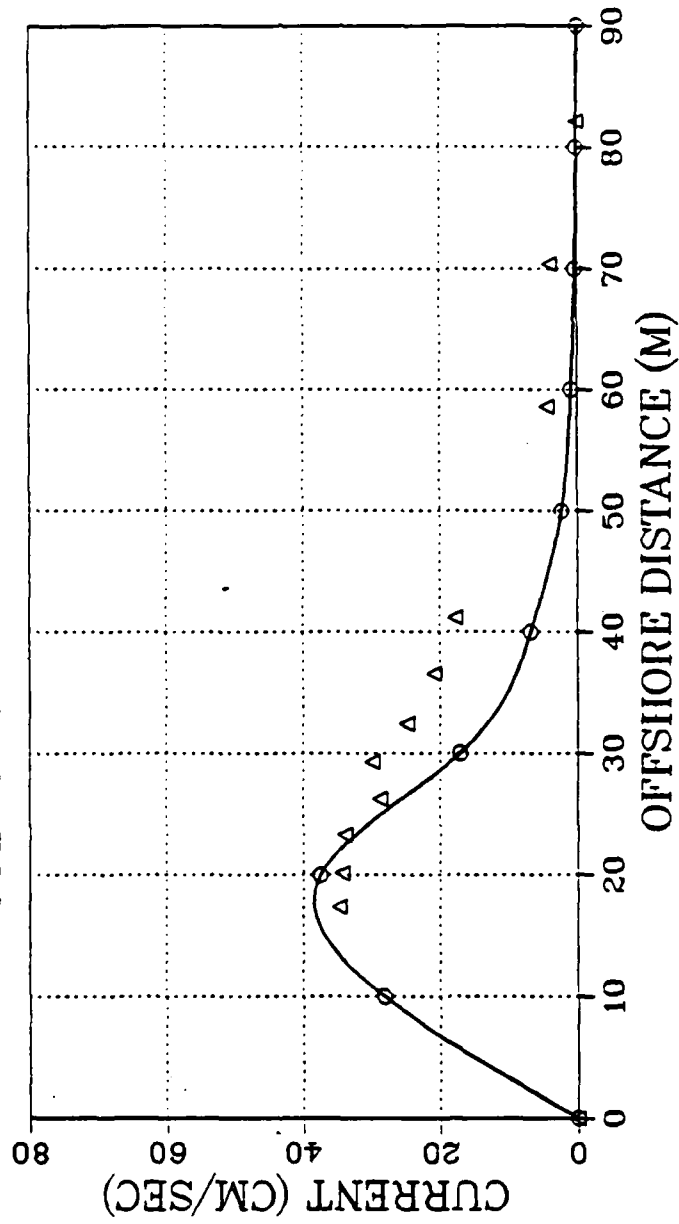


Figure 5.9. Comparison between the model output (solid) and the observed data from Santa Barbara on 5 Feb., 1980 (triangles).

MODEL OUTPUT VS OBSERVED DATA
3 FEB 1980 B = 1.00 GAMMA = .45

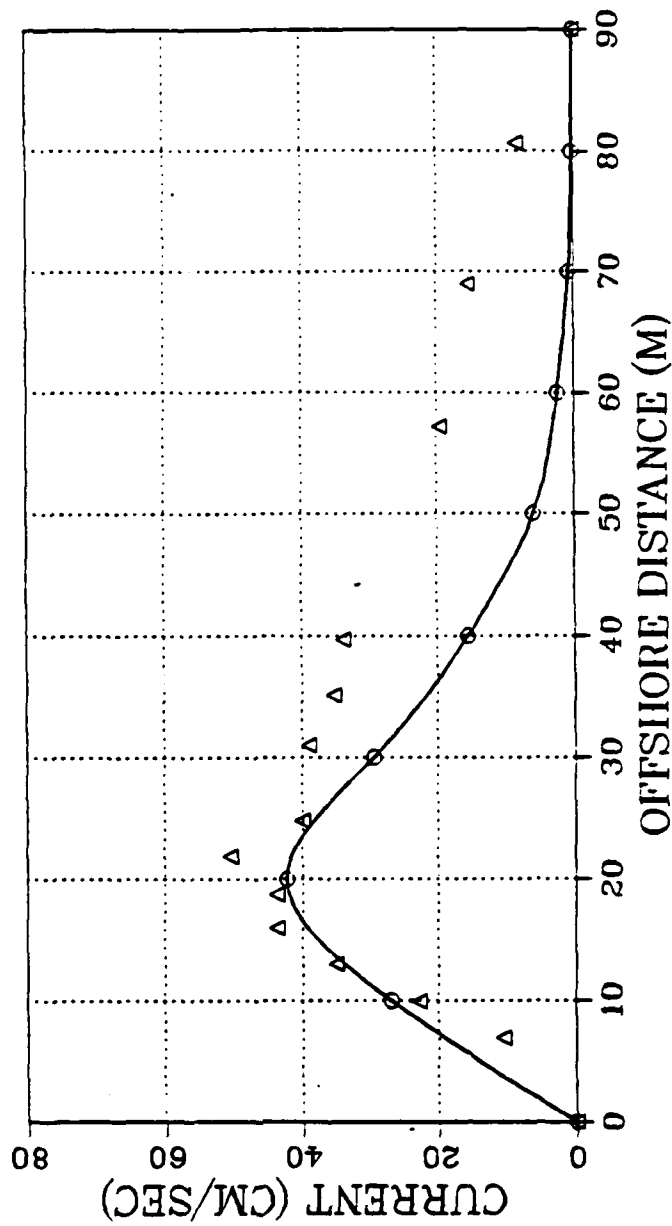


Figure 5.7. Comparison between the model output (solid) and the observed data from Santa Barbara on 3 Feb., 1980 (triangles).

MODEL OUTPUT VS OBSERVED DATA
4 FEB 1980 B = 1.00 GAMMA = .45

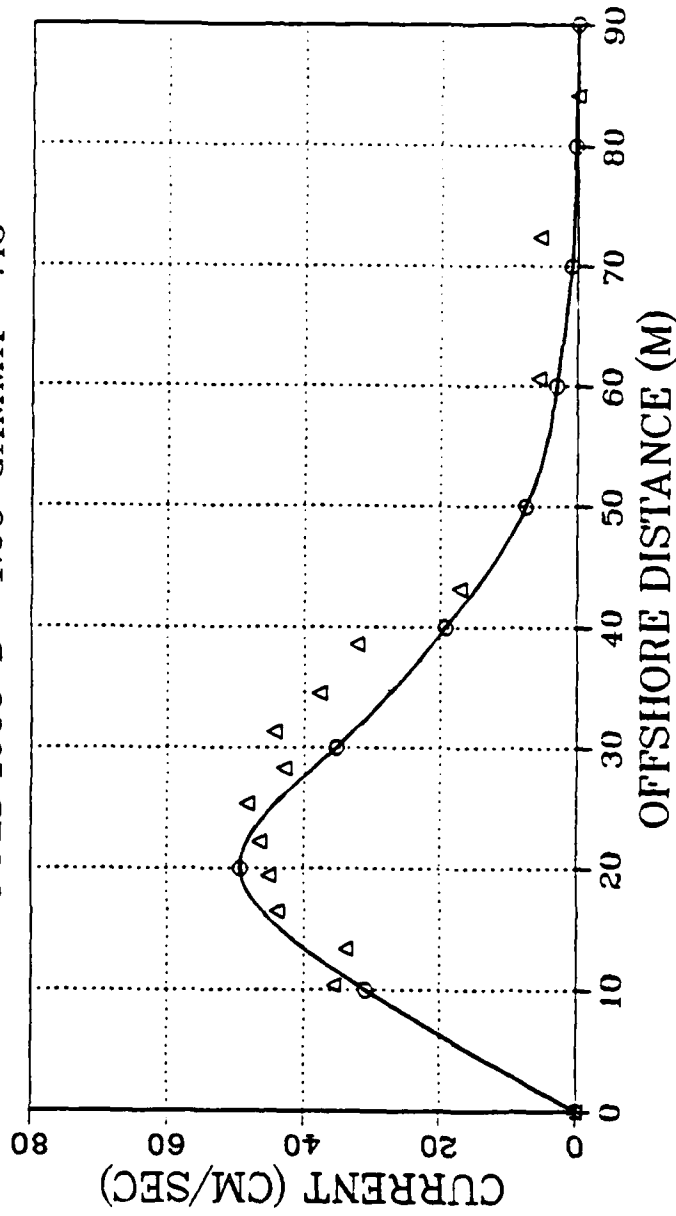


Figure 5.8. Comparison between the model output (solid) and the observed data from Santa Barbara on 4 Feb., 1980 (triangles).

VI. SUMMARY AND CONCLUSIONS

A. SUMMARY

In 1981, the U.S. Navy contracted to have a Sea, Swell and Surf Program (SSSP) developed to provide input to the planning efforts of Naval Oceanographers at sea and amphibious operational planners. The model was developed in FORTRAN and designed to run on a main frame computer (Wang and Chen, 1983). The completed SSSP was then translated into BASIC for use on the currently available shipboard micro-computers, the HP-9845B/275 (Devendorf, 1985). The SSSP was modular in nature, with separate subroutines for offshore wind wave generation, surf zone calculations and nearshore circulation.

The original SSSP had several problems which prevented its use by operational planners. The offshore wind wave generation module overbuilt the wave heights for high wind speeds. Some of the surf condition calculations were inaccurate and the nearshore circulation subroutine had stability problems. These problems were addressed by this thesis in an attempt to improve and upgrade the SSSP.

The open water module shows satisfactory wind wave generation for wind speeds of 15 knots or less. For higher wind speeds, the predicted wave generation occurs too quickly, both spatially and temporally. Sensitivity analysis indicated that the Phillips linear term was responsible for the rapid development, but no improvements to the model physics were made. Several ad hoc "fixes" were recommended. This problem will require further research.

Two subroutines are called to calculate the wave transformation as the wave proceeds from offshore to onshore. Several numeric improvements were made which eliminated minor instabilities in the wave direction and height subroutines. The original no flux boundary conditions were changed to cyclic boundary conditions in both subroutines. This change allows the wave heights and directions to more accurately reflect the conditions required by the model physics at the model boundaries.

The most serious problem, the instability of the nearshore circulation module, is solved by substituting a one dimensional longshore current model for the original two dimensional scheme. Although there is a loss of two dimensional current resolution within the surf zone due to the assumptions of straight and parallel contours, stationary wave conditions, and shallow water initial waves, it was felt that a model that gives the important longshore current information quickly and accurately is an improvement over the original unstable, two-dimensional model. The new current model is a simple, longshore momentum flux balance equation. It retains the wave induced momentum flux and neglects the turbulent Reynold's stress. The new model is fast and accurate, requiring only a few calculations once the wave height field is generated.

To take advantage of state of the art breaker height modeling, a random wave model was implemented for the calculations of the wave heights in the nearshore area. The random wave model assumes that wave heights, in the nearshore region, follow a Rayleigh distribution and that, even after the waves break, this distribution is retained. As a future project, the random wave model could be developed into a two dimensional model by applying the proper longshore numerical differencing.

The random wave model assumes that wave breaking can be described by a periodic bore. Two parameters are introduced by the model, which must be chosen based on the initial conditions. The Gamma term is part of the proportionality coefficient which modifies the initial Rayleigh distribution, and is found to be strongly correlated with the beach slope. The breaker parameter, B, describes the amount of the wave face that is breaking and appears to be related to the surf parameter Eta. The criterion for choosing the two breaker parameters was developed empirically.

The wave height and current models were next tested against wave tank and natural beach data sets. Although the model did not necessarily choose optimum values for the breaker parameters, the model is fairly robust, and slight deviations in the parameter values do not degrade the wave height calculations significantly. Good agreement was found between the observed wave heights and the model's predicted values. The longshore current, based on the model's predicted wave height field, were also in close agreement with observations.

The calculation of Effective Surf, an amphibious planning guideline, was improved. The algorithm was implemented in accordance with the Joint Surf Manual (1976) with respect to its input requirements and its formatted output.

A simple users manual, tutorial in nature, was developed for this version of the SSSP. It is short, and assumes some knowledge of the host computer and basic oceanographic terms. It is written within the guidelines set forth by the Navy for development of computer models for the Shipboard Numerical Aid Program (Brown, 1984).

B. CONCLUSIONS

The improved Sea, Swell and Surf Program (SSSP) can provide much useful information to the Naval Oceanographer at sea or amphibious planner. It has several problems which have not been resolved, so its use is recommended with several caveats. The offshore wind wave generation module is felt to be accurate for low wind speeds only. Useful information on offshore wave growth can be obtained for input wind speeds of 15 knots or less. The results obtained for higher wind speed inputs must be examined carefully before use. The requirement for providing an initial wave energy spectrum is probably impractical for shipboard use. The option of providing a single initial wave height and period will be of more value to the operational user.

The new random wave breaker height model appears to work well. The breaker heights and locations as well as the longshore current field are accurately predicted by the model. Due to its one-dimensional nature and the assumption of straight and parallel contours, longshore wave height and current resolution is restricted. However, the assumption that an amphibious landing beach is uniform in the longshore direction is a reasonable one over a wide range of operational areas. The small grid size of the model supports the use of a one dimensional model to compute an average set of characteristics for a "mean" beach. The speed and stability of the new model make it a viable tool for operational planners. Recommendations for further improvement of the SSSP include:

1. Pursue the problem of the overbuilding of the offshore wind waves.
2. Development of better predictors for the breaker parameters Gamma and B by including a wider data base. As was seen in the optimized tests, correct choice of these parameters will provide a

very good fit to observations, even with very complicated bathymetry.

3. Explore the feasibility of using the random wave model two dimensionally. This would offer the advantages of this more realistic approach to wave height modeling, while retaining the details that two dimensional spatial resolution provides.

The improved SSSP offers the Naval Oceanographer at sea and amphibious operational planners a new and useful tool that, when used in conjunction with surf observations, weather information, and other available data, can be a great aid in the safe planning and execution of beach landing operations.

LIST OF REFERENCES

- Abbott, M.D., Computational Hydraulics, p. 155, Pitman, London, 1979.
- Arthur, R.S., "Variability in Direction of Wave Travel," Annals of the New York Academy of Sciences, 51, pp. 511-522, 1949.
- Barnett, T.P., "On the Generation, Dissipation and Prediction of Ocean Wind Waves," J. Geophys. Res., 73, pp. 513-530, 1968.
- Bascom, T.P., Waves and Beaches, Anchor Press/Doubleday, New York, New York, 1980.
- Bishop, C.T., "Comparison of Manual Wave Prediction Models," J. Waterways Harbors Coastal Eng. Div. Am. Soc. Civ. Eng., 109, pp. 1-17, 1983.
- Battjes, J.A., "Set-up Due to Irregular Waves," Proceedings of the 13th International Conference Coastal Engineering, pp. 1993-2004, Am. Soc. Civ. Eng., New York, New York, 1972.
- Battjes, J.A. and Janssen, J.P.F.M., "Energy Loss and Set-up Due to Breaking of Random Waves," Proceedings of the 16th International Conference Coastal Engineering, p. 569, Am. Soc. Civ. Eng., New York, New York, 1978.
- Battjes, J.A. and Stive, M.J.F., "Calibration and verification of a dissipation Model for Random Breaking Waves," Accepted in J. Geophys. Res., 1985.
- Brown, T., "Programming Guide for Shipboard Numerical Aid Programs (SNAP)," NAVENVPREDRSCHFAC Technical Report TR 84-06, Naval Environmental Prediction Facility, Monterey, California, June, 1984.
- Chen, Y.H. and Wang, H., "Numerical Model for Nonstationary Shallow Water Wave Spectral Transformation," J. Geophys. Res., 88, pp. 9851-9863, November 20, 1983.
- Collins, J.I., "Predictions of Shallow Water Spectra," J. Geophys. Res., 77, pp. 2693-2701, 1972.
- Collins, J.I., "Probabilities of Breaking Wave Characteristics," Proceedings of the 13th International Conference Coastal Engineering, pp. 399-412, Am. Soc. Civ. Eng., New York, New York, 1970.
- COMNAVSURFPAC/COMNAVSURFLANT Instruction 3840.1A (Joint Surf Manual), Department of the Navy, 04 December, 1976.

- Devendorf, L.E., Wave and Surf Forecast Model For Use on a Micro-Computer, Master of Science Thesis, Naval Postgraduate School, Monterey, California, March, 1985.
- Gill, M.J., SSSP User's Guide, in press, 1985.
- Haltiner, G.J. and Williams, T.W., Numerical Prediction and Dynamical Meteorology, 2nd ed., John Wiley and Sons, 1980.
- Hasselmann, K., "Grundgleichungen der Seegangsvoraussage," Schiffstechnik, 7, pp. 191-195, 1960.
- Hasselmann, K. and Collins, J.I., "Spectral Dissipation of Finite Depth Gravity Waves Due to Bottom Friction," J. Mar. Res., 26, pp. 1-12, 1968.
- Hunt, J.N., "Direct Solution of Wave Dispersion Equation," J. Waterway, Port, Coastal and Ocean Div., 105, No. WW4, pp. 457-460, 1979.
- Hwang, L.S. and Divoky, D. "Breaking Wave Set-up and Decay on Gentle Slopes," Proceedings of the 12th International Conference Coastal Engineering, pp. 377-389, Am. Soc. Civ. Eng., New York, New York, 1970.
- Karlsson, T., "Refraction of Continuous Ocean Wave Spectra," J. Waterways Harbors Coastal Eng. Div. Am. Soc. Civ. Eng., 105, pp. 437-448, 1969.
- Kitaigorodski et al., "On Phillips Theory of Equilibrium Range in the Spectra of Wind Generated Gravity Waves," J. Phys. Oceanogr., 5, pp. 410-420, 1975.
- LeBlond, P.H. and Mysak, L.A., Waves in the Ocean, pp. 490-500, Elsevier Scientific Publishing Company, 1978.
- LeMahaute', B., "On Non-saturated Breakers and the Wave Run-up," Proceedings of the 8th International Conference Coastal Engineering, pp. 77-92, Am. Soc. Civ. Eng., New York, New York, 1962.
- Longuet-Higgins, M.S., "Longshore Currents Generated by Obliquely Incident Sea Waves," J. of Geophys. Res., 75, 6778-6801, 1970.
- Longuet-Higgins, M.S. and Stewart, R.W., "The Changes in Amplitude of Short Gravity Waves on Steady, Non-Uniform Currents," J. Fluid Mech., 8, pp. 568-583, 1960.
- Longuet-Higgins, M.S. and Stewart, R.W., "Radiation Stresses in Water Waves: A Physical Discussion With Applications," Deep Sea Res. II, pp. 529-562, 1964.

- Longuet-Higgins, M.S. and Stewart, R.W., "Radiation Stresses and Mass Transport in Gravity Waves, With Applications to Surf Beats," J. Fluid Mech., 13, pp. 481-504, 1962.
- Miles, J.W., "On the Generation of Surface Waves by Shear Flows," J. Fluid Mech., 3, pp. 185-204, 1957.
- Miles, J.W., "On the Generation of Surface Waves by Shear Flows, II," J. Fluid Mech., 6, pp. 568-582, 1959a.
- Miles, J.W., "On the Generation of Surface Waves by Shear Flows, III," J. Fluid Mech., 6, pp. 583-598, 1959b.
- Miles, J.W., "On the Generation of Surface Waves by Shear Flows, IV," J. Fluid Mech., 13, pp. 433-448, 1962.
- Noda, E.K., "Rip Currents," Proceedings of the 13th International Conference Coastal Engineering, pp. 653-668, Am. Soc. Civ. Eng., New York, New York, 1972.
- Noda, E.K., Sonu, J., Rupert, V.C. and Collins, J.I., "Nearshore Circulation Under Sea Breeze Conditions and Wave Current Interaction in the Surf Zone," Tetra Tech Report TC-149-4, 1974.
- Pierson, W.J. and Moskowitz, L., "A Proposed Spectral Form for Fully Developed Wind Seas Based on the Similarity Theory of S. A. Kitaigorodski," J. Geophys. Res., 69, pp. 5181-5190, 1964.
- Phillips, O.M., "On the Generation of Waves by Turbulent Wind," J. Fluid Mech., 2, pp. 417-445, 1957.
- Phillips, O.M., The Dynamics of the Upper Ocean, 2nd ed., pp. 23-24, Cambridge University Press, New York, 1977.
- Sallenger, A.H. and Holman, R.A., "Wave-Energy Saturation on a Natural Beach of Variable Slope," Accepted in J. Geophys. Res., 1985.
- Shiau, J.C., and Wang, H., "Wave Energy Transformation Over Irregular Bottom," Waterways Port Coastal Div. Am. Soc. Civ. Eng., 103, pp. 57-68, 1977.
- Sorensen, R.M., Basic Coastal Engineering, 2nd ed., John Wiley and Sons, New York, New York, 1978.
- Thornton, E.B., "Rederivation of the Saturation Range in the Frequency Spectrum of Wind Generated Gravity Waves," J. Phys. Oceanogr., 7, (1), pp. 137-140, 1977.

- Thornton, E.B., "Variations of Longshore Current," Proceedings of the 12th International Conference Coastal Engineering, pp. 291-308, 1970.
- Thornton, E.B. and Guza, R.T., "Surf Zone Longshore Currents and Random Waves: Models and Field Data," Accepted in J. Phys. Oceanog, 1985.
- Thornton, E.B. and Guza, R.T., "Transformation of Wave Height Distribution," J. Geophys. Res., 88, (C10), pp. 5925-5938, 1983.
- Vincent, C.L., "Energy Saturation of Irregular Waves During Shoaling," Accepted in J. Waterway, Port, Coastal and Ocean Division, Am Soc. Civ. Eng. 1985.
- Wang, H. and Chen, Y.H., Sea, Swell and Surf Program (SSSP)," Coastal and Offshore Engineering and Research, Inc., 1983.
- Wang, H. and Yang, W.C., "Wave Spectral Transformation Measurement at Sylt, North Sea," Coastal Engineering, 5, pp. 1-34, 1981.
- Wiegel, R.L., Waves, Tides, Currents and Beaches: Glossary of Terms and List of Standard Symbols, Council on Wave Research, The Engineering Foundation, July, 1953.
- Wu, C.S. and Liu, P.L.F., "Finite Element Modeling of Breaking Wave Induced Nearshore Currents," J. of Waterway, Port, Coastal and Ocean Division, Am. Soc. Civ. Eng., 111, 2, pp. 417-432, 1985.

INITIAL DISTRIBUTION LIST

	No. Copies
1. Defense Technical Information Center Cameron Station Alexandria, VA 22304-6145	2
2. Library, Code 0142 Naval Postgraduate School Monterey, CA 93943-5100	2
3. Chairman (Code 68Mr) Department of Oceanography Naval Postgraduate School Monterey, CA 93943-5100	1
4. Chairman (Code 63Rd) Department of Meteorology Naval Postgraduate School Monterey, CA 93943-5100	1
5. Prof. E.B. Thornton, Code 68 Tm Department of Oceanography Naval Postgraduate School Monterey, CA 93943-5100	3
6. Prof. C.S. Wu, Code 68 Wu Department of Oceanography Naval Postgraduate School Monterey, CA 93943-5100	2
7. Lieutenant Michael J. Gill Naval Coastal Systems Center Panama City, FL 32407	2
8. Commanding Officer Naval Environmental Prediction Research Facility Monterey, CA 93940	1
9. Commanding Officer Fleet Numerical Oceanography Center Monterey, CA 93943	1
10. Department of Oceanography Library University of Washington Seattle, WA 98105	1

11. **Commanding Officer** 1
Naval Ocean Research and Development
Activity
NSTL Station
Bay St. Louis, MS 39522
12. **Office of Naval Research (Code 420)** 1
Naval Ocean Research and Development
Activity
800 N. Quincy Street
Arlington, VA 22217

END

FILMED

12-85

DTIC